Assessment of Sediment Transport Pathways Inshore of HARS from Near-bottom Current and Turbidity Measurements Fall/Winter 2000 and Spring 2001

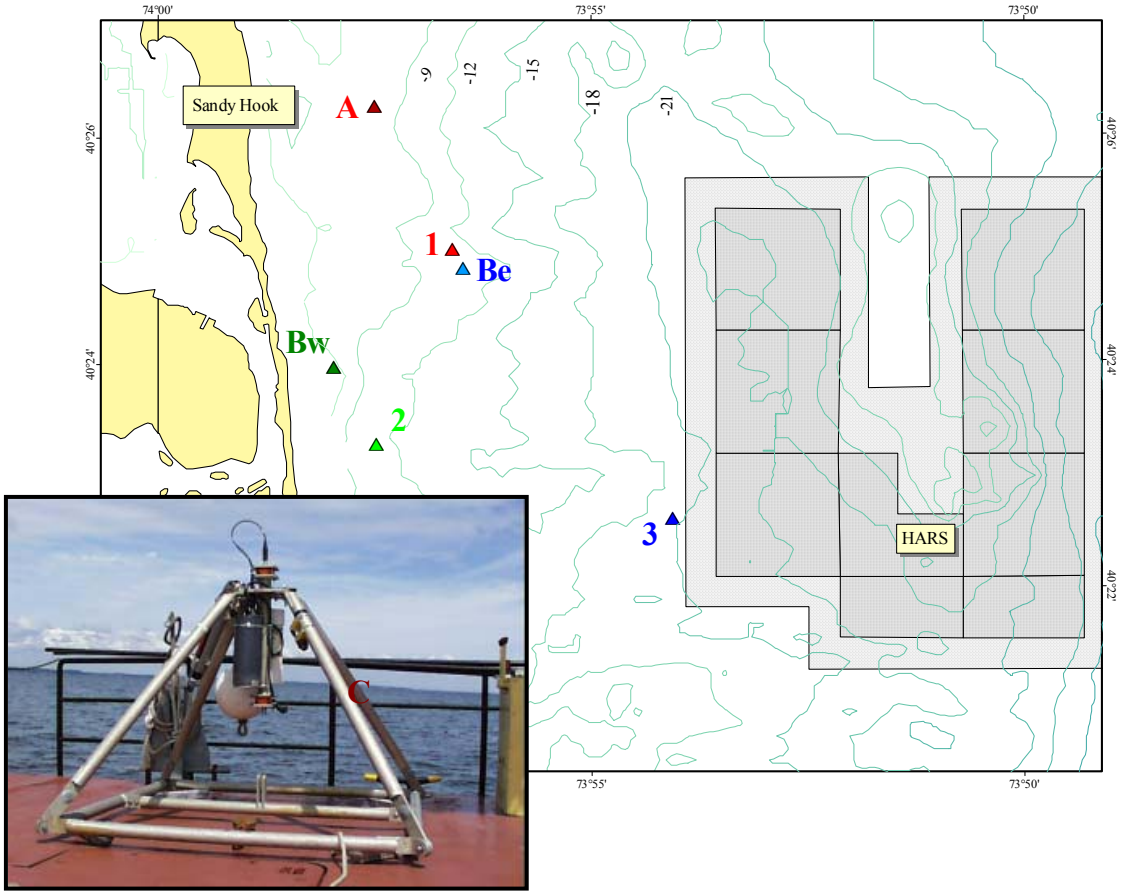

Prepared for:

U.S. Army Corps of Engineers
New York District,
Operations Division
26 Federal Plaza
New York, NY 10278-0090

Prepared by:

Science Applications International Corporation
Admiral's Gate
221 Third Street
Newport, RI 02840

July 2002
SAIC Report Number 585

TABLE OF CONTENTS

TABLE OF CONTENTS (continued)

ACKNOWLEDGEMENTS

Funding for this extensive oceanographic measurement program performed by SAIC in the NY Bight derived from the U.S. Army Corps of Engineers, New York District under contract number GS-35F-4461G. Mr. Brian May was responsible for the project initiation, and Dr. Stephen Knowles was the Program Manager for the Army Corps over the course of the measurement program.

All field operations were based out of the Army Corps field facility in Caven Point, NJ, and mooring deployments and recovery were conducted aboard the Army Corps vessel *M/V Gelberman*. The various deployment and recovery efforts were conducted by employees of the Army Corps Operations Division Tim LaFontaine, Rich Goudreau, Eddie Quirk, Dan Florio, Bill Cobb and Liz Finn and SAIC Scientists Dr. Scott McDowell, Steven Pace, Marc Wakeman and Kate Pickle.

Dr. Scott McDowell was the SAIC lead oceanographer and program manager for the duration of the project. Mr. Steven Pace oversaw and managed the development and deployment of the Automated Resuspension Surveillance System, which provided the excellent near-bottom current and turbidity datasets. Processing of the ARESS and ADCP data was performed by Mr. Paul Blankinship under the direction of Dr. Peter Hamilton. Data analysis, report writing and figure production was performed by Mr. Kurt Rosenberger under the direction of Dr. Scott McDowell and Mr. Tom Waddington. Report production was conducted by Mr. Tom Fox and Mrs. Michelle San Antonio.

LIST OF TABLES

LIST OF TABLES (continued)

Page

LIST OF FIGURES

LIST OF FIGURES (continued)

Page

LIST OF FIGURES (continued)

Page

LIST OF FIGURES (continued)

Page

LIST OF FIGURES (continued)

Page

EXECUTIVE SUMMARY

Since September 1997, the U.S. Army Corps of Engineers, New York District (NYD) has been performing environmental monitoring of the Historic Area Remediation Site (HARS), following the guidelines of the Site Management and Monitoring Plan (SMMP) developed by the NYD and the U.S. Environmental Protection Agency (EPA). This plan calls for a variety of periodic monitoring efforts, designed primarily to measure any changes in bathymetry, benthic habitat, and sediment chemistry. In addition, the NYD has funded oceanographic monitoring to answer general questions on circulation patterns in the region as well as specific questions on sediment resuspension and transport.

As part of this ongoing effort to understand the oceanographic conditions at the HARS, SAIC performed a 6-month monitoring program from the fall of 2000 into the spring of 2001. The two primary objectives of this study were to determine whether or not sediment in the HARS could be resuspended and transported toward the shore of New Jersey, and to determine what the likely sources of suspended sediment in this region may be. To answer the first question, three bottom mounted instrument arrays measuring wave heights, near-bottom currents, and turbidity were deployed inshore of the HARS in the fall and winter of 2000, the time of year when oceanographic conditions are likely to be most favorable for sediment resuspension and transport. In response to the second question four bottom-mounted arrays, as well as some water-column instruments, were deployed in the same region but focused along the inshore areas. The primary intent of the spring measurement program was to attempt to assess the impact of discharge from the New York Harbor Estuary (NYHE) system. In addition to near-bottom currents, the water column currents were monitored at two locations in each measurement program.

Based on this two-phase oceanographic study, it appears there is little potential for sediment from the HARS to migrate into the near-shore areas of the New Jersey coast. The six months of oceanographic data acquired over both phases of this project demonstrated that the highest observed turbidity conditions were attributed to seafloor sediment resuspension caused by large waves from ocean storms. During these infrequent events, the average progressive near-bottom currents were consistently weak and oriented primarily along a northward/southward direction. During the entire course of this study, there was only one period of consistent westward near-bottom currents at all three sites, and this occurred during a period of low turbidity. Overall, observed currents were dominated by tidal influences and flowed primarily in a northward/southward direction along the coast. During the few periods of high river discharges detected through USGS river gauge data, significantly lower near-surface salinities were noted at the near-shore instrument moorings. However, because the data did not show any corresponding increase in near-bottom turbidity during these periods, this measurement program did not highlight any significant impacts from the NYHE.

1.0 INTRODUCTION

On 1 September 1997, the New York Bight Dredged Material Disposal Site, known as the Mud Dump Site (MDS), was de-designated as an official ocean disposal site by the U.S. Environmental Protection Agency (EPA). This action was the culmination of more than a year of cooperation and coordination between the Department of the Army, the Environmental Protection Agency, and the Department of Transportation. The closure of the MDS on 1 September 1997 ended its use as a repository for dredged sediments removed from the Port of New York for over three-quarters of a century.

Simultaneous with the closure of the MDS, the site and surrounding areas that have been used historically for placement of contaminated material were re-designated as the Historic Area Remediation Site (HARS). The planned remediation for this site has consisted of placing a minimum one-meter "cap" layer of uncontaminated dredged material on top of the existing surface sediments within the nine Priority Remediation Areas (PRAs) of the HARS. The "remediation material" to be used for capping is defined as dredged material that meets current Category I standards and will not cause significant undesirable effects, including bioaccumulation.

The regional office of the EPA (Region II) and the U.S. Army Corps of Engineers New York District (NYD) share joint responsibility for managing and monitoring of the HARS. The two agencies have prepared a Site Management and Monitoring Plan (SMMP) for the HARS that identifies a number of actions, provisions and practices to manage the remediation activities and monitoring tasks (USEPA/USACE 1997). The monitoring program includes state-of-the-art technologies to collect data on waves, currents, and suspended particulate material using remotely installed field instrumentation.

In addition to the HARS monitoring, routine water quality monitoring is conducted along the New Jersey coastline and in the coastal bays by several agencies, including the New Jersey Department of Environmental Protection's (NJDEP) Bureau of Marine Water (BMW), many coastal county Health Departments (such as Monmouth County), and the EPA. The primary objective of these monitoring efforts is to determine the suitability of the coastal waters for shellfishing and bathing activities. During the summers of 1987 and 1988, floating trash such as wood, plastic, paper, and medical waste washed up on several different New Jersey beaches (including Sandy Hook), leading to many beach closures during that period. In most cases where the cause could be determined, the sources for this floating waste were traced to illegally dumped trash that washed onto area beaches following heavy rains and combined sewer overflow.

Other than the well-publicized beach closures during the late 80's, routine sampling conducted along the northern New Jersey shoreline over the last several years has not highlighted any significant water quality problems associated specifically with the Sandy Hook area. Despite the lack of significant water quality evidence, many claims have been made over the last several years implicating the dredged material placement at the HARS as a likely and significant contributor to water quality degradation along the northern New Jersey shoreline. Though the claims appear to be based primarily on anecdotal evidence or the generally negative perceptions

associated with "ocean dumping," the responsible agencies have recently made efforts to research and analyze the validity of these claims.

Numerous past oceanographic studies have been conducted in the region of the HARS, focusing either on the HARS itself (SAIC (1995)), or the New York Bight apex in general (Dittsworth (1978), Charnell (1974), Lyne (1990), Scheffner (1994), Harris (1999)). Past studies conducted by SAIC have focused on currents and turbidity and the mechanisms responsible for sediment resuspension within the HARS site (SAIC 1995). Because of the lack of data specifically focused on the areas inshore of the HARS, this recent study was initiated by the NYD to assess patterns of circulation and potential transport pathways along the New Jersey coastline. This study was intended to answer two basic questions:

1. What is the potential for transport of near-bottom waters (and any associated turbidity) from the offshore HARS area to the shoreline?

2. What is the potential for outflow from the New York Harbor Estuary (NYHE) to contribute turbid waters to the New Jersey coastal environment, thus degrading water quality?

To help answer these questions, SAIC conducted a 6-month oceanographic measurement program (from fall/winter 2000 to spring 2001) extending from the HARS in toward the New Jersey shoreline. The fall/winter measurement program was primarily designed to answer the first question (because of the higher likelihood of large wave storm events), while the spring program was primarily intended to answer the second question (because of the likelihood of higher volumes of outflow from the NYHE). Bottom-mounted Automated REsuspension Surveillance System (ARESS) arrays as well as upward-looking Acoustic Doppler Current Profilers (ADCP) were utilized to observe the near-bottom currents and turbidity, and water column currents in the study area. Periodically during this program, water mass properties (temperature, salinity, and density) also were observed utilizing both real-time, in-situ measurement devices and stationary, vertical profiles in an effort to relate changes in the water mass characteristics to changes in circulation patterns.

2.0 FIELD MONITORING AND DATA PROCESSING

2.1 Overview of Field Monitoring Activities

As indicated in Table 2-1, there were three distinct oceanographic measurement phases that provided the data presented in this report. The two main phases occurred in the fall/winter of 2000 and during the spring of 2001. In addition, oceanographic data from an abbreviated program conducted in the fall of 1999 are also included as supplemental data to the primary measurement program. An overview of the methods employed during each of these measurement phases is presented below.

Each of the measurement phases entailed the deployment of at least three specially designed oceanographic arrays strategically located on the seafloor to assess water column and hydrodynamic characteristics. These Automated REsuspension Surveillance System (ARESS) arrays have been used successfully in numerous past studies to accurately quantify water near-bottom currents and turbidity as well as wave height and period over extended time periods. The locations for the ARESS arrays were selected based upon the primary area of focus for each of the two phases. In addition to the data from the continuously-recording ARESS arrays, periodic discrete sampling operations were conducted to provide supplemental full water-column data (e.g., suspended solids, salinity, temperature, etc.).

2.1.1 Fall/Winter 2000 ARESS Deployments

For the fall/winter 2000 measurement program, three sites were chosen to measure near-bottom currents and turbidity (Figure 2-1): one site adjacent to the HARS (Site 3), one near-shore site (Site 2), and one site in between (Site 1). Depths at the sites and deployment locations are listed in Table 2-1. The primary purpose of this site plan was to monitor east-west, across-shelf flow. The ARESS instrument arrays consisted of aluminum frame quadrapods equipped with two Anderaa acoustic current sensors at 0.76 m and 1.52 m off the seafloor and two optical backscatter sensors (OBS) at 0.76 m and 1.52 m off the seafloor (Figure 2-2). Site 1 and Site 3 were also equipped with an RDI acoustic Doppler current profiler (ADCP) measuring currents throughout the water column. The bottom-mounted arrays were deployed twice in the fall for approximately 1 month each deployment, and for approximately 2 months in the winter, with short interruptions for data recovery and instrument turnaround (Table 2-2).

2.1.2 Spring 2001 ARESS Deployments

In the spring of 2001, ARESS arrays were deployed at three near-shore sites (Sites A, Bw, and C) as well as near the location (Site Be) of Site 1 from the fall/winter deployment period (Figure 2-1). The primary focus of this effort was to measure the along-shore flow and the potential impacts associated with spring outflow from the NYHE system. The bottom-mounted ARESS arrays were deployed for approximately one month in both April and May at Sites A, Bw, and Be, with a short interruption between deployments for data recovery and instrument turnaround (Table 2-3). Deployment locations and water depths are listed in Table 2-1. The

Table 2-1.

Deployment locations and approximate water depths for the three measurement programs. Note: only deployment locations where reliable data was collected are listed for the fall/winter 1999 program.

Site Name	Period	Latitude	Longitude	Water Depth (m)
1	Fall 1999	40.41670	-73.94311	16
3	Fall 1999	40.36952	-73.86950	26
1	Fall 2000	40.41695	-73.94350	16
2	Fall 2000	40.38820	-73.95812	12
3	Fall 2000	40.37726	-73.90123	21
A	Spring 2001	40.43800	-73.95850	7.5
Bw	Spring 2001	40.39950	-73.96633	7.5
Be	Spring 2001	40.41417	-73.94150	13
C	Spring 2001	40.35100	-73.96667	10

Table 2-2.

Log of all data collected during the fall/winter 2000 deployment period

Data Type	Sites	Deployment #1 (09/18/00–10/06/00)	Deployment #2 (10/13/00–11/09/00)	Deployment #3 (11/16/00–1/12/01)
CTD Casts	(All Sites)	**X**	**X**	**X**
Surface Temperature Data	Sites 1, 2, and 3		**X**	**X**
ADCP Data	Sites 1 and 3	**X**	**X**	**X**
Pressure (waves)	Site 3 then 1	**X (3)**	**X (3)**	**X (1)**
ARESS Data (OBS and Velocity)	Sites 1, 2, and 3	**X**	**X**	**X**

Table 2-3.

Log of all data collected during the spring 2001 deployment period

Data Type	Sites	Deployment #4 (04/04/01-05/01/01)	Deployment #5 (05/03/01-06/06/01)
CTD Casts	All Sites	**X**	**X**
Drouge Tracks	Sites A and Be	**X**	**X**
Surface Temperature Data	Sites A, Be and C	**X**	**X**
ADCP Data	Sites Bw and Be	**X**	**X**
MicroCat CT Data	Site Bw, surf. And bott.	**X**	**X**
Aquadopp Data (OBS and Velocity)	Site C (4/24 - 6/6)		**X**
ARESS Data (OBS and Velocity)	Sites A, Bw and Be	**X**	**X**

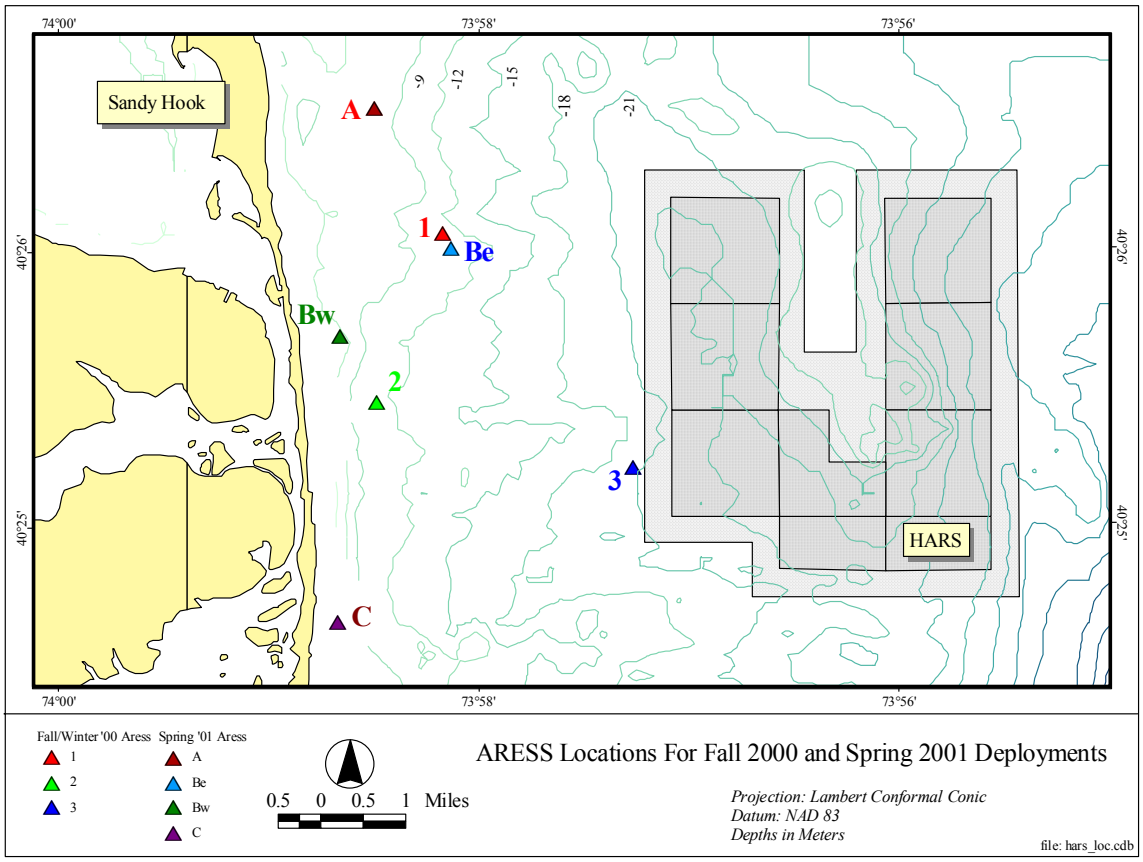

Figure 2-1. Locations of ARESS deployments in fall/winter 2000 and spring 2001

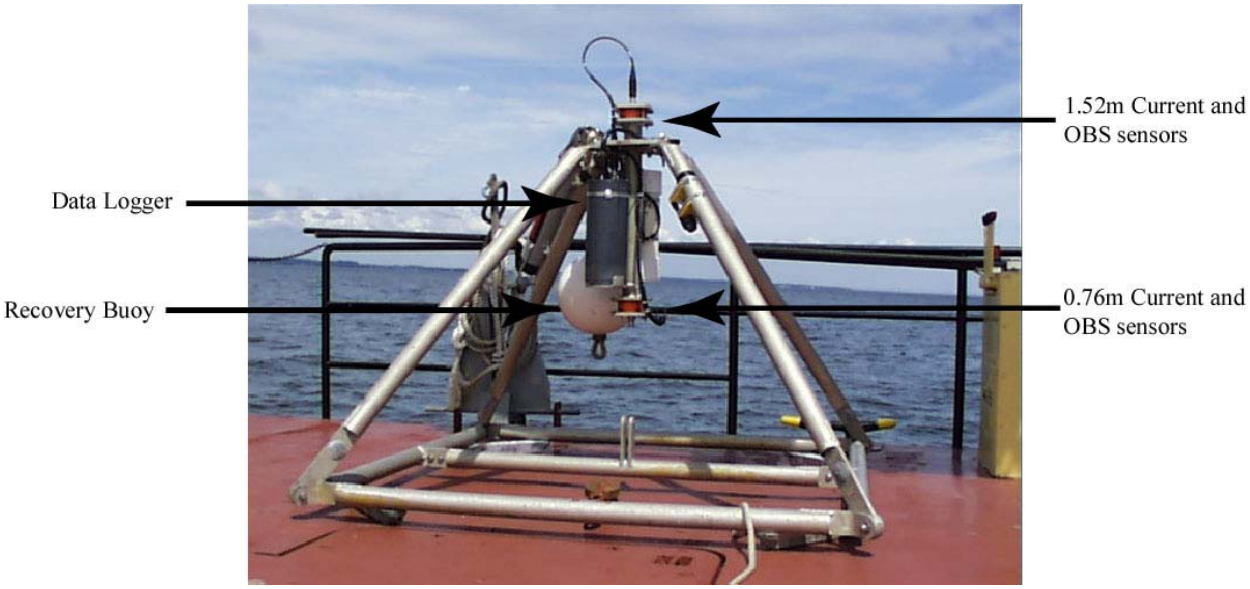

Figure 2-2. Diagram of the ARESS array with current and OBS sensors at two levels

sensor levels on the ARESS arrays were identical to the fall program. At Site C, a steel tripod mounted with a Nortek Aquadopp acoustic Doppler current meter (ADCM) and a D&A Sensors OBS sensor was set to measure near-bottom currents and turbidity for a single 44-day deployment. Each sensor was approximately 1 m off the seafloor. The ADCM also recorded temperature and pressure for the duration of the deployment. In addition, ADCP data were acquired at the two near equal-latitude sites (Bw and Be).

2.1.3 Drogue Deployments

Free-drifting holey-sock drogues were deployed and tracked for one day each at the end of each spring mooring deployment. The drogues have subsurface sails that consist of a long nylon tube approximately 1m in diameter and approximately 3m long with holes to catch the current (Figure 2-3). These drogues were set at different depths in order to track the water currents at various depth levels. Two depths were chosen for these deployments—a near-surface level, and a mid-depth level at approximately 6 m below the surface. Accurate DGPS positions were obtained for the drogues at deployment and retrieval, as well as periodically during their drift.

2.1.4 Measurement of Water Column Properties

During each ARESS deployment, a vertical hydrocast with a Seabird SBE-19 conductivity-temperature-depth instrument was taken adjacent to the mooring. For the spring 2001 deployment period, multiple CTD casts were taken along a transect running from near-shore to offshore to enable a more broad-scale assessment of water column properties. CTD casts were acquired along two transects on 24 April and along one transect on 4 June.

In addition to the CTD casts, time series temperature and conductivity data were collected at selected sites. For each deployment period, one bottom-mounted ARESS array included a temperature sensor (Site 3 in the first two deployments, Site 1 in the third deployment) and both ADCPs also contained a temperature sensor. In the fall and winter of 2000, temperature sensors were placed at the surface on the chain of the mooring buoy for the second and third deployments at all three sites. The temperature sensors also were deployed at the surface for the spring deployments at Sites A, Be, and C. Additionally, Seabird 37-SM Microcat conductivity-temperature recorders were used at both the surface and bottom at Site Bw, to detect stratification that may occur due either to freshwater input or surface warming.

2.2 Instrumentation and Data Processing Techniques

2.2.1 ARESS Sampling Procedures

A self-contained electronics package controlled sampling and data logging on the ARESS arrays. Both the current sensors and OBS turbidity sensors recorded data in short bursts that lasted 2.5 minutes and were spaced two hours apart. The newer and older Anderaa current sensors

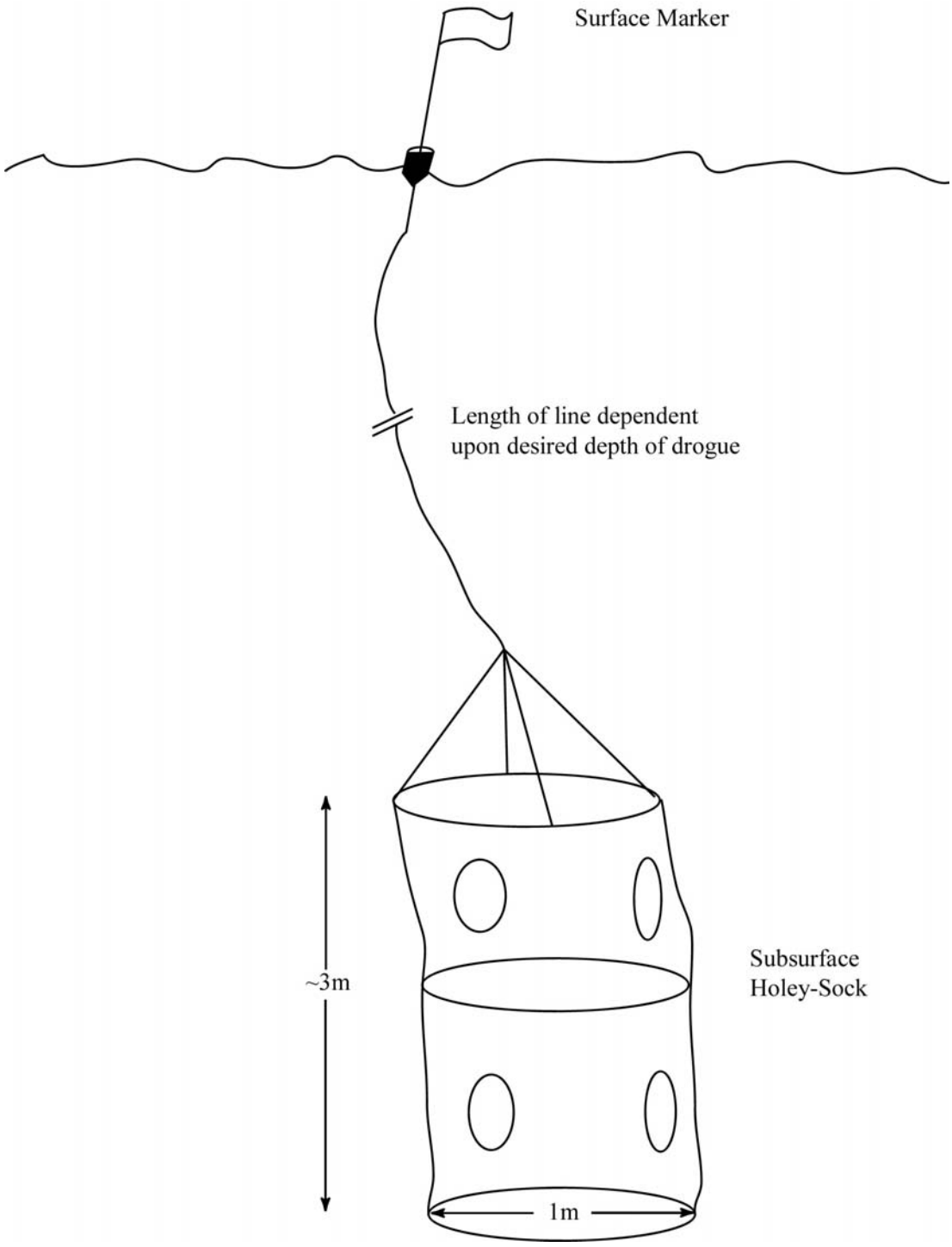

Figure 2-3. Diagram of the holey-sock current drogue. Drogue positions were recorded by monitoring position of surface marker.

recorded at differing intervals, but averaged approximately 3 Hz, providing approximately 450 samples from which an average current velocity was computed. The OBS sensors sampled at a two-second interval, providing approximately 75 samples per data burst. The ARESS array pressure sensor sampled at 3 Hz, providing 450 samples per data burst on average.

2.2.2 ADCP Sampling Procedures

For the fall/winter 2000 measurement program, the ADCPs were deployed in water depths of approximately 16 m and 21 m at Sites 1 and 3, respectively. The ADCPs were set to begin collecting data at 2 m off the seafloor in multiple, vertical, one-meter bins at Sites 1and 3. Because the velocities within the depth bins are vertically averaged, the data represent the velocity at the center of the one-meter bins. Thus, processed data begins at 2.5 m off the seafloor (this includes the height of the instrument off the seafloor, plus a region above the sensors in which the instrument cannot sample). Because surface waves can scatter the ADCP acoustic signal, some of the upper water column vertical current bins are often unreliable. A review of the data indicated that vertical bins 1 through 11 contained reliable data for Site 1 (or from 13.5 m up to 3.5 m depth), and vertical bins 1 through 16 contained reliable data for Site 3 (or from 18.5 m up to 3.5 m depth). The instruments were set to collect velocity data every 10 seconds and to compute an average current velocity every half hour.

In the spring of 2001, the ADCPs were deployed in water depths of approximately 7.5 and 13 m at Sites Bw and Be, respectively. Because of the shallower water depths, a half-meter bin length could be used, thereby providing increased resolution for the vertical current data. Reliable data were recovered from 2.25 m to 5.25 m depth at Site Bw, and from 2.75 m to 10.75 m depth at Site Be. The sampling intervals were comparable with the fall/winter 2000 deployment period, to assist with subsequent analyses.

2.2.3 Data Processing

All data from the ARESS arrays (currents, turbidity, pressure, and temperature) were processed by physical oceanographers in the SAIC Raleigh, NC office. The data were initially run through standard QA/QC processing routines to remove any unreliable data, and an average current, turbidity, and temperature value was calculated for each data burst. The individual pressure observations in each data burst were used to calculate the height and period of waves at the given site.

Currents were recorded in earth coordinates as north-south and east-west components. Basic processing of the current data included calculating a magnitude and direction for each sample as well as a mean speed and direction for each deployment. Current data were then filtered using a 30-hour, 2^{nd} order Butterworth low-pass filter (LPF) to remove the major tidal constituents and view the currents in a sub-tidal sense.

3.0 RESULTS

The following section provides a detailed discussion of the analyses conducted on the extensive oceanographic data acquired during the course of this study. Detailed results from the two primary measurement programs (fall/winter 2000 and spring 2001) are provided, as well as the supplemental data from the fall 1999 measurement program. Because of the volume of data included in this study, only selected representative figures have been included within the main body of the report to help illustrate the types of data being discussed. For instance, though the fall/winter 2000 measurement program consisted of three separate instrument deployment periods, only data from one of these periods are included in the main report. Similar figures representing all of the data from this study have been included in the Appendix. In some cases, the results discussed in this section may be illustrated by figures included in the Appendix.

In addition, summary results have been provided at the end of the three main sub-sections, highlighting the key results from each of the three distinct measurement programs. Readers not interested in the in-depth review and discussion of the extensive oceanographic data acquired during this study may want to review just these key summary results at the end of each main sub-section.

3.1 Fall/Winter 2000 Measurement Program

The first phase of the measurement program was conducted in fall/winter 2000 and was primarily intended to determine if resuspended sediment from the HARS was likely to migrate toward the inshore areas of the New Jersey shore. This time period was selected because it represented the time of year when storms and large wave events are both larger and more frequent, demonstrating the worst-case scenario that might be encountered. Past oceanographic studies have shown that large waves are the primary forcing mechanism for resuspending seafloor sediment in this area (SAIC 1995).

In this section, the term ‘fall’ is generally used to refer to the first two deployments, whereas ‘winter’ refers to the third deployment from November to January, unless otherwise specified.

3.1.1 Water Column Characteristics

CTD Casts

Casts of CTD data showed markedly different water properties between onshore and offshore locations. A common means of presenting data from CTD casts is in the form of a T/S plot, in which individual temperature and salinity pairs are plotted against one another (Figures 3-1 and 3-2). In these plots, the dotted lines in the background represent lines of constant density, or isopycnals. The density units are in Sigma-T units (kg/m^3), represented as a departure from pure fresh water at 1000 kg/m^3 (thus, 20 Sigma-T units represents 1020 kg/m^3). A cast was taken at each site at the beginning and end of the first deployment on 18 September and 6 October. Data collected from Site 3 on 18 September was deemed unreliable and is therefore not

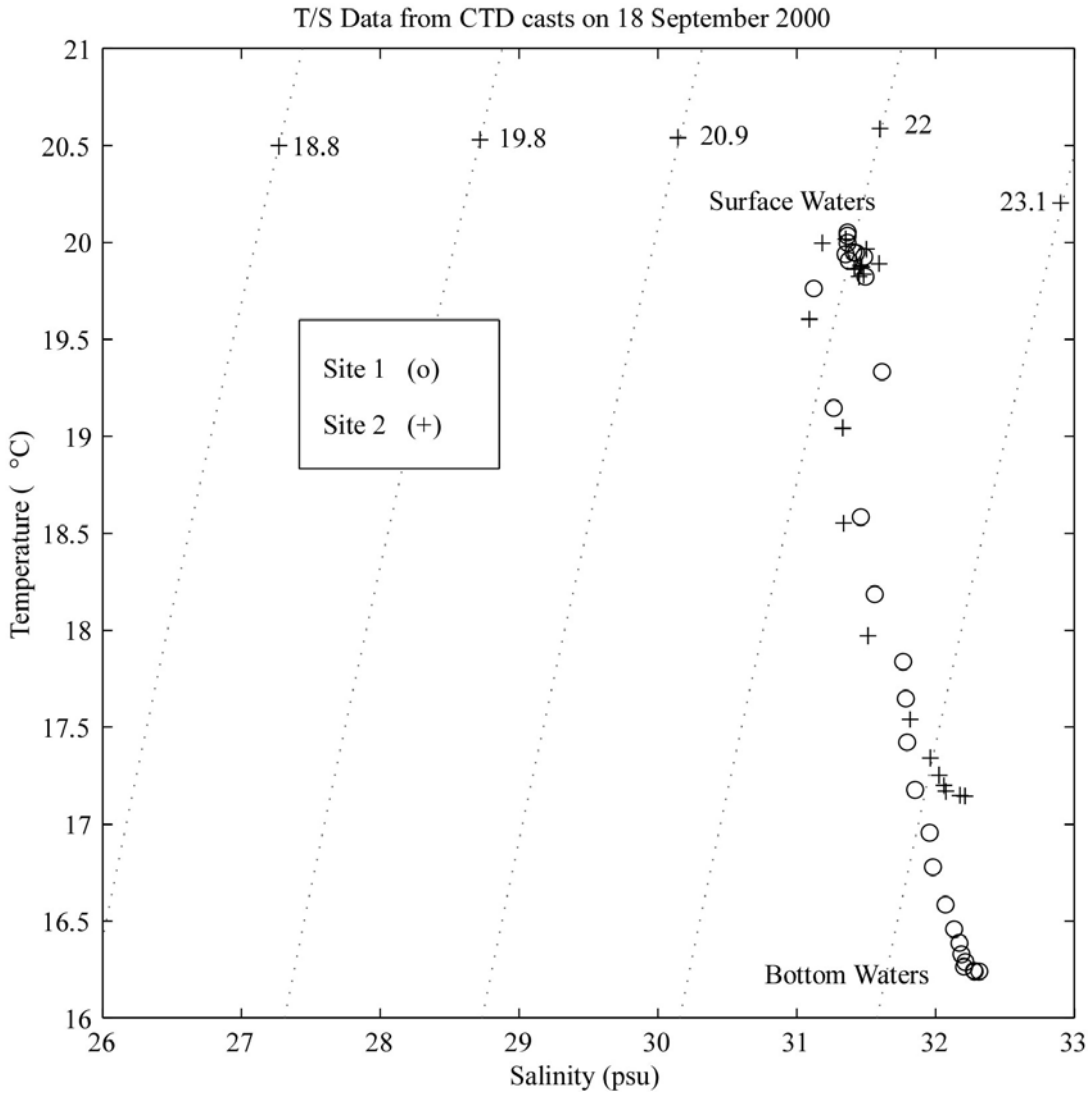

Figure 3-1. T/S plot of CTD data collected on 18 September 2000. Dotted lines in the background represent lines of constant density (isopycnals) and the numbers at each dotted line represent density values in Sigma-T units, which increase from left to right.

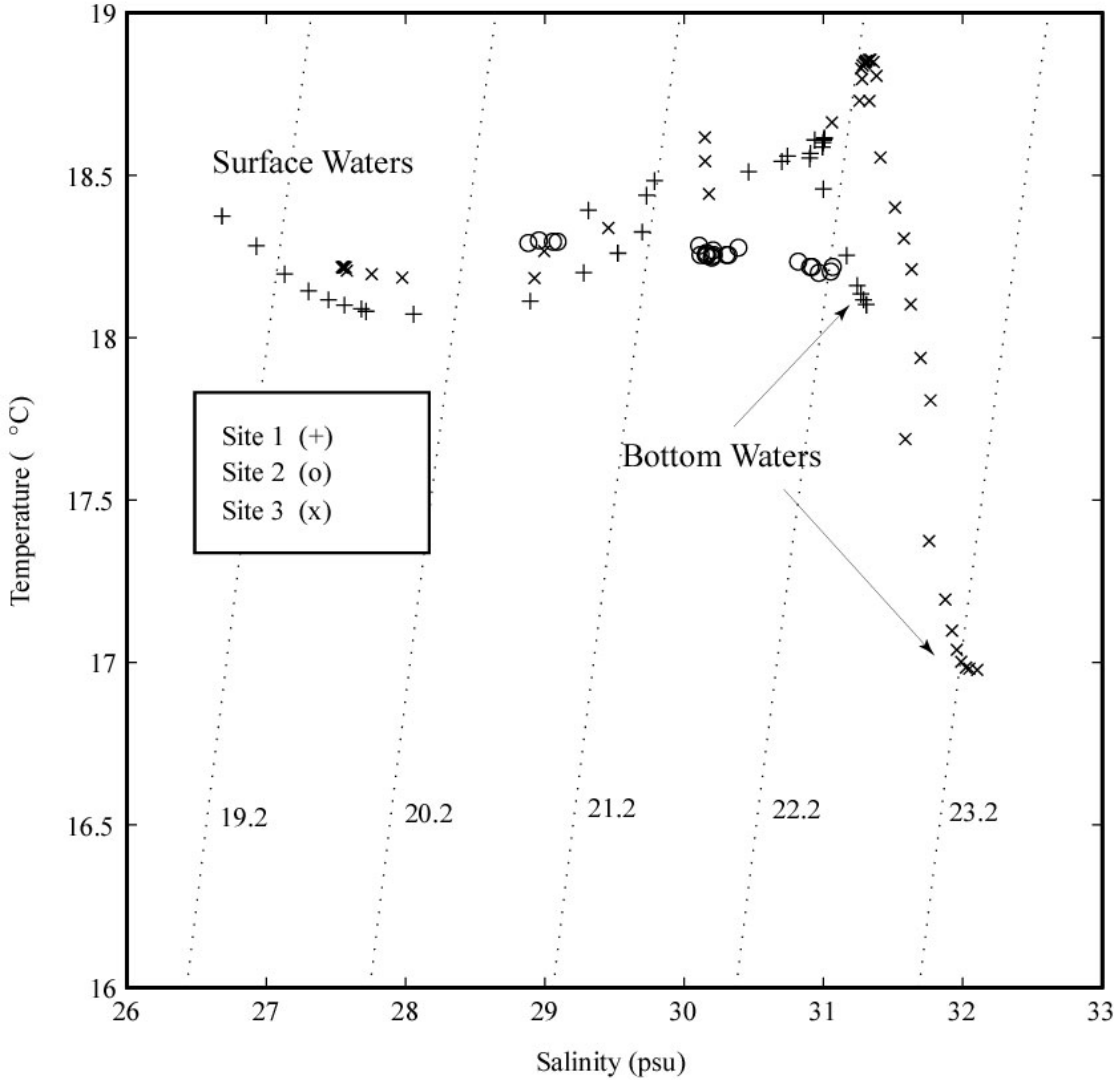

Figure 3-2. T/S plot of CTD data collected on 6 October 2000. Dotted lines in the background represent lines of constant density (isopycnals) and the numbers at each dotted line represent density values in Sigma-T units, which increase from left to right.

presented. At Sites 1 and 2 only a slight density gradient of approximately 2.0 sigma-t units from surface to bottom was detected; both of these stations also exhibited a low salinity gradient. Based on casts taken on 6 October, water column properties had changed noticeably, with thermal stratification breaking down and saline stratification intensifying, particularly for the inshore sites (Figure 3-2); this is most likely due to water column mixing and overturning caused by strong winds out of the north in late September. The inshore sites (Sites 1 and 2) were characterized by slightly colder, fresher surface waters overlying warmer, more saline waters, and a density stratification of approximately 2 sigma-t units. In general, bottom temperatures rose and surface temperatures dropped at all sites from the beginning of the first deployment to the beginning of the second deployment as water-column mixing broke down the thermal stratification.

It can also be instructive to view the CTD data in a vertical profile of the cast, as in Figures 3-3 and 3-4. Salinity is plotted in Practical Salinity Units (PSU), Temperature in Degrees Celsius, and Density in Sigma-T units. Here we note the breakdown in the thermal stratification from September to October, (note the small range in temperature in October at sites 1 and 2). At site three, however, the thermal stratification remains through 6 October, but is typically vertically mixed come winter.

Near-bottom and Surface Temperature

Near-bottom water temperature data were recorded by the ADCPs at Sites 1 and 3 for all three deployments and surface temperature was recorded at all three sites by thermistors attached to the surface buoys (Figure 3-5). Breaks in the near-bottom record (green) show the periods of ADCP turnaround. These data provide a view of stratification in the water column through time. The beginning of the record shows a well developed thermal stratification with near bottom temperatures at 12° and 14° C at Sites 1 and 3 respectively and near surface temperatures of 20° C at Sites 1 and 2 and variable temperatures around 15° -16° C at Site 3. From 25 to 27 September a strong northeasterly storm (as outlined in the next section) thoroughly mixed the water column and input a flux of fresh water to the system, which is represented in the temperature data as near-bottom temperatures rose and near surface temperatures fell to a final value of approximately 17° C at all three sites.

Over the course of the fall and winter, both near-bottom and surface temperatures showed a monotonic decrease to final values of 4° –6° C. Some periods show warmer temperatures at the near-bottom than on the near surface as on 5 to 10 November and around 30 November. This would seem to contradict the notion of a stable water column with colder water overlying warmer water. However, as we will see in the next section, these periods correspond to periods of high freshwater input, indicating that the surface waters were, in fact, cold and fresh, leaving slightly warmer and more salty water at depth, thus indicating stable water column stratification. Another point to note is that this difference between surface and bottom temperatures is more significant at Site 1 than Site 3, which could be explained by less dense freshwater outflow from the NYHE following the coastline as it exits the harbor.

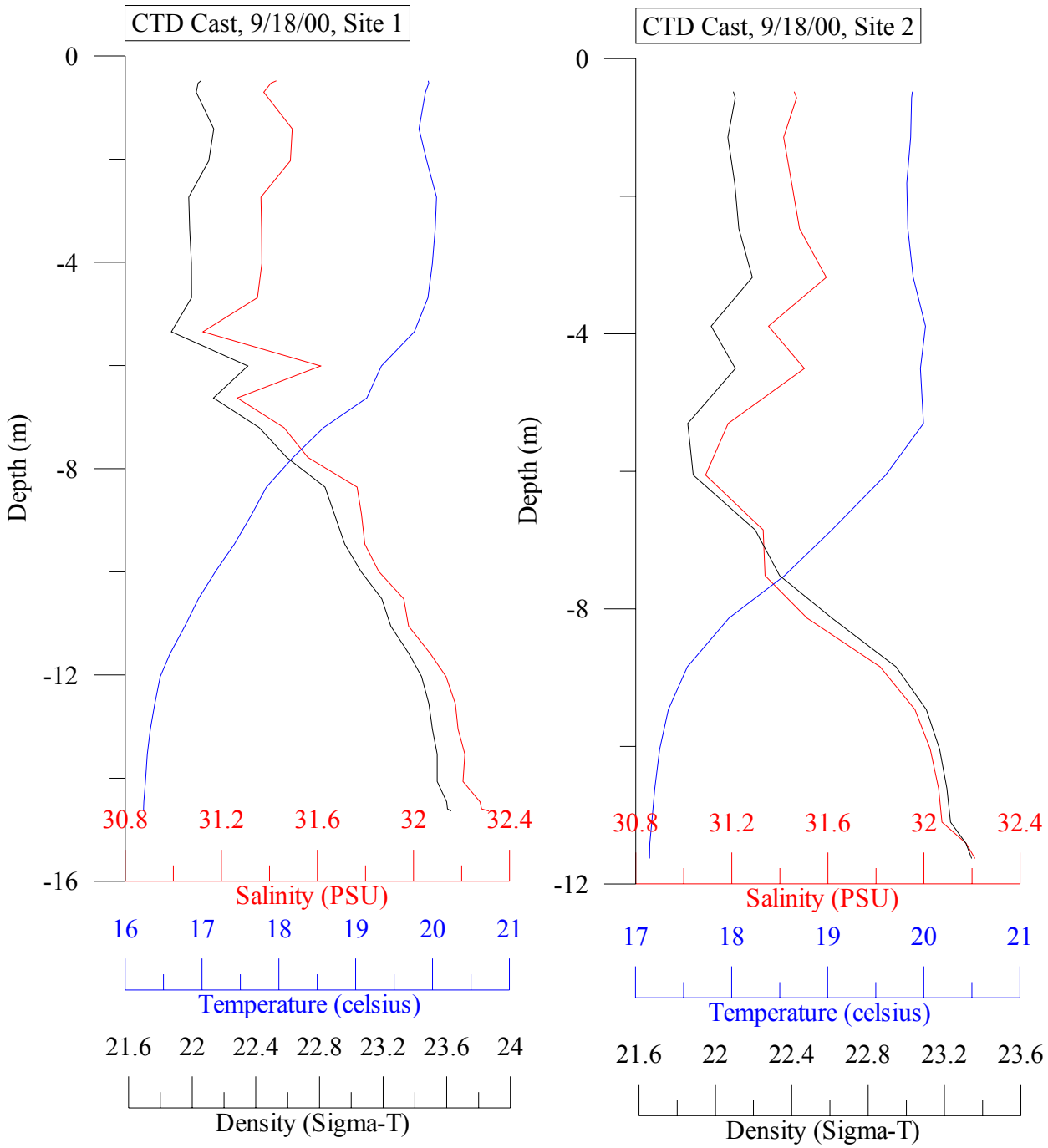

Figure 3-3 Vertical plots of CTD casts collected on 18 September 2000. Salinity is plotted in Practical Salinity Units, Temperature in Degrees Celsius, and Density in Sigma-T units.

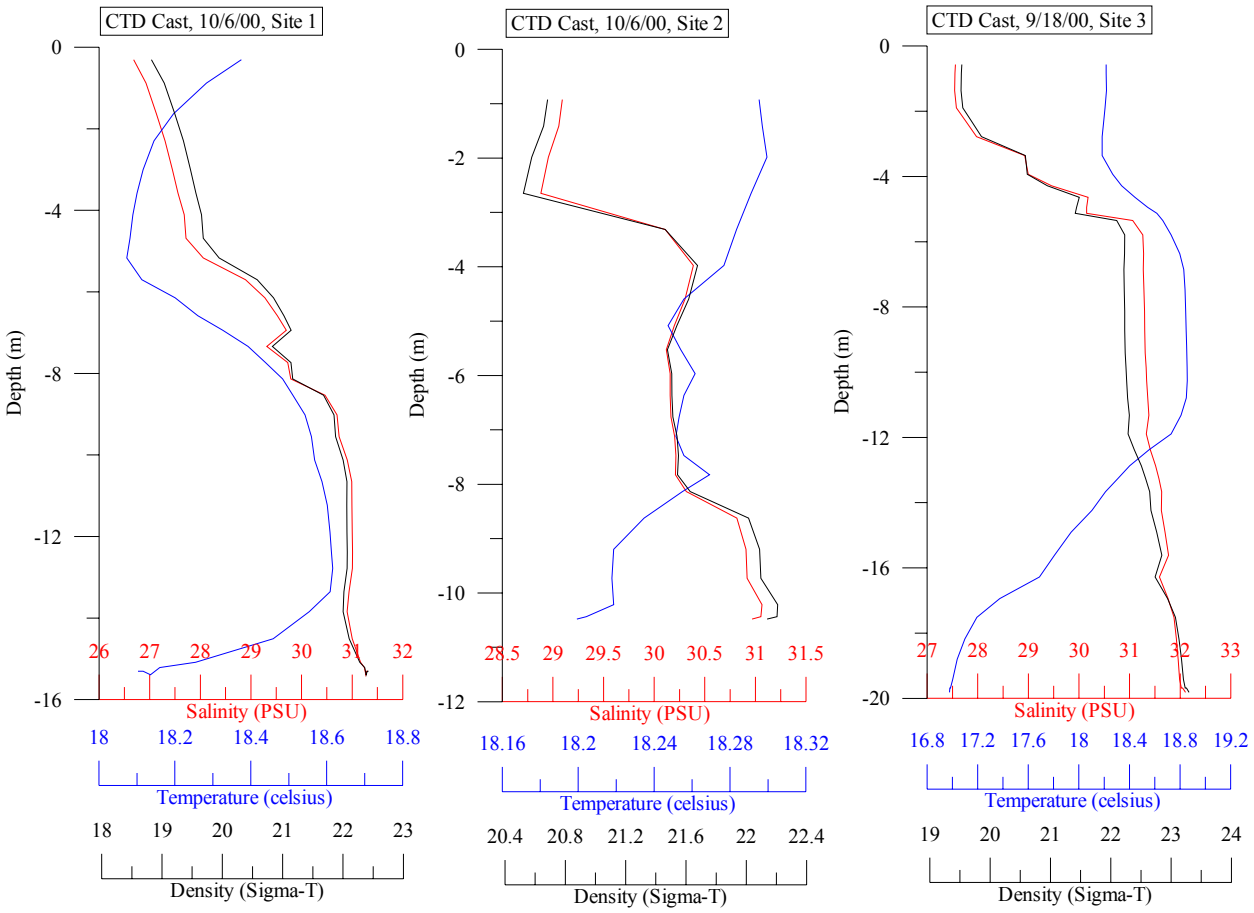

Figure 3-4. Vertical plots of CTD casts collected on 6 October 2000. Salinity is plotted in Practical Salinity Units, Temperature in Degrees Celsius, and Density in Sigma-T units.

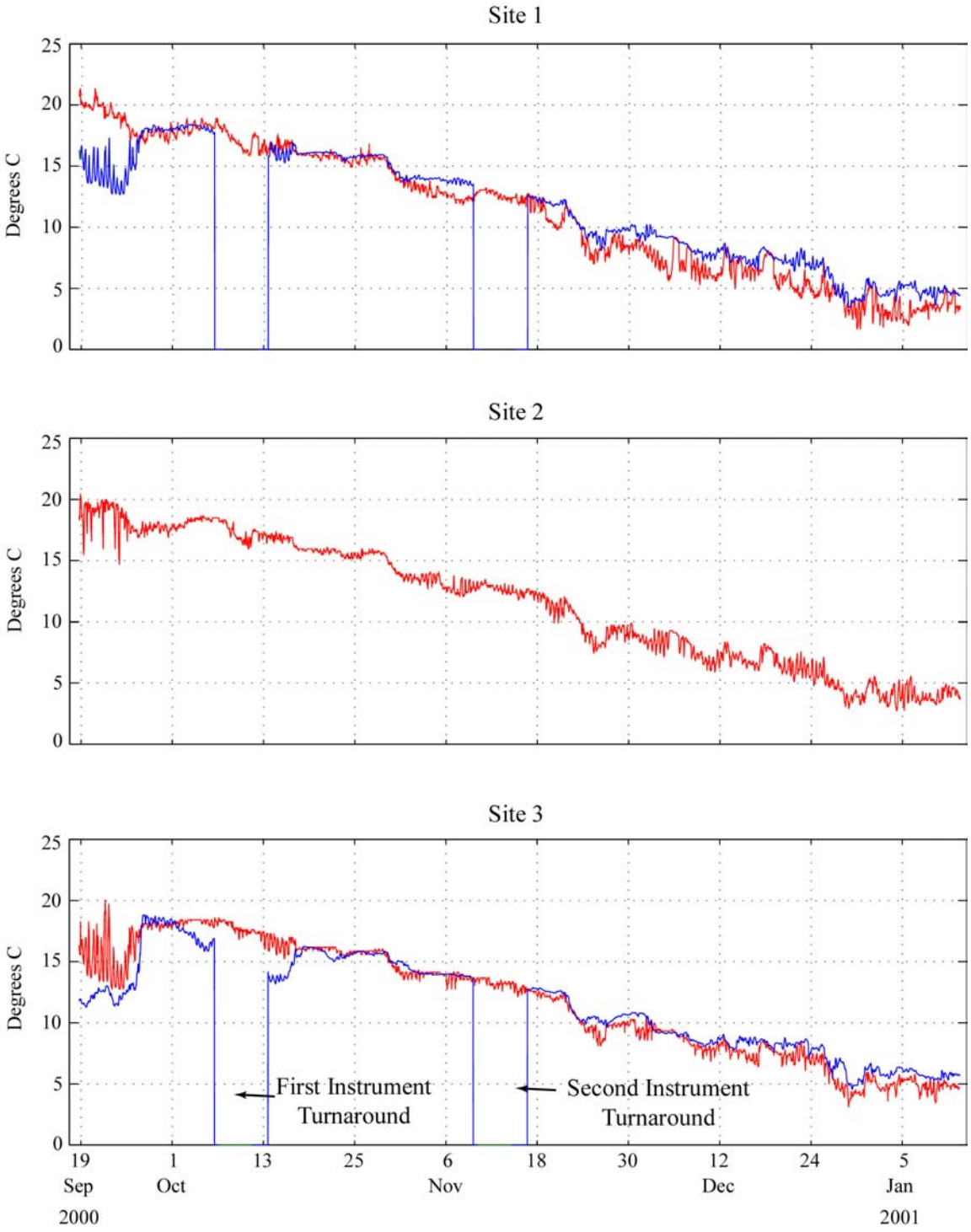

Figure 3-5. Time series of surface (red) and bottom (blue) temperature as recorded by ADCP (bottom) and Tidbit thermistors (surface) at Sites 1 and 3 for the fall/winter 2000 deployment period.

3.1.2 Time Series Observations

Meteorological, Waves, and River Flow Data

Data on wind speed and direction were obtained from the NOAA National Data Buoy Center Ambrose Light Tower station for the periods of array deployment. A pressure sensor on the Site 1 ARESS array collected 2.5 minute burst pressure data during the first two deployments; during the third deployment the pressure data was acquired at the Site 3 ARESS array. Based on the burst pressure data, significant wave height, mean period, and peak period were calculated. The significant wave height represents the average of the highest one-third of the waves observed during the period of measurement. An example of the time series of waves and winds for the winter deployment is presented in Figure 3-6 (wave and wind data from the first two deployments are presented in Figures A-1 and A-2).

In the fall, wind events over 15 m/s were rare (only two or three in the first two deployments) and subsequently, waves over 2 m were also rare (Figures A-1 and A-2). In the winter, however, there were several wind events exceeding 15 m/s, and a few above 20 m/s. Previous investigations at the HARS determined that winds out of the northeast, east, and southeast produced the greatest significant wave height and thus created the strongest wave-generated currents (SAIC 1995). During the present study, the largest wave event of the first two deployments (over 3 m, 26 to 27 September) was associated with strong winds blowing out of the north and northeast. Other wave events with wave heights exceeding 2 m were associated with winds from the east or southeast, including the event with the highest recorded waves (exceeding 4 m) at the end of November (Figure 3-6). Because of the limited fetch over water, sustained strong winds out of the west or northwest (as from 25 to 30 December) did not produce significant waves. In general, the larger wave events started with a shorter peak period than average (about 5s), and increased gradually to just above average, at about 10s.

Freshwater discharge data were tabulated from several tributaries of the lower Hudson River, in order to gauge the relative magnitude of river flow over the entire study period (Figure 3-7). While the highest discharge occurred in late winter and early spring, the spring measurement program did not coincide with an individual, localized event. Two discharge events of note occurred in mid-November and the beginning of December, but these events were not as large as those noted between the deployment periods in January and February.

Water Column Currents

The simplest means of viewing the moored current data are to plot the time series of the speed and direction with no filtering applied. This presents the actual velocities recorded and enables a direct comparison between short-term trends both vertically within the water column and horizontally between stations. The depth at ADCP Site 1 was approximately 16 m, and the depth at ADCP Site 3 (adjacent to the HARS) was approximately 21 m. For each of the two ADCP sites, time series current data were generated for the upper, middle, and lowest bins, providing good quality data. This corresponded to time-series currents from depths of 3.5 m, 8.5 m, and 13.5 m at Site 1 (Figure 3-8) and 3.5 m, 11.5 m, and 18.5 m at Site 3 (Figure 3-9).

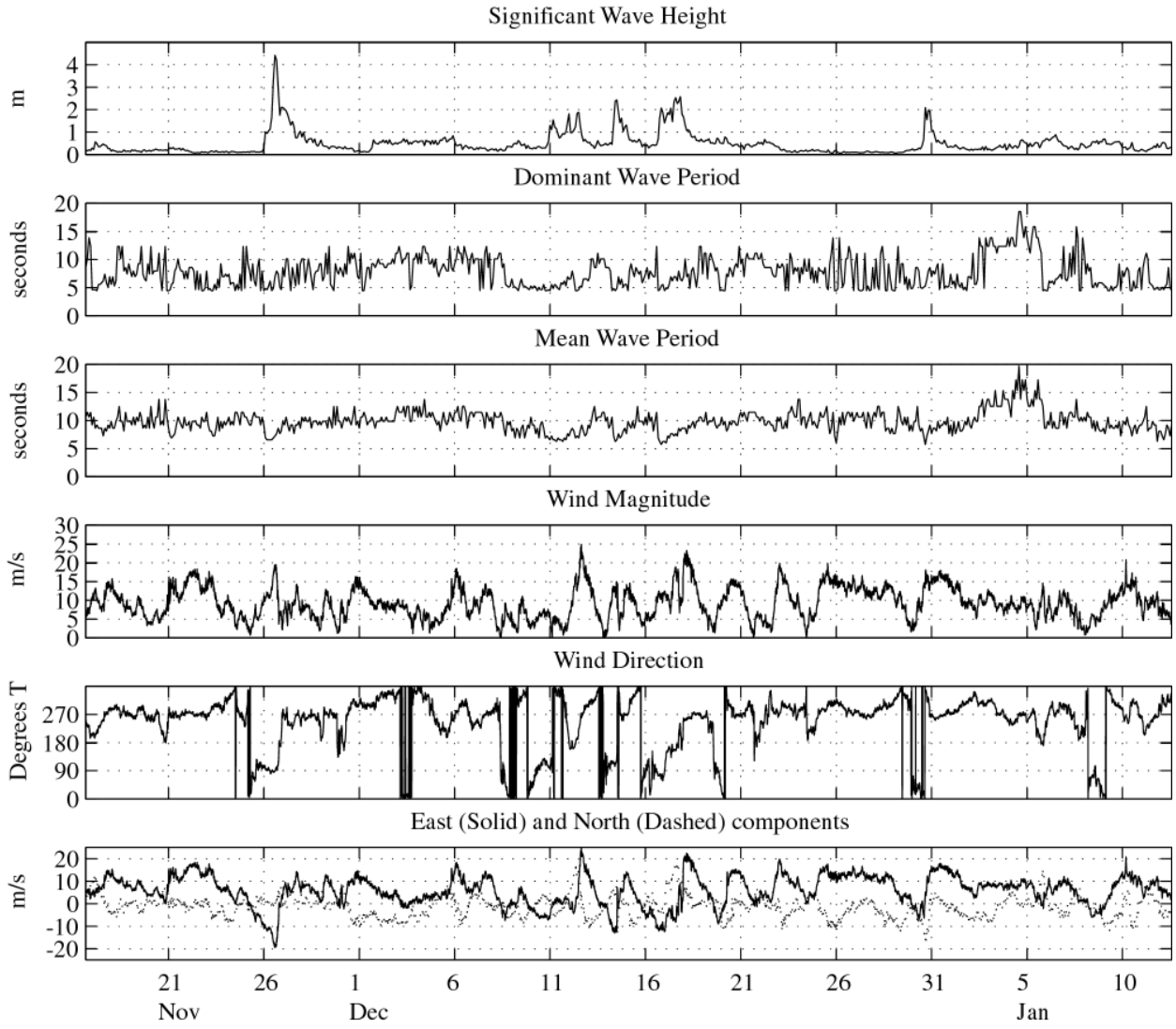

Figure 3-6. Time series of wave and wind data for Deployment 3, winter 2000–01. Wave data was derived from a bottom-mounted pressure sensor at Site 1, presented as significant wave height, and wind data was downloaded from the NOAA Ambrose Light Tower station.

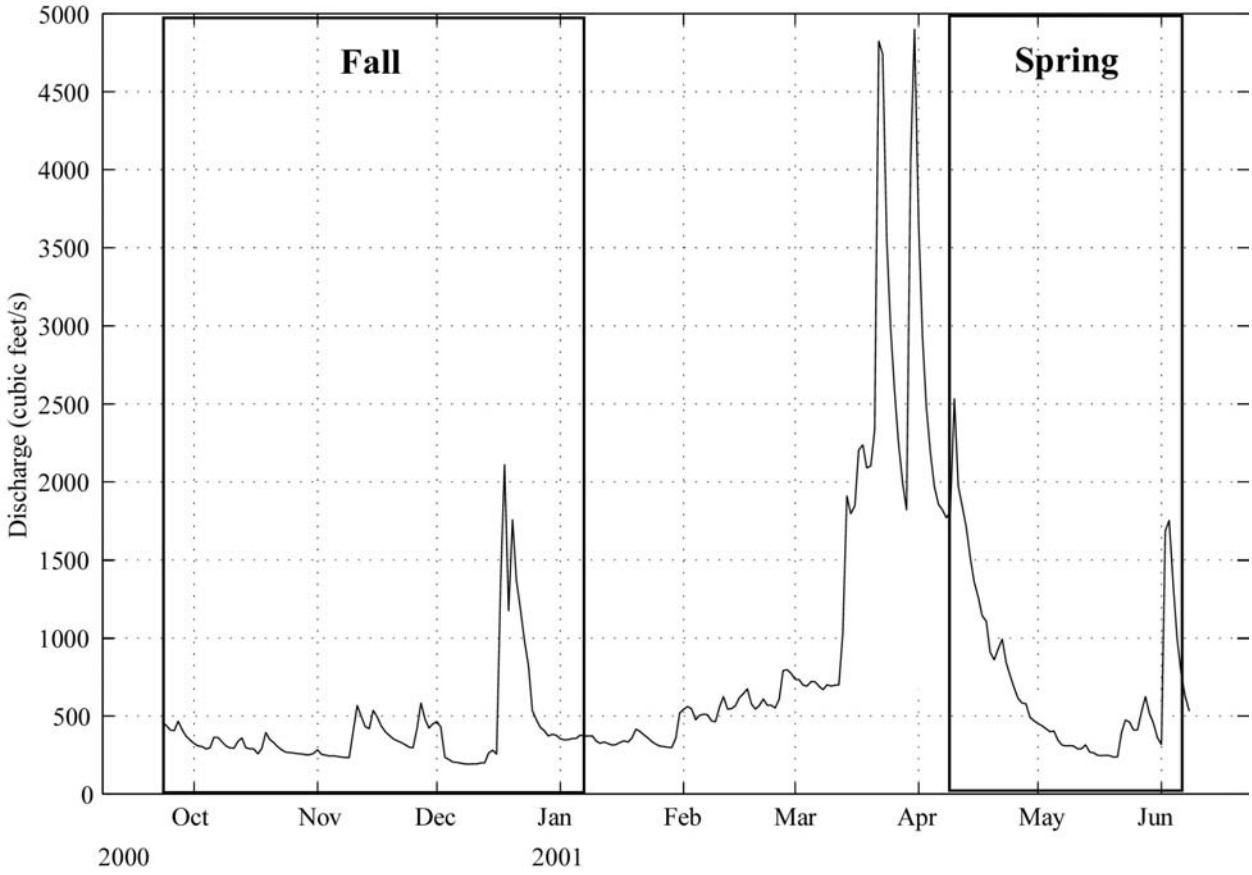

Figure 3-7. Time series of river discharge tabulated from the lower tributaries of the Hudson River over the entire study period. The two boxes delineate the fall 2000 and spring 2001 measurement program periods. Mean discharge was greater in late winter and early spring, as might be expected, however, the largest single discharge event occurred in late December 2000.

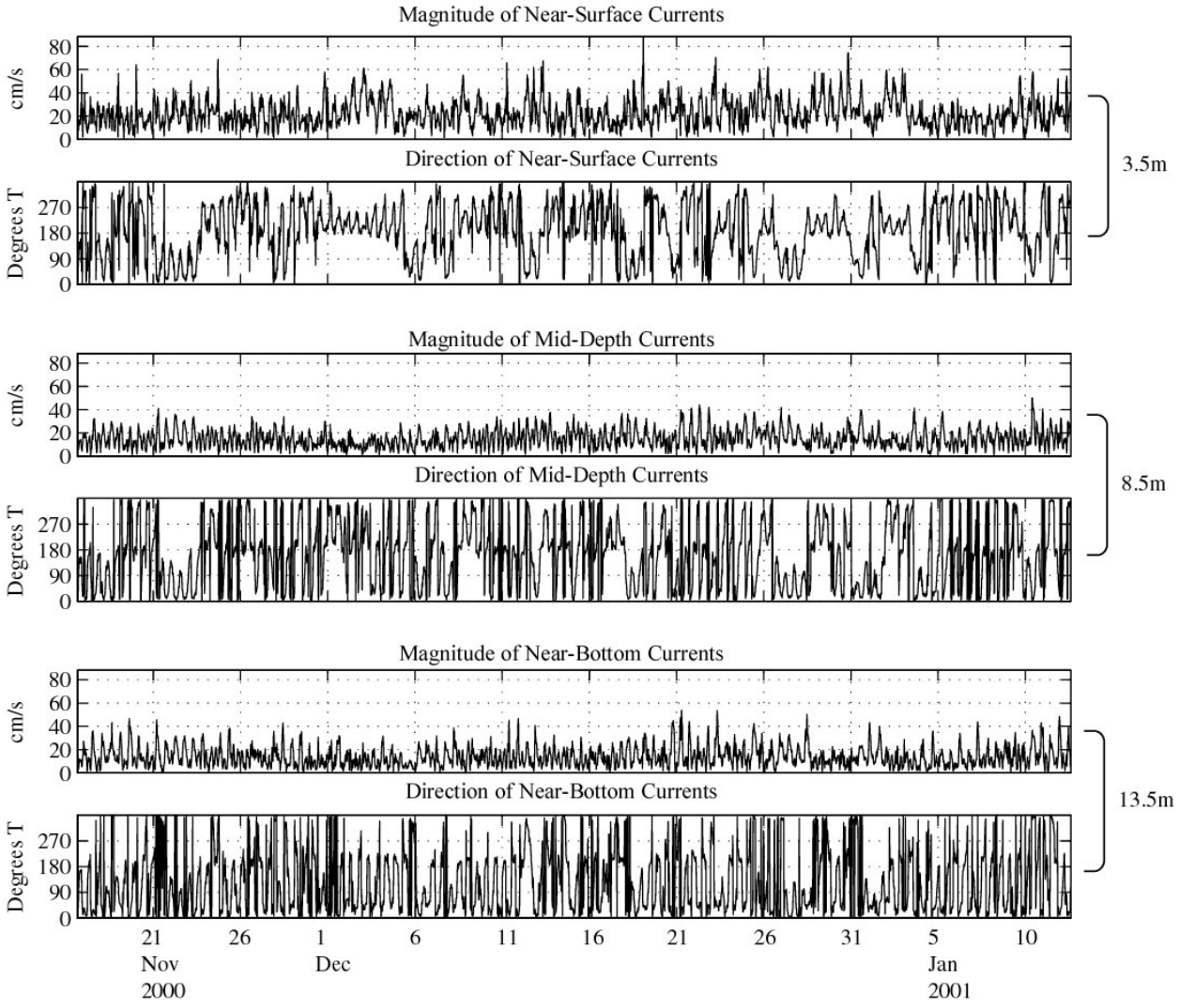

Figure 3-8. Time series of current magnitude and direction acquired by ADCP from three depth levels, Site 1, Deployment 3, winter 2000–01. Values to the right of plots indicate measurement depth.

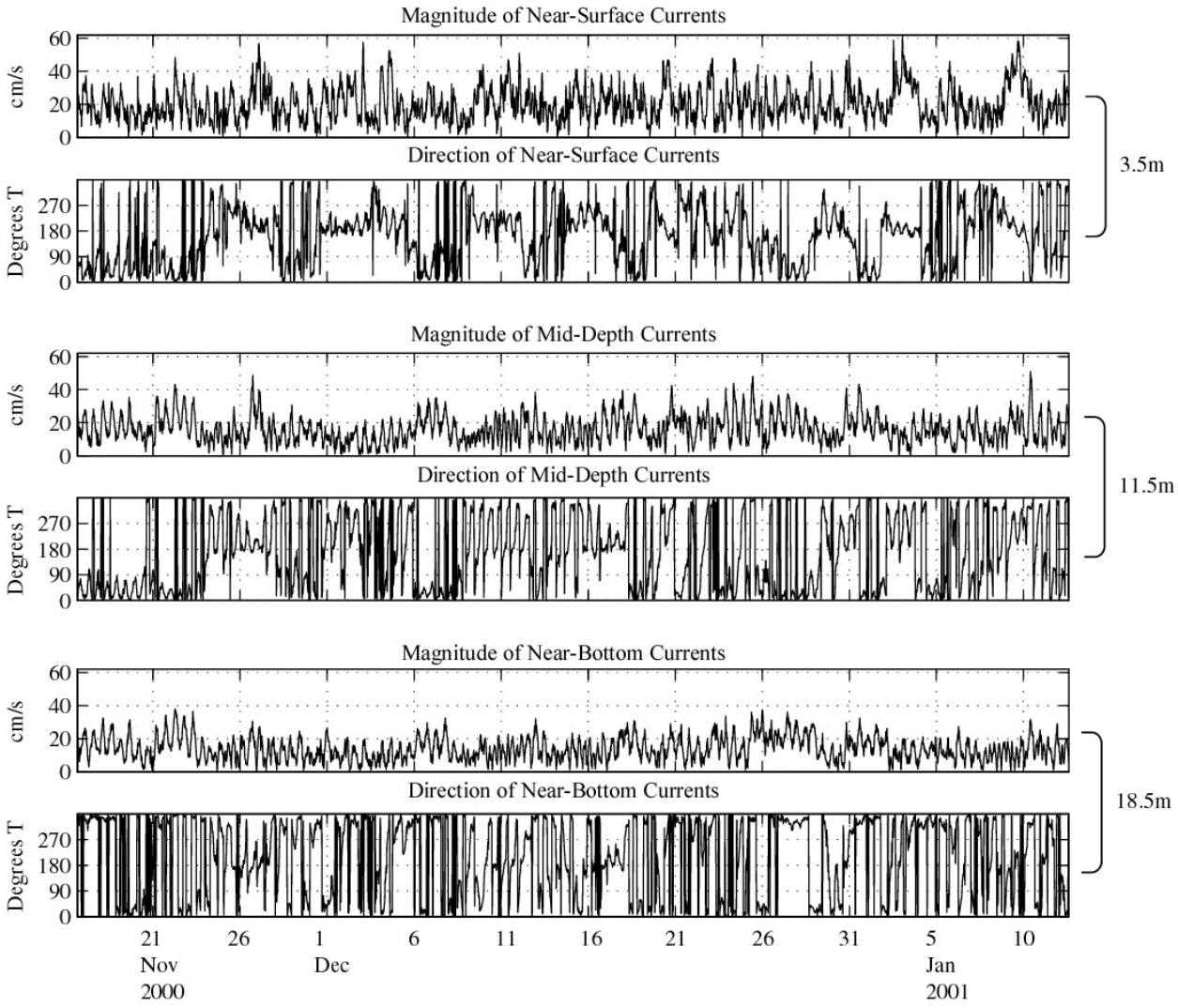

Figure 3-9. Time series of current magnitude and direction acquired by ADCP from three depth levels, Site 3, Deployment 3, winter 2000–01. Values to the right of plots indicate measurement depth.

As expected, the periodic nature of the lunar semi-diurnal tides (with a period of 12.42 hrs) was the most obvious feature in the current records from Site 1 (Figures 3-8 and A-3 – A-4). Current direction demonstrated the periodic bi-directional nature of the tides flowing either north or south, with sporadic departures from this periodicity possible for more than one day. Velocities increased into late fall and winter, on average, at all depth levels. Even more departures from the dominant semi-diurnal tides were noted in the surface layers, particularly in the winter, when a mean flow appeared to suppress the opposing flow of the tides for several days, as was noted just before and after 3 December (see upper two tiers in Figure 3-8). Velocities at mid-depth and near-bottom showed enhanced peaks at the tidal frequencies and an overall increase in average velocities in late fall and winter, as well.

Overall, the current records at Site 3, near the HARS, appeared less influenced by the semi-diurnal tide (Figures 3-9 and A-5 – A-6). Current direction was much more variable at this site, with extended mean flows noted at all depth levels, particularly those tending southward. Velocities increased into late fall and winter, with peaks in winter of approximately 55 cm/s near surface, and 50 cm/s at mid-depth. Peak velocities did not appear to change at the bottom. Near-surface direction showed the semi-diurnal tide superimposed on mean flows that persisted for several days. The lower water column also showed mean flows, but the semi-diurnal tide was more dominant.

Near-bottom Currents

As with the ADCP data, it is also enlightening to view the raw current and turbidity data recorded by the ARESS arrays as time series. Examples from the three sites during the winter deployment are plotted in Figures 3-10 to 3-12; additional plots for other deployment periods are provided in Figures A-7 through A-12. These figures provide the magnitude and direction of the currents, along with OBS data, for both of the sensor pairs on each ARESS array. Turbidity data are presented in the Formazin Turbidity Unit (FTU), a standard turbidity measure. The semi-diurnal tide was the primary component of the velocity signal in the near-bottom measurements. Peak velocities at Site 1 ranged from 15 cm/s to over 40 cm/s in the first two deployments, with a background of approximately 5 cm/s. Velocities were slightly stronger at the upper sensor, most likely due to reduced effects of seafloor bottom friction. During the third deployment (Figure 3-10) velocities were generally higher than during the prior deployments, with many more events noted above 25 cm/s, and a higher background of approximately 10 cm/s in the upper sensor.

At Site 2, closer to shore, near-bottom velocities were somewhat less than at Site 1, with peak events reaching only 12 to 25 cm/s in the upper sensor and a background less than 5 cm/s (Figure 3-11). Current direction was predominantly northwestward or southeastward, with quick transitions between the two. In addition, there were periods of consistently northwestward currents (~3 days in duration), showing almost no tidal fluctuations. Peak speeds increased in winter, with many observations above 20 cm/s at the upper level, and several in the lower level as well. Periods of elevated background as well as tidal velocities are noted in the record as on 22 November and 27 December. These low frequency events could be due to a spring-neap or monthly modulation of the semi-diurnal tide, or could simply represent stronger current flows associated with meteorological forcing. Given that these periods of elevated current correspond to periods of consistent current direction, the latter is more likely the case.

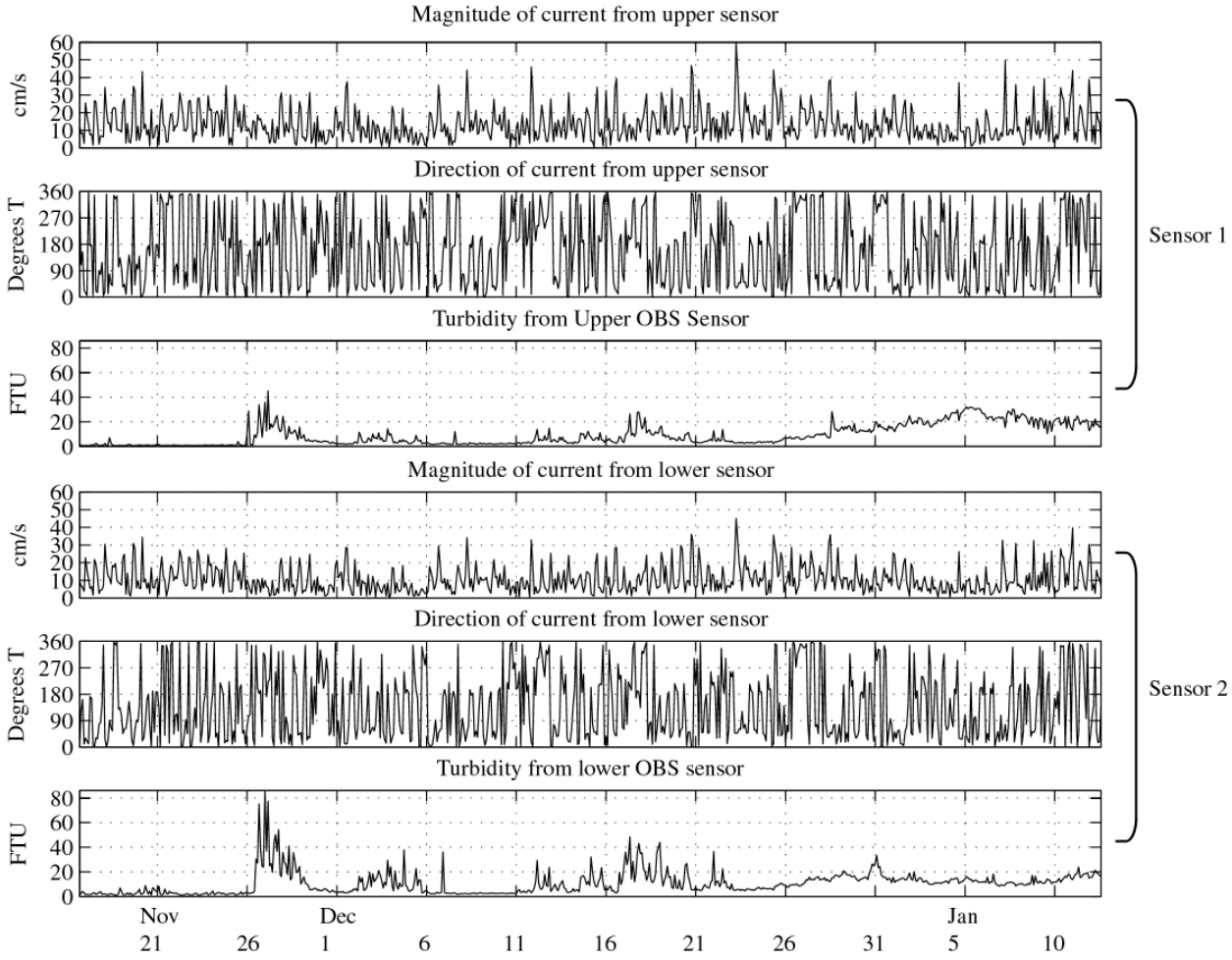

Figure 3-10. Time series of near-bottom current speed and direction, and turbidity from two depth levels; 1.52 m (Sensor 1) and 0.76 m (Sensor 2), Site 1, Deployment 3, winter 2000–01.

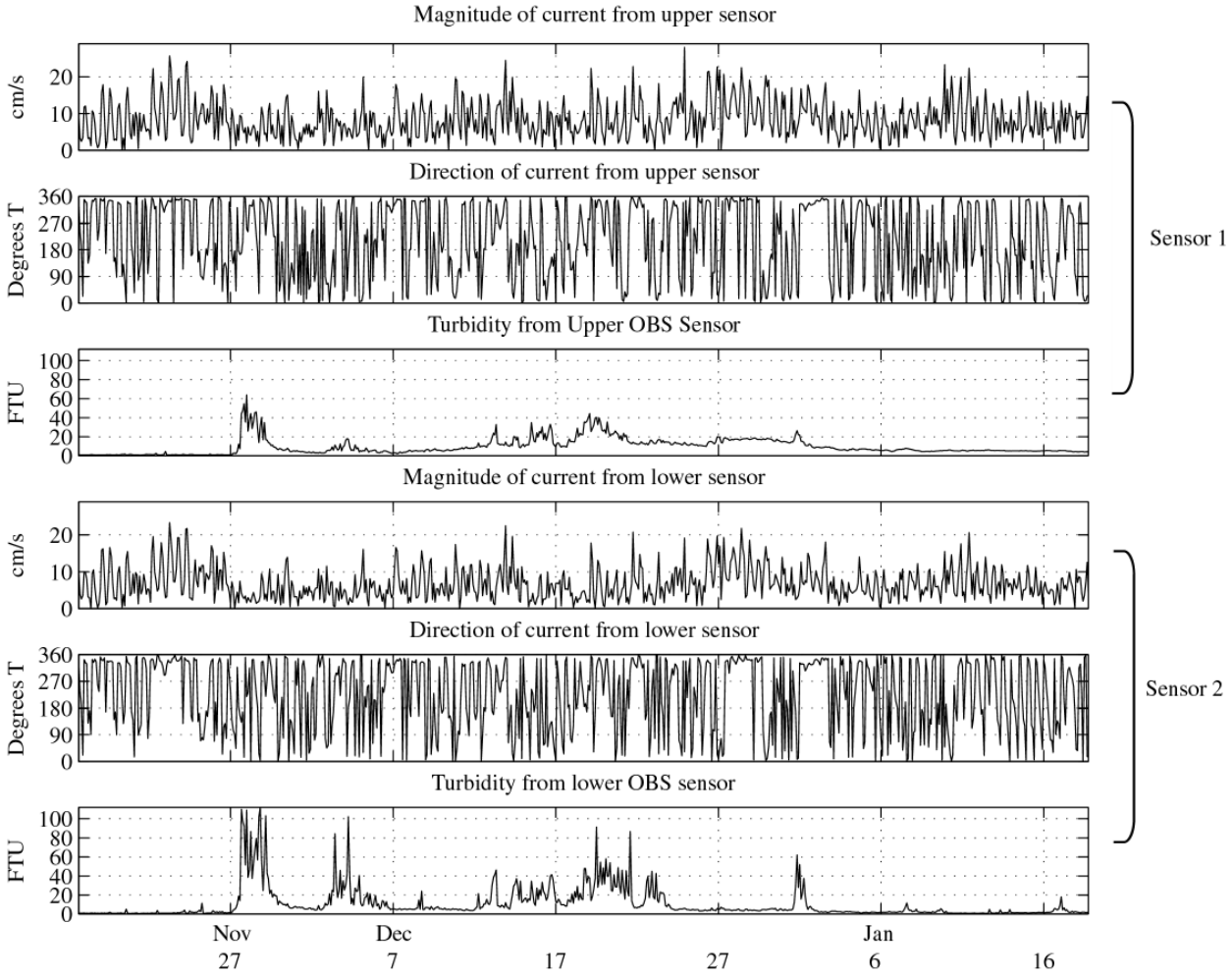

Figure 3-11. Time series of near-bottom current speed and direction, and turbidity from two depth levels; 1.52 m (Sensor 1) and 0.76 m (Sensor 2), Site 2, Deployment 3, winter 2000–01.

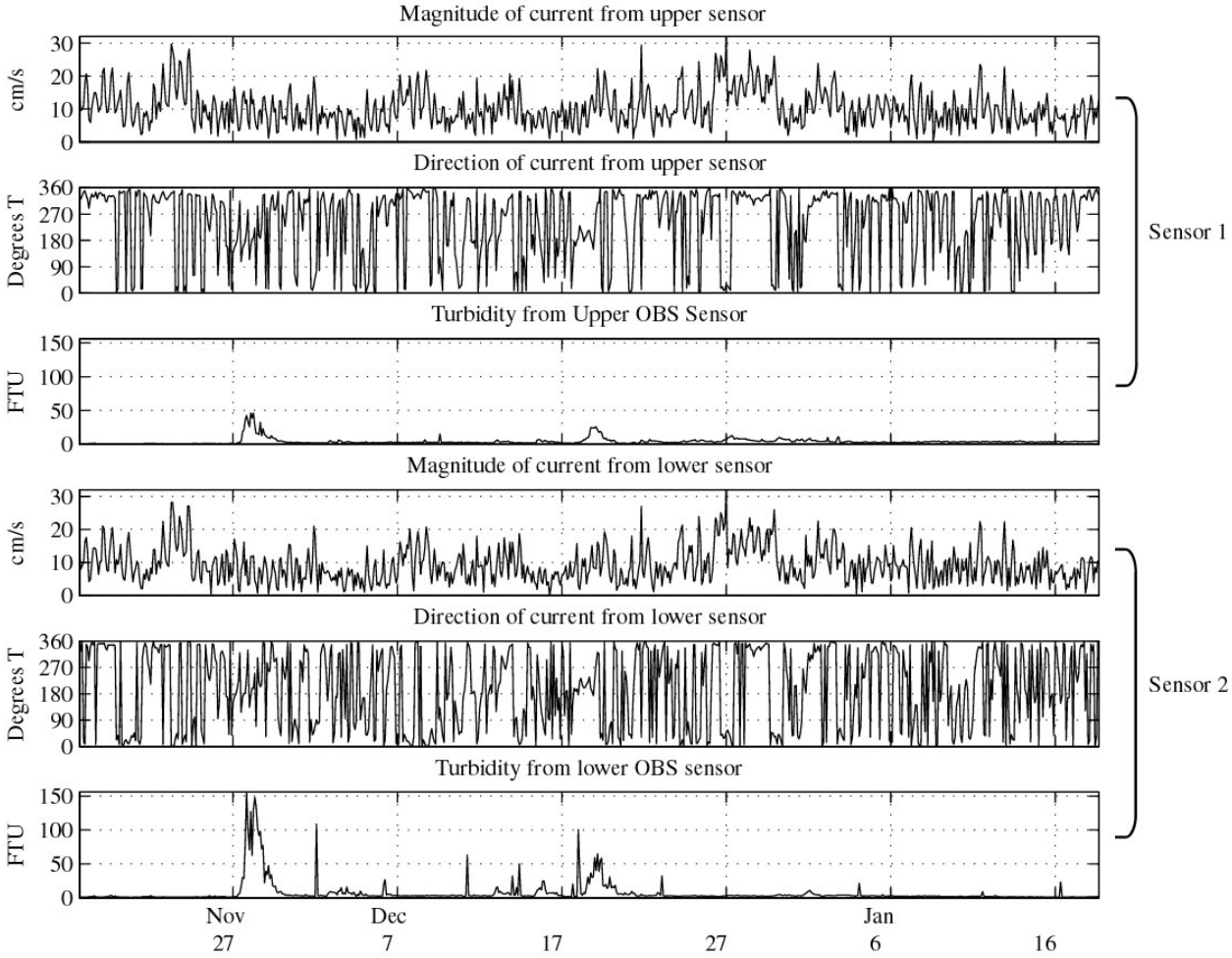

Figure 3-12. Time series of near-bottom current speed and direction, and turbidity from two depth levels; 1.52 m (Sensor 1) and 0.76 m (Sensor 2), Site 3, Deployment 3, winter 2000–01.

Similar trends are noted at Site 3, with somewhat stronger currents than Site 2, (Figure 3-12). Current direction alternated between northwestward and southeastward, with a tendency towards northern flow. As with the other sites, the winter velocities increased, with numerous observations above 25 cm/s. Longer duration velocity events were noted here as well, with events that correspond to those described for Site 2 (although somewhat stronger than at Site 2). A sensor failure was the result of a shortened current record in the first deployment at this site (Figure A-9).

Near-bottom Turbidity

Site 1 to the north showed distinct peaks in OBS readings that typically occur at both sensor levels, as well as smaller peaks that occurred at only one level. For example, a sharp peak in suspended sediment was recorded at both levels on 27 November (Figure 3-10); however, a quick increase in turbidity was recorded in the lower sensor on 31 December, which was barely noted in the upper sensor. The larger events increased turbidity to 20 FTU on average for the upper sensor (maximum of ~43) and to approximately 40 FTU for the lower sensor (maximum of ~80), with background levels less than 10 FTU for the upper sensor and less than 20 FTU for the lower sensor. Events lasted from one day to several days in either sensor. A broad period of elevated turbidity was noted during the second deployment, where levels were above 30 FTU for approximately 5 days (20 to 26 October) in the lower sensor (Figure A-8).

Higher turbidity values were recorded at Site 2, with major events showing values of up to 120 FTU in the lower sensor and less than 70 FTU in the upper sensor (Figure 3-11). Background turbidity was still low, however, typically 10 FTU or less. An anomaly was noted at the end of the first deployment (Figure A-9), with a monotonic increase at the lower sensor, from 30 FTU to >150 FTU. This was most likely due to sensor fouling by organisms growing on the sensor face. A similar trend was noted in the lower sensor in the second deployment as well, however, the values only reached 40 FTU (Figure A-10). Events typically lasted one day or less at this location and were represented in both sensors.

Greater variability was noted at Site 3, with low background levels (below 10 FTU for both sensors) and high peaks, with a maximum of 50 FTU for upper sensor and ~150 FTU for lower sensor (Figure 3-11). Several sharp peaks were recorded during the first deployment in the upper sensor (70-130 FTU), which corresponded to broader peaks (30-50 FTU) in the lower sensor (Figure A-11). Significant events typically lasted for a day or less.

3.1.3 Long-Term Mean and Statistics

To obtain information on the potential for long-term transport of material into and out of a particular site, it is instructive to examine the velocity records in the context of long period changes. Statistics of the current observations were calculated for the entire record of each individual deployment to obtain an understanding of changes on a monthly basis, and subsequent deployments were then compared to gain insight on seasonal changes.

Three methods of examining the current record mean were employed:

- The first method consisted of calculating a mean of the U and V components for the entire deployment, and then constructing a record mean vector of magnitude and direction. These vector mean values represented the theoretical direction and the rate at which a suspended particle would drift over the cumulative period of the entire instrument deployment.

- The second method consisted of calculating the vector magnitude for each observation, and then computing a mean speed from these values. This scalar quantity represented the speed that might be encountered at a given depth level at any point in time, independent of current direction. It is important to note that the scalar mean speeds are always higher than vector means because the current magnitude is always assigned a positive value. For the vector means, the north-south and east-west components have opposing signs and will tend to cancel each other out over time.

- The third method of examining current means entailed the creation of compass rose histograms that provided the relative current magnitudes through 15^{o} direction bands around the compass. In addition, some basic statistics on the current observations were computed and presented in tabular form. The results are presented first for the ADCP data and then for the bottom-mounted ARESS arrays.

Water Column Current Statistics—Vertical Means

Examples of the vertical profiles of mean vector magnitude, mean speed, and mean direction for the winter deployment at Sites 1 and 3 are presented in Figure 3-13. Means and maxima as well as statistics on the percentage of observations in certain velocity ranges for Sites 1 and 3 are provided in Tables 3-1 and 3-2, respectively. At Site 1, the vertical structure of current velocity showed a noticeable difference between surface and bottom for each deployment. In the early fall (Deployment 1), mean vector magnitudes were stronger near the surface, dropping to below 1 cm/s at a mid-depth of approximately 7.5 m, and increasing again to approximately 3.5 cm/s near bottom (Figure A-13). Current direction showed southwestward trends in the surface layers, with a sudden shift at 7.5 m depth to northeastward flow in the bottom layers. The same structure was noted in fall and winter, with magnitudes increasing in both surface and bottom in the fall (Deployment 2). In the winter, magnitudes continued to increase near the bottom and decrease slightly near the surface (Figure 3-13).

Offshore at Site 3 in September, mean vector magnitudes were low, from below 1 cm/s to 7 cm/s, showing a peak at mid-depth. This was the only site and deployment in which mean direction was consistent in one direction throughout the water column. Mean magnitude decreased at mid-depth and increased in the surface layers into the late fall, while direction shifted to southwest in the surface, rotating clockwise through west to northwest at depth. The winter deployment showed increased separation between surface and bottom, with bottom magnitudes increasing to 8 cm/s, and magnitude decreasing to 1 cm/s at 6 m depth (Figure 3-13).

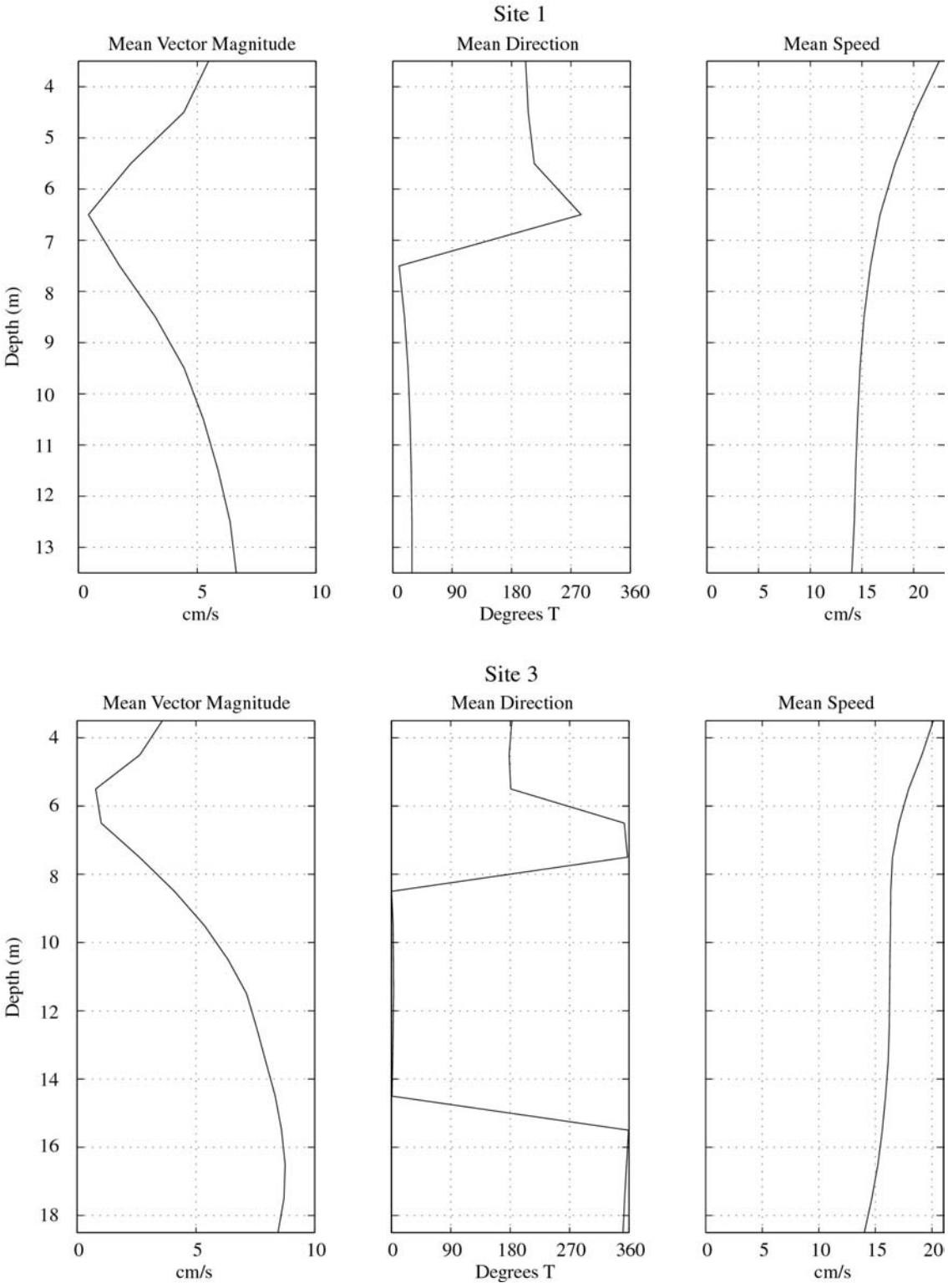

Figure 3-13. Vertical profiles of mean vector magnitude and direction, and mean speed from ADCP data at Sites 1 and 3, Deployment 3, winter 2000–01.

Table 3-1.

Statistics of ADCP data collected at Site 1 during the fall/winter 2000 deployment period. Note: an asterisk denotes an observed maximum speed for which there were not enough observations to represent in the statistics at that speed level)

Deployment Number and dates	Depth Level (m)	Mean Vector Magnitude (cm/s)	Mean Direction	Mean Speed (cm/s)	Max Speed (cm/s)	Percentage of Observations in Speed ranges below								
						0-10	10-20	20-30	30-40	40-50	50-60	60-70	70-80	80-90
ONE 9/18/2000 to 10/6/2000	3.5	8.8	240.1	19.1	54.6	17.8	41.4	26.1	11.0	3.5	0.2	0.0	0.0	0.0
	8.5	1.5	4.2	15.6	47.2	26.7	48.0	19.9	4.5	0.8	0.0	0.0	0.0	0.0
	13.5	4.1	32.8	12.8	44.6	43.8	41.0	10.0	4.1	1.0	0.0	0.0	0.0	0.0
TWO 10/13/2000 to 11/9/2000	3.5	10	214.8	19.4	65.3	20.4	37.0	26.5	11.3	3.2	1.2	0.2	0.0	0.0
	8.5	1.5	234.8	14.1	41.5	31.9	48.5	16.0	3.2	0.3	0.0	0.0	0.0	0.0
	13.5	5.0	12.2	13.4	46.3	42.3	39.0	11.9	6.0	0.8	0.0	0.0	0.0	0.0
THREE 11/16/2000 to 1/12/2001	3.5	5.5	201.5	22.5	88.3	13.4	34.0	29.7	14.3	5.3	2.6	0.5	0.1	0.0
	8.5	3.2	17.9	15.2	50.1*	28.1	46.7	20.3	4.2	0.6	0.0*	0.0	0.0	0.0
	13.5	6.6	29.2	14	53.7	38.2	40.8	14.9	5.0	1.0	0.1	0.0	0.0	0.0

Table 3-2.

Statistics of ADCP data collected at Site 3 during the fall/winter 2000 deployment period. Note: an asterisk denotes an observed maximum speed for which there were not enough observations to represent in the statistics at that speed level)

Deployment Number and dates	Depth Level (m)	Mean Vector Magnitude (cm/s)	Mean Direction	Mean Speed (cm/s)	Max Speed (cm/s)	Percentage of Observations in Speed ranges below								
						0-10	10-20	20-30	30-40	40-50	50-60	60-70	70-80	80-90
ONE 9/18/2000 to 10/6/2000	3.5	5.6	336.1	20.4	74.1	19.8	35.3	27.6	10.3	3.7	2.1	1.0	0.1	0.0
	11.5	6.7	20.2	15.1	43	29.1	45.3	19.0	6.1	0.5	0.0	0.0	0.0	0.0
	18.5	0.5	325.1	10.7	33.4	52.0	41.0	6.1	0.9	0.0	0.0	0.0	0.0	0.0
TWO 10/13/2000 to 11/9/2000	3.5	9.6	217.4	20.8	81.5	16.9	36.2	28.0	14.0	3.3	0.9	0.1	0.5	0.1
	11.5	2.9	313.6	13.6	53.3	35.4	46.2	15.3	2.4	0.5	0.2	0.0	0.0	0.0
	18.5	3.8	354.7	11.2	32.9	46.7	45.0	7.9	0.5	0.0	0.0	0.0	0.0	0.0
THREE 11/16/2000 to 1/17/2001	3.5	3.6	182.6	20.1	62*	16.4	39.8	26.2	13.0	3.8	0.7	0.0*	0.0	0.0
	11.5	7.1	3.5	16.2	51.1*	24.9	45.5	22.5	6.1	1.0	0.0*	0.0	0.0	0.0
	18.5	8.5	350.9	14	37.8	32.4	47.4	18.2	2.0	0.0	0.0	0.0	0.0	0.0

Thus, as the seasons progressed from fall to winter, the water column offshore that appeared to act as a whole in early fall demonstrated more distinct flow characteristics in winter months.

As mentioned previously, mean speeds were higher than mean vector magnitudes, as they did not take into account the direction of the current, only the absolute magnitude. Site 1 showed mean speeds higher in the surface layers than at depth for all three seasons, ranging from ~20 cm/s near surface to 13 cm/s at depth, which increased slightly into the winter (Table 3-1). Maximum velocities steadily increased at the near-surface from early fall into winter, with the highest recorded velocity of 88.3 cm/s in the winter (Deployment 3). Mid-depth maxima varied from season to season, with a maximum of ~50 cm/s recorded in the winter (Deployment 3), but only 41.5 cm/s in fall (Deployment 2). Near-bottom maximum velocities were more similar from season to season, with the highest velocity recorded in winter at ~54 cm/s.

Similar observations were made offshore at Site 3, with near-surface mean speeds relatively consistent at approximately 20 cm/s from late summer into winter, and bottom velocities increasing from ~11 cm/s to 14 cm/s. Maximum velocities at the near-surface were quite variable from one deployment to the next, with the highest recorded velocity of 81.5 cm/s occurring in fall (Deployment 2). Mid-depth maxima showed less variability, with highest velocities in the fall of 53.3 cm/s. Near-bottom maxima increased into the winter to 37.8 cm/s, exhibiting the least inter-seasonal variability.

Water Column Current Histograms

In addition to examining means and maxima, it is useful to examine the currents in terms of frequency of observations within velocity bands (Tables 3-1 and 3-2 for Sites 1 and 3, respectively). In general, at the near-surface and mid-depth levels at Site 1 (over all three deployments), the highest frequency of measurements occurred in the 10-20 cm/s range. The next highest percentage was in the 20-30 cm/s range for near-surface, but in the 0-10 cm/s range for mid-depth. At near-bottom levels, frequencies were almost evenly distributed between the 0–10 cm/s and 10-20 cm/s range. At mid-depth and bottom levels, less than one percent of the observations were above 40 cm/s, whereas approximately 3 to 9 percent of the near-surface velocities were above this range. In general, the winter deployment exhibited higher percentages in the higher velocity ranges. Results from Site 3 were very similar, except that near-bottom winter currents showed higher percentages in the higher velocity ranges.

Plotting the direction data in terms of the number of observations per 15-degree band on a compass rose for an entire deployment revealed departures from the vector mean direction. The results for each deployment at both sites equipped with an ADCP for surface, mid-depth, and near-bottom are plotted in Figures 3-14 and 3-15. Similar trends were noted between seasons at Site 1 (Figure 3-14). Near-surface measurements showed the most scatter, with a near equal number of measurements of direction recorded from northwest to south. During the second fall deployment, southward near-surface currents were most prevalent, and during the winter the near-surface current direction was more scattered. Mid-depth and near-bottom currents showed a more north-south bi-directional nature in each season. At mid-depth, the prevalent direction shifted from more northward during the first deployment to southward in the

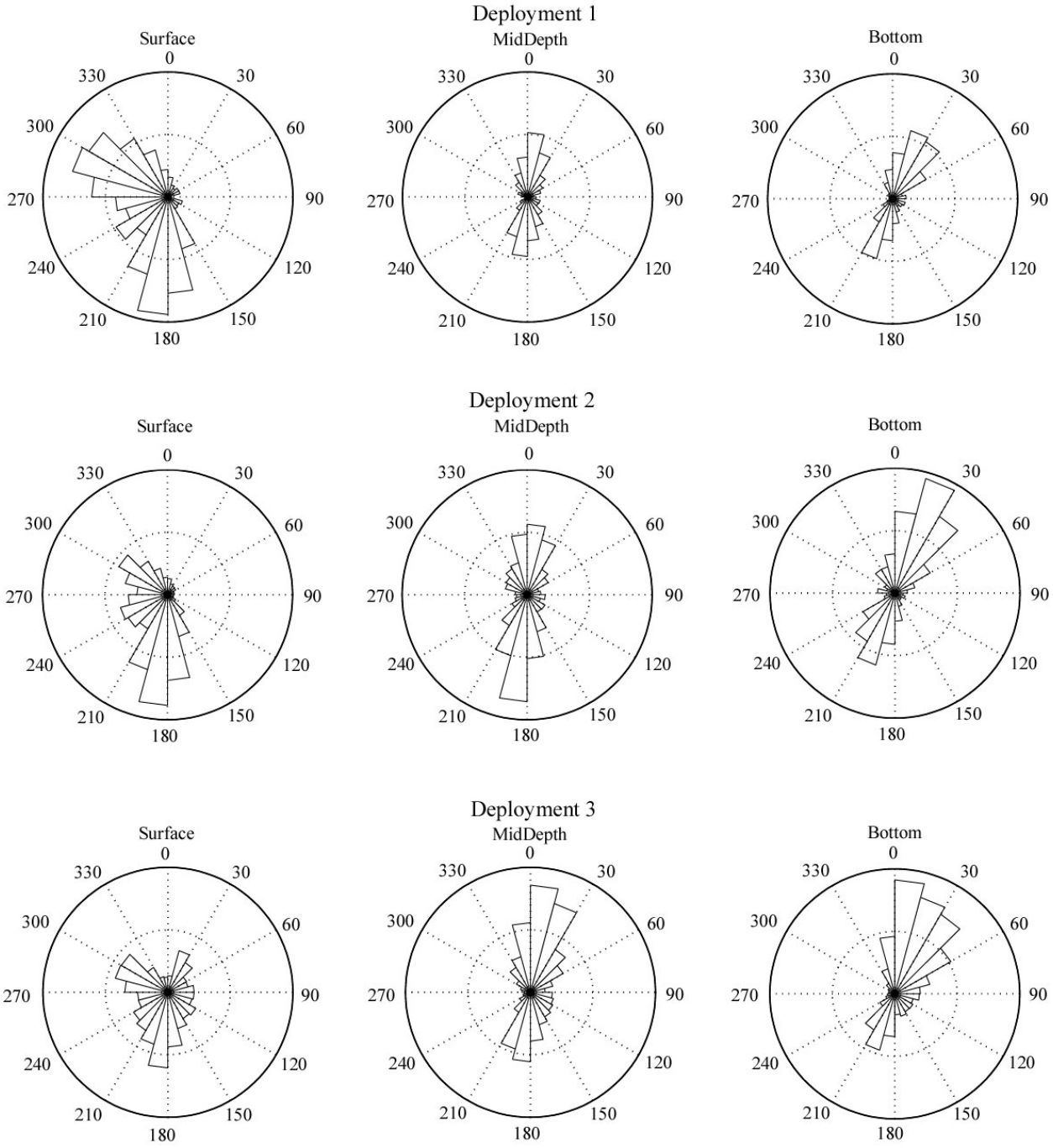

Figure 3-14. Rose histograms of current meter data from ADCP at three depth levels for fall/winter 2000 deployment period at Site 1.

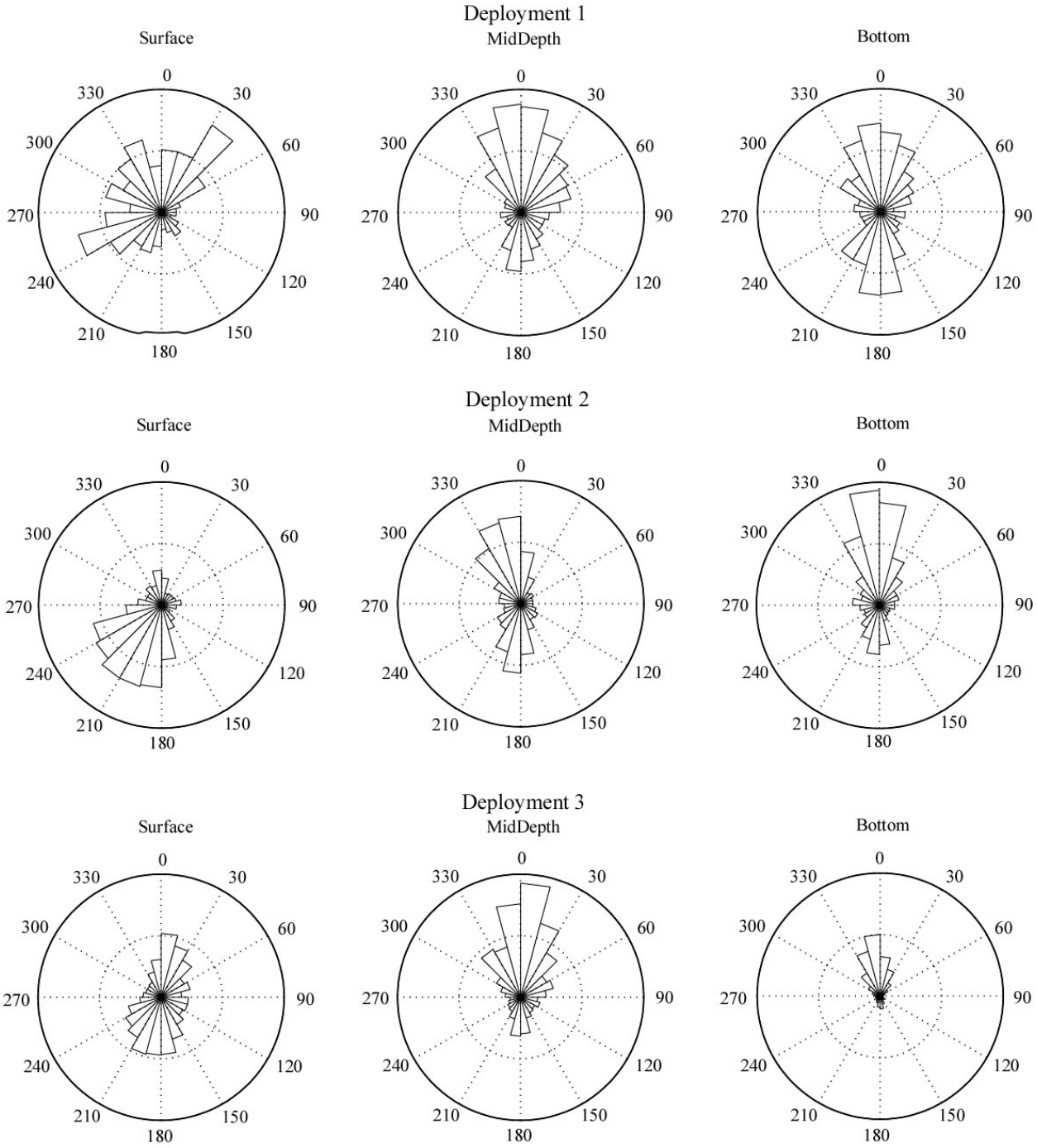

Figure 3-15. Rose histograms of current meter data from ADCP at three depth levels for fall/winter 2000 deployment period at Site 3.

second deployment, and back to northward in the third. At the near-bottom level, the prevalent direction was north-northeastward in fall and shifted to more northward in the winter.

Similar trends were noted at Site 3 (Figure 3-15), with some differences. Near-surface current direction showed more scatter in early fall than late fall or winter, in contrast to Site 1. The fall data indicated that southwestward near-surface currents were most prevalent, whereas winter showed more of a bi-directional nature between northward and southward. Mid-depth currents showed bi-directional structure as well, though there was a noticeable prevalence of northward flow. Near-bottom currents exhibited an even stronger tendency toward northward flow than the upper water column currents, particularly during the second and third deployments.

Near-bottom Current Statistics—Means

Near-bottom water velocities in the north-south and east-west directions were recorded by the ARESS arrays at each site at two levels—30 inches (0.76 m) and 60 inches (1.52 m) off the seafloor. Statistics of the velocity data for each deployment are listed in Tables 3-3, 3-4, and 3-5 for Sites 1, 2, and 3, respectively. The mean vector magnitude at Site 1 was fairly weak, around 5 cm/s at the upper sensor and 4 cm/s at the lower sensor in fall, increasing to 7 cm/s for the upper sensor and 6 cm/s for the lower sensor in winter; the direction was predominantly to the north for all of the deployments. Maximum speeds of 32 cm/s and 27 cm/s in the fall increased to 60 cm/s and 45 cm/s in the winter for the upper and lower sensors, respectively.

Mean vector magnitudes at Site 2 were quite low in the fall (from 1-2 cm/s at each sensor), but picked up in early winter (~5 cm/s and ~4 cm/s at the upper and lower levels respectively). Mean direction was to the northeast in early fall, shifting to the northwest in late fall/winter. Maximum speeds of about 25 cm/s and 21 cm/s in the upper and lower sensors, respectively, did not change significantly from fall to winter.

Site 3 showed mean vector magnitudes closer to those of Site 2, with values for the upper and lower sensors of about 2.5 cm/s and 1.5 cm/s in the fall, which increased to approximately 6 cm/s and 5 cm/s in the winter. Mean directions shifted from southeast in early fall to north-northwest in late fall and winter. Maximum speeds increased from ~25 cm/s to ~32 cm/s in the upper sensor and from ~18 cm/s to 32 cm/s in the lower sensor from the fall to the winter.

Near-bottom Current Histograms

Statistics on the percentage of values recorded within a velocity range for each instrument at each site are shown in Tables 3-3, 3-4, and 3-5. Velocities were predominantly below 10 cm/s (above 50% in all cases), and some site-to-site variability was noted in the percentage of observations in higher ranges. Site 1 showed more observations above 30 cm/s than either of the other sites. Site 2 showed the lowest current magnitudes, with less than one percent of observations above 20 cm/s on average, and the highest percentage of observations below 10 cm/s. In comparing differences between sensor readings at each site, the least variability between velocity ranges existed at Site 1 and the most variability existed at Site 3. In terms of temporal variability, all three stations showed higher percentages in the upper velocities ranges in winter than in fall. For example, the lower sensor at Station 3 showed less than 0.3 percent of the observations above 20 cm/s for the fall, but over 5 percent for the same sensor and

Table 3-3.
Statistics of near-bottom currents as recorded by ARESS at Site 1 during the fall/winter 2000 deployment period

Deployment Number and dates	Sensor Level (cm)	Mean Vector Magnitude (cm/s)	Mean Direction	Mean Speed (cm/s)	Max Speed (cm/s)	Percentage of Observations in Speed ranges					
						0-10	10-20	20-30	30-40	40-50	50-60
ONE 9/18-10/6/2000	152	3.8	348.8	10.4	31.9	54.7	36.0	7.9	1.4	0.0	0.0
	76	2.8	339.6	8.6	27.2	66.8	26.2	7.0	0.0	0.0	0.0
TWO 10/13-11/9/2000	152	4.9	350.6	10.4	39.2	58.8	30.1	7.7	3.4	0.0	0.0
	76	5.5	339.6	9.7	37.7	63.4	25.0	9.5	2.1	0.0	0.0
THREE 11/16/2000 - 1/17/2001	152	6.7	16.1	13.2	59.5	44.6	35.7	13.0	5.3	1.3	0.1
	76	5.7	29.8	10.5	45.1	58.9	28.4	10.2	2.4	0.1	0.0

Table 3-4.
Statistics of near-bottom currents as recorded by ARESS at Site 2 during the fall/winter 2000 deployment period

Deployment Number and dates	Sensor Level (cm)	Mean Vector Magnitude (cm/s)	Mean Direction	Mean Speed (cm/s)	Max Speed (cm/s)	Percentage of Observations in Speed ranges					
						0-10	10-20	20-30	30-40	40-50	50-60
ONE 9/18-10/6/2000	152	1.1	38.6	6.8	25.6	78.0	21.0	1.0	0.0	0.0	0.0
	76	0.7	9.7	5.1	20.9	89.7	9.8	0.5	0.0	0.0	0.0
TWO 10/13-11/9/2000	152	1.3	334.7	7.3	19	76.3	23.7	0.0	0.0	0.0	0.0
	76	1.9	4.7	6.6	19.9	78.4	21.6	0.0	0.0	0.0	0.0
THREE 11/16/2000 - 1/17/2001	152	4.6	358.1	8.3	28	68.4	29.1	2.5	0.0	0.0	0.0
	76	3.7	349.3	6.7	23.4	79.3	19.7	1.0	0.0	0.0	0.0

Table 3-5.

Statistics of near-bottom currents as recorded by ARESS at Site 3 during the fall/winter 2000 deployment period

Deployment Number and dates	Sensor Level (cm)	Mean Vector Magnitude (cm/s)	Mean Direction	Mean Speed (cm/s)	Max Speed (cm/s)	Percentage of Observations in Speed ranges					
						0-10	10-20	20-30	30-40	40-50	50-60
ONE 9/18-10/6/2000	152	1.0	141.6	9.1	24.7	62.5	32.9	4.6	0.0	0.0	0.0
	76	1.3	140.8	6.5	17.6	82.9	17.1	0.0	0.0	0.0	0.0
TWO 10/13-11/9/2000	152	2.6	339.7	9.3	28	61.7	34.9	3.4	0.0	0.0	0.0
	76	1.5	333.4	6.3	22.1	84.9	14.8	0.3	0.0	0.0	0.0
THREE 11/16/2000 - 1/17/2001	152	6.7	337.0	10.2	31.9	55.2	38.0	6.7	0.1	0.0	0.0
	76	5.4	358.1	9.3	32	61.5	33.3	5.1	0.1	0.0	0.0

range in the winter. Similarly, the percentage of observations for this sensor in the 10-20 cm/s range was twice as high in the winter than in the fall. Rose histograms of velocity measurements for the bottom sensor at each site for all three deployments are presented in Figure 3-16. At Site 1, a north-northwest trend at the bottom sensor through the fall shifted to a more northeastward trend in the winter. Site 2, closer to shore, showed more variability in the fall than other sites, with more observations in the east and west bands. However, a significant shift to predominantly northward currents was noted in the winter. Site 3 showed predominantly southward currents in early fall, with a few observations noted in the eastward and westward directions. By late fall, the prevalent current direction shifted toward a north-northwest direction that continued through the winter deployment period.

3.1.4 Event-Based Processes

In order to examine sub-tidal changes, a 30-hr LPF was applied to the U and V current components to remove any changes in the record that took place on timescales shorter than 30 hrs. A filtered vector magnitude and direction was calculated for each observation and then depicted as a vector plot. The vector plots provide a view of the temporal variability within the dataset without the dominant tidal signal. In particular, major flow events could be examined in terms of relative magnitude, direction, and duration. It should be kept in mind that the absolute magnitude of the current flow has been averaged in the filtering process, and therefore the raw time series plots should be referred to for the true velocity magnitude (including tides and high-frequency processes) at a specific time.

Water Column Low-Pass Filtered Currents

Vector plots for the winter deployment at Sites 1 and 3 are presented in Figures 3-17 and 3-18; as with the mean velocity analysis, three depth levels were chosen for the vector plot analysis (3.5, 8.5, and 13.5 m depths for Site 1 and 3.5, 11.5, and 18.5 m depths for Site 3). Each stick on the vector plot represents one vector-averaged, two-hour measurement. The most noticeable feature detected on the Site 1 vector plots was the predominant north-south nature of the currents. Interestingly, near-surface and near-bottom events often demonstrated opposing flow, with primarily southward flow near surface and northward flow at depth. Also, events were typically considerably stronger at the near-surface. This trend continued into late fall and winter with a greater frequency of strong-current events. Mid-depth currents showed both northward and southward events, with a tendency towards northward flow. The magnitude of events increased in winter, and direction was more sporadic at near-surface, occurring in almost any direction (Figure 3-17). Mid-depth and near-bottom current events were primarily north to northeastward, with one or two events directed southwestward.

Similar results were obtained from Site 3 offshore, with some notable differences. In late summer and early fall, vertical structure tended to be more coherent, with strong events typically following similar patterns from surface to bottom. Strong outflow events to the south were not necessarily augmented in near-surface layers, but appeared to be of near equal magnitude throughout the water column. By winter, a strong average northward flow developed in near-bottom layers, which was interrupted only by southward events that affected much of the water column (Figure 3-18). Winter events in the near-surface layer were more rotary, and tended not

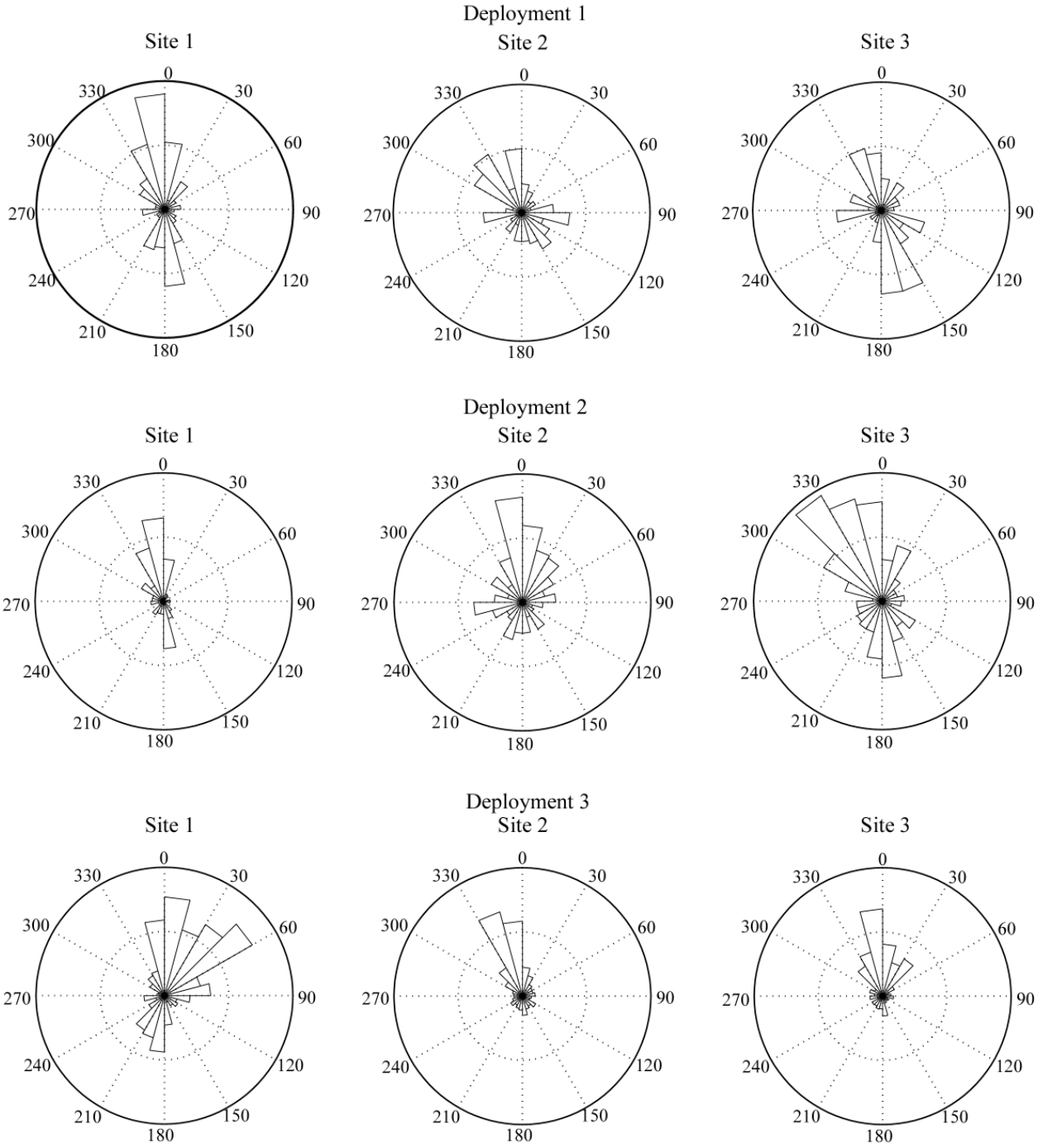

Figure 3-16. Rose histograms of near-bottom current meter data from ARESS at the lower depth level (0.76 m) for the fall/winter 2000 deployment period at all Sites.

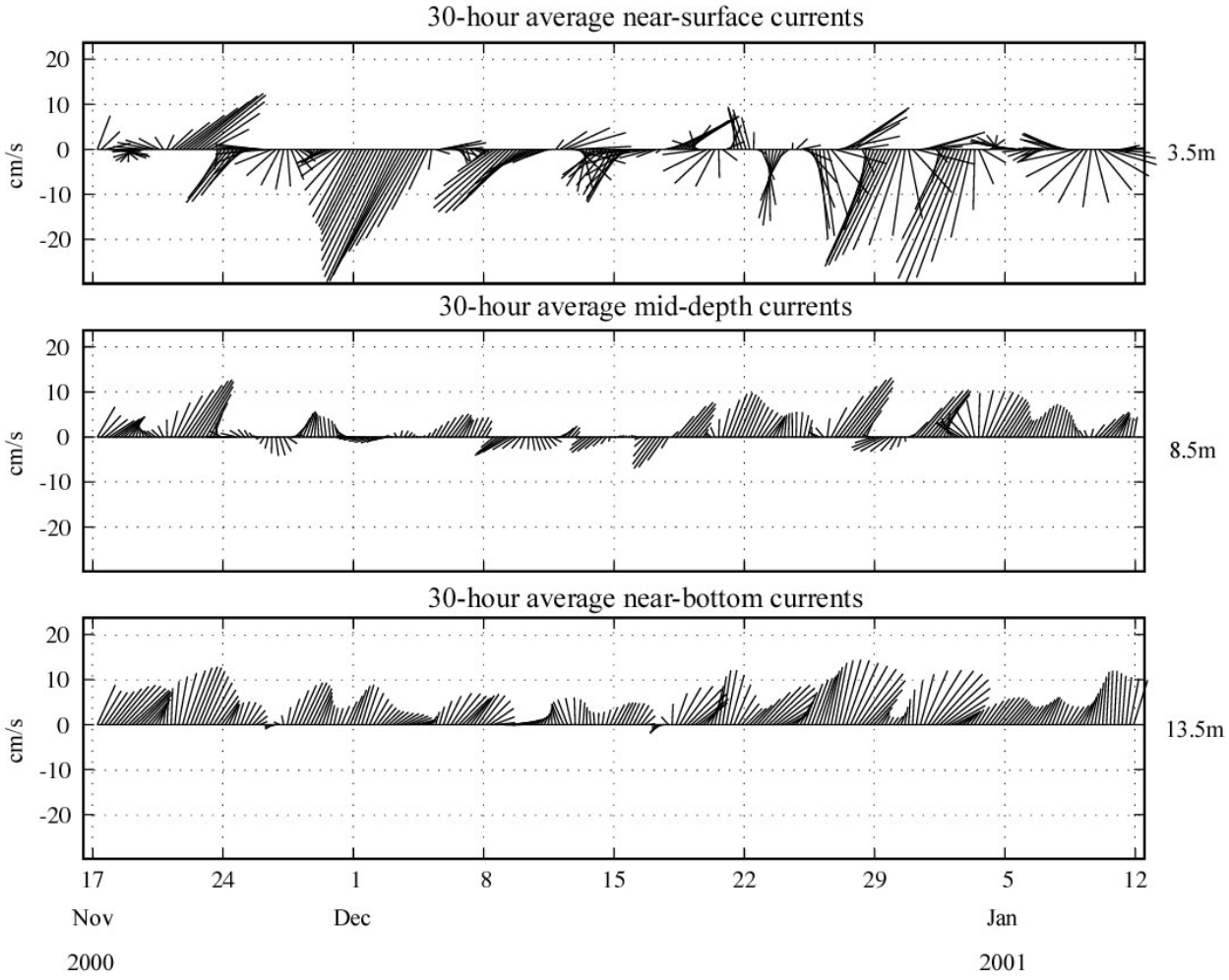

Figure 3-17. Time series vector plots of 30-hr LPF ADCP data from three depth levels for Deployment 3, winter 2000–01 at Site 1. Values to the right of plots indicate measurement depth.

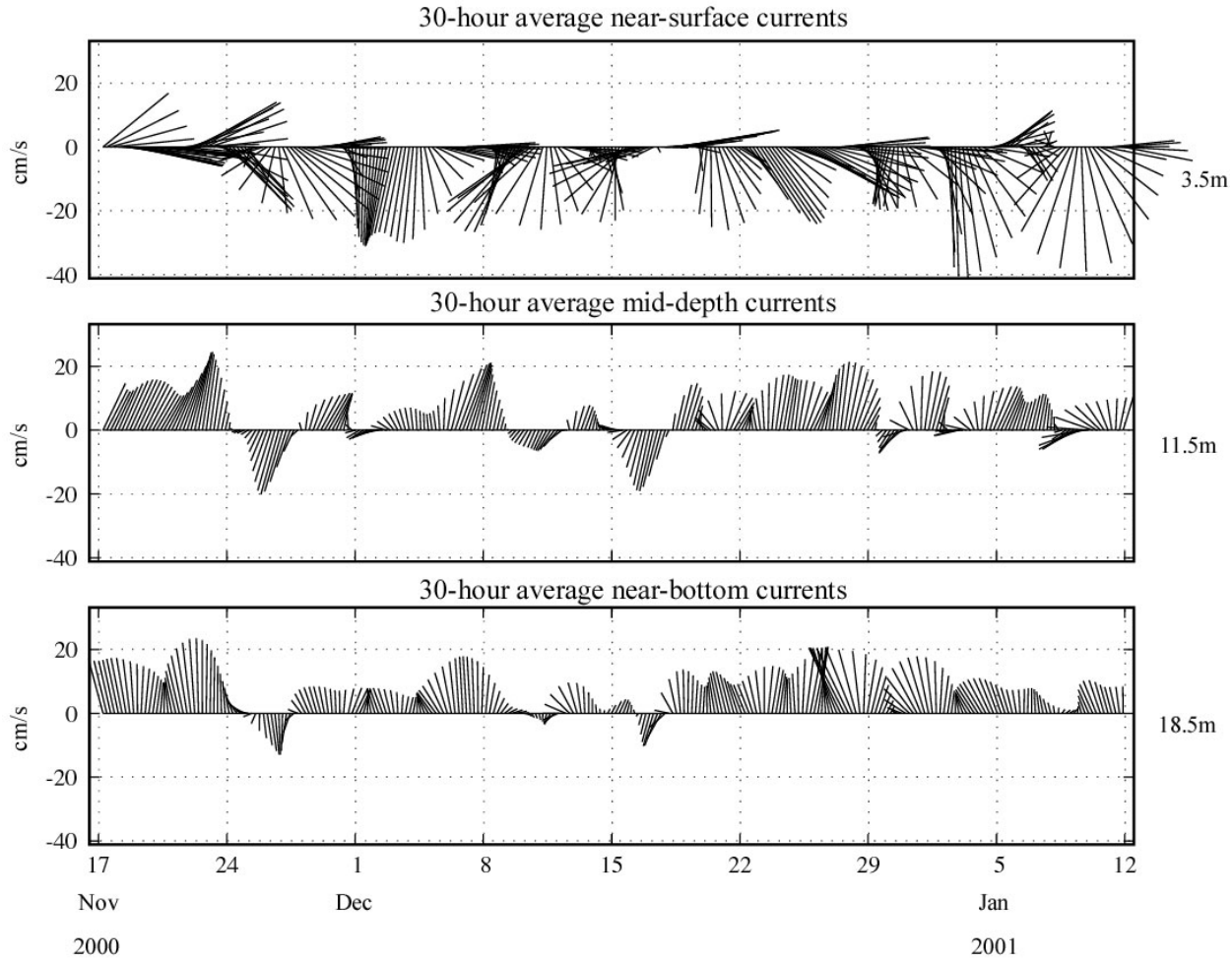

Figure 3-18. Time series vector plots of 30-hr LPF ADCP data from three depth levels for Deployment 3, winter 2000–01 at Site 3. Values to the right of plots indicate measurement depth.

to be as bi-directional as in previous deployments. Strong events were also more frequent in winter than in late summer or early fall.

Near-bottom Low-Pass Filtered Currents

As with the ADCP data, the ARESS near-bottom current data were also run through a low-pass filter to remove any variability associated with the tides and higher frequency processes, and plotted as time series vectors (Figure 3-19). Once again, the dominant north-south orientation of the flows was obvious in the vector plots. At Site 1 in particular, very little low-frequency flow occurred to the south, and all of the major events occurred in the northward direction. The shift from a predominant north-northwest direction in fall to north-northeast in the winter that was noted in the rose diagrams was also evident in the low-pass vector plots. There were almost no events in the east-west direction, and those that did occur were short in duration, of small magnitude, and typically appeared to be associated with a shift in the dominant direction for that given period. These periods also appeared to be correlated with periods of higher wind and wave activity. It was also noted that the magnitude and frequency of these events increased into late fall and winter, with one or two per week noted in fall, and two to three per week in winter.

Site 2, closer to shore, showed stronger low-pass velocities to the south than at the other two sites, particularly in the fall. Larger events to the north and south were observed in early to late fall, and at times contained a smaller eastward or westward component. By winter, the dominant direction was clearly to the north-northwest (Figure 3-19), as was noted previously in rose diagrams. As with Site 1, the frequency and magnitude of flow events at Site 2 also increased from fall to winter. At Site 3, events primarily occurred flowing northward or southward, with one or two strong flow events to the southeast in the fall. By mid-October, trends had shifted to predominantly northward net velocities, with two stronger events to the south in late fall/winter. As at the other two sites, the frequency and magnitude of the strong current events increased into the winter, with three to four per week. In addition, there were no indications of any prominent east-west current events near the bottom.

3.1.5 Summary of Fall/Winter 2000 Results

- Winds exceeding 15 m/s were rare in the fall, but more common in the winter. Wave heights reached 2 m or more only seven times during the fall and winter deployments, and exceeded 3 m only twice. Typically, higher waves were associated with winds blowing from the northeast, east, or southeast.

- Time series observations of ADCP data revealed that the semi-diurnal tide was the most significant portion of the velocity signal, particularly at deeper depths. In addition, the tides were primarily bi-directional, trending either northward or southward.

- As with the water-column currents, the near-bottom currents were primarily bi-directional and also most influenced by the semi-diurnal tidal signal. In addition, the near-bottom currents showed enhanced magnitudes on a two-week cycle, concurrent with the spring-neap cycle of the tide that was noted in the pressure data.

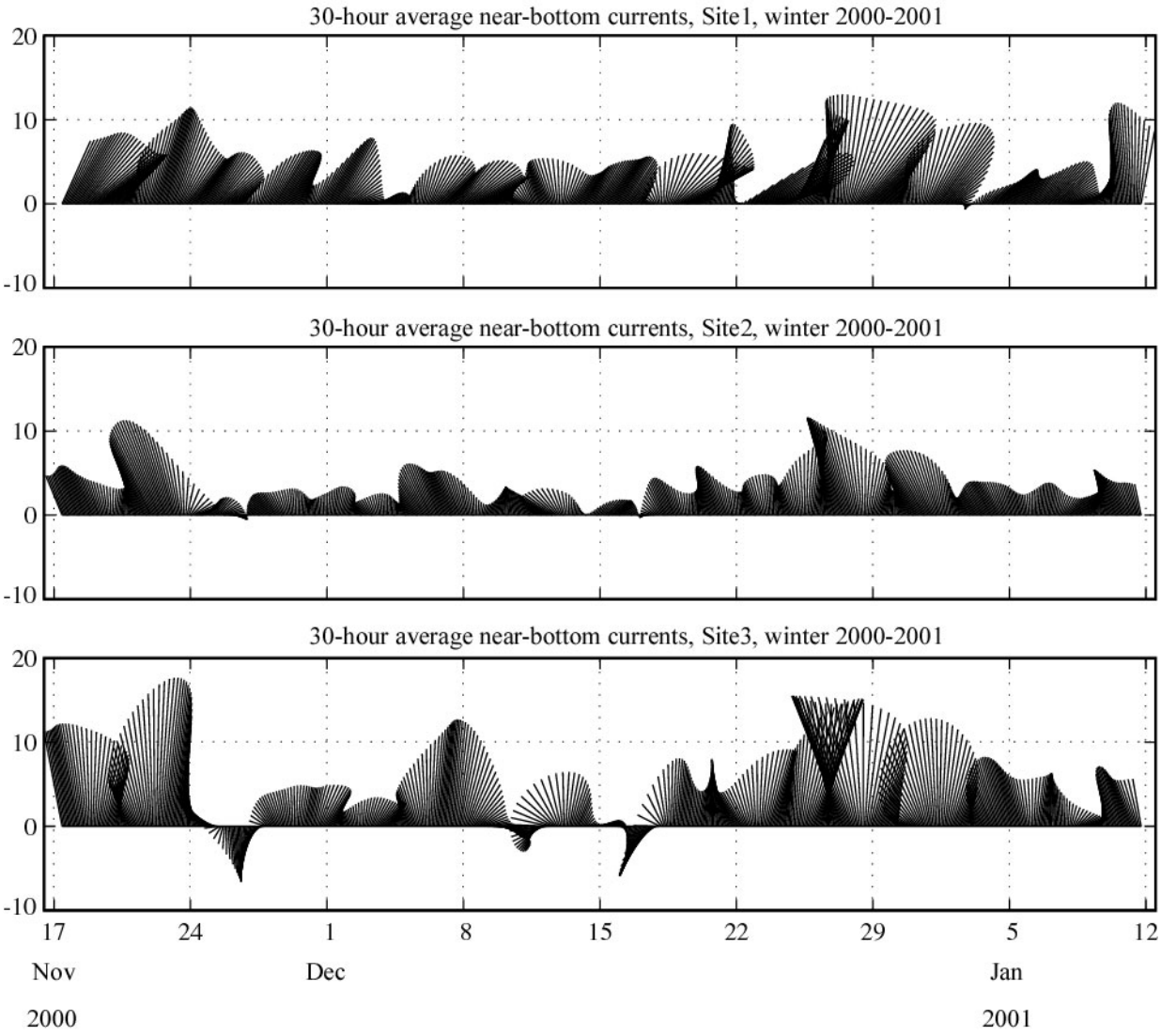

Figure 3-19. Time series vector plots of near-bottom currents from the lower sensor level (0.76 m off seafloor) for Deployment 3, winter 2000–01 at Site 1 (top tier), Site 2 (middle tier), and Site 3 (bottom tier).

- Turbidity data showed generally low background values at all sites, with distinct short-term peaks as well as some broader, longer-term increases. Increases in turbidity were almost always associated with periods of higher waves. Generally, turbidity values were somewhat higher at the sensor mounted lower on the ARESS array.

- Long-term means of ADCP data demonstrated that currents were primarily northward at depth and southward near the surface. Mean speeds were highest at the near-surface, and mean currents were generally stronger in the winter. This was corroborated by the histogram analysis that showed a higher percentage of values in the higher velocity ranges at both measurement sites (1 and 3) in the winter. Histograms of current direction data also supported the conclusion that currents were primarily bi-directional in either a northward or southward direction.

- Vector plots of low-pass filtered currents demonstrated that average flows noted in long-term means were representative of flows that occur on a 2-4 day timescale. All major velocity events occurred primarily in a northward or southward direction. Near-bottom response to surface events was sometimes concurrent with, and sometimes in opposition to, the surface flow. Events in the cross-shelf direction (east-west) were rare, typically low in magnitude, and short in duration.

- Examination of mean ARESS current data revealed similar trends as the ADCP data, showing primarily weak, northward currents at the near-bottom. Mean current speeds increased into the winter along with the number of observations in higher velocity ranges.

3.2 Spring 2001 Measurement Program

The second field phase was conducted from April 2001 through May 2001 and focused primarily on measuring the impacts associated with the outflow from the New York/New Jersey Harbor Estuary (NY/NJHE) system. This phase was conducted during this time because spring represented the season when generally higher volumes of outflow could be expected from the NY/NJHE system.

3.2.1 Water Column Characteristics

CTD Casts – Spring 2001

Individual CTD hydrocasts made at the beginning of each spring deployment at each bottom-mounted instrument location (Figure 2-1) are shown as T/S plots in Figures 3-20 and 3-21. Each site is represented by a different symbol, and the dashed lines in the background represent lines of constant density. At the beginning of the first deployment, water column properties were fairly homogeneous throughout the region, with little temperature stratification (thermocline) and a more pronounced saline stratification (a well developed halocline). By the beginning of May, a more pronounced thermocline had developed, and the halocline was beginning to disintegrate.

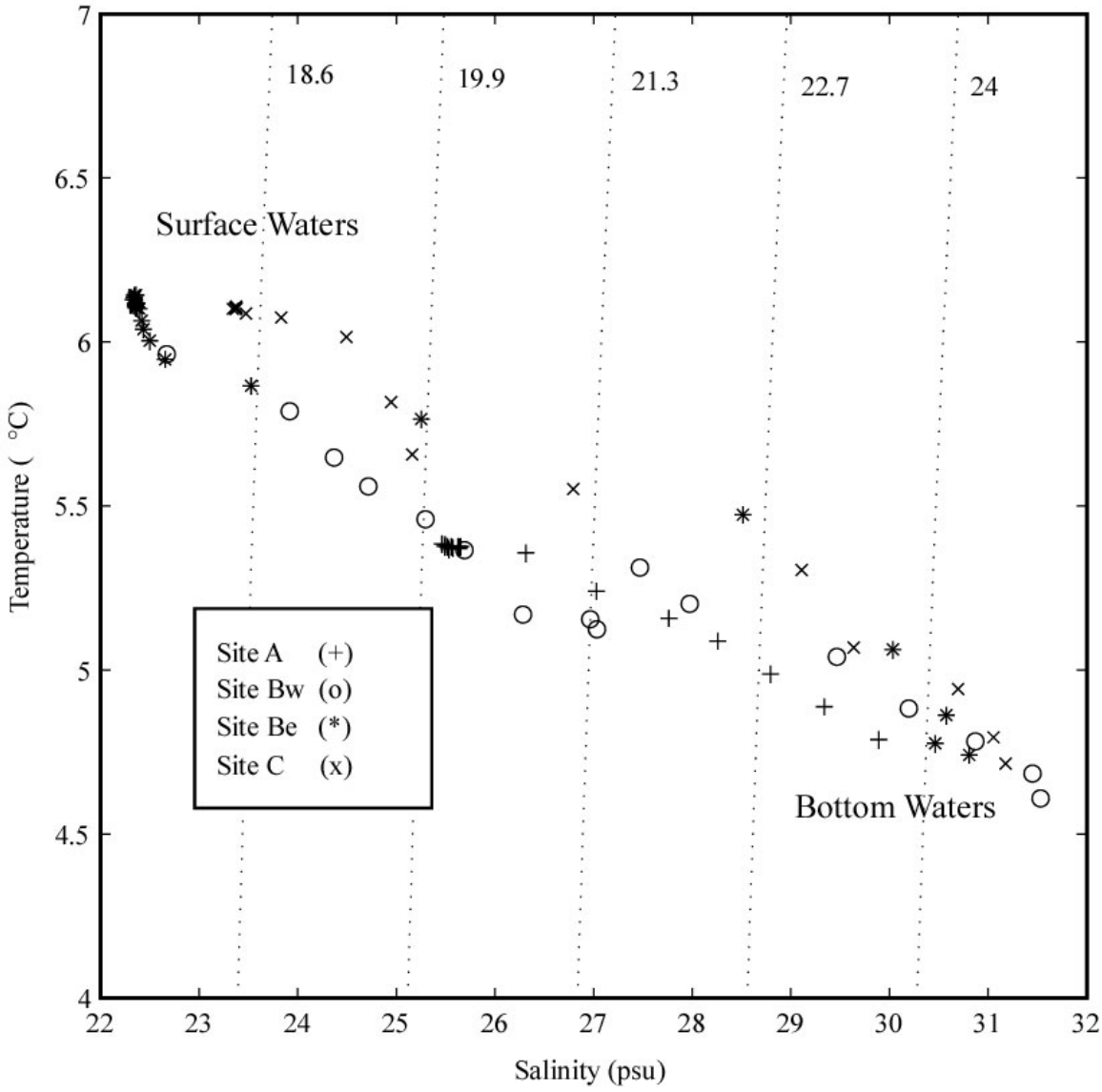

Figure 3-20. T/S plot of CTD data collected on 5 April 2001. Dotted lines in the background represent lines of constant density (isopycnals), which increase from left to right.

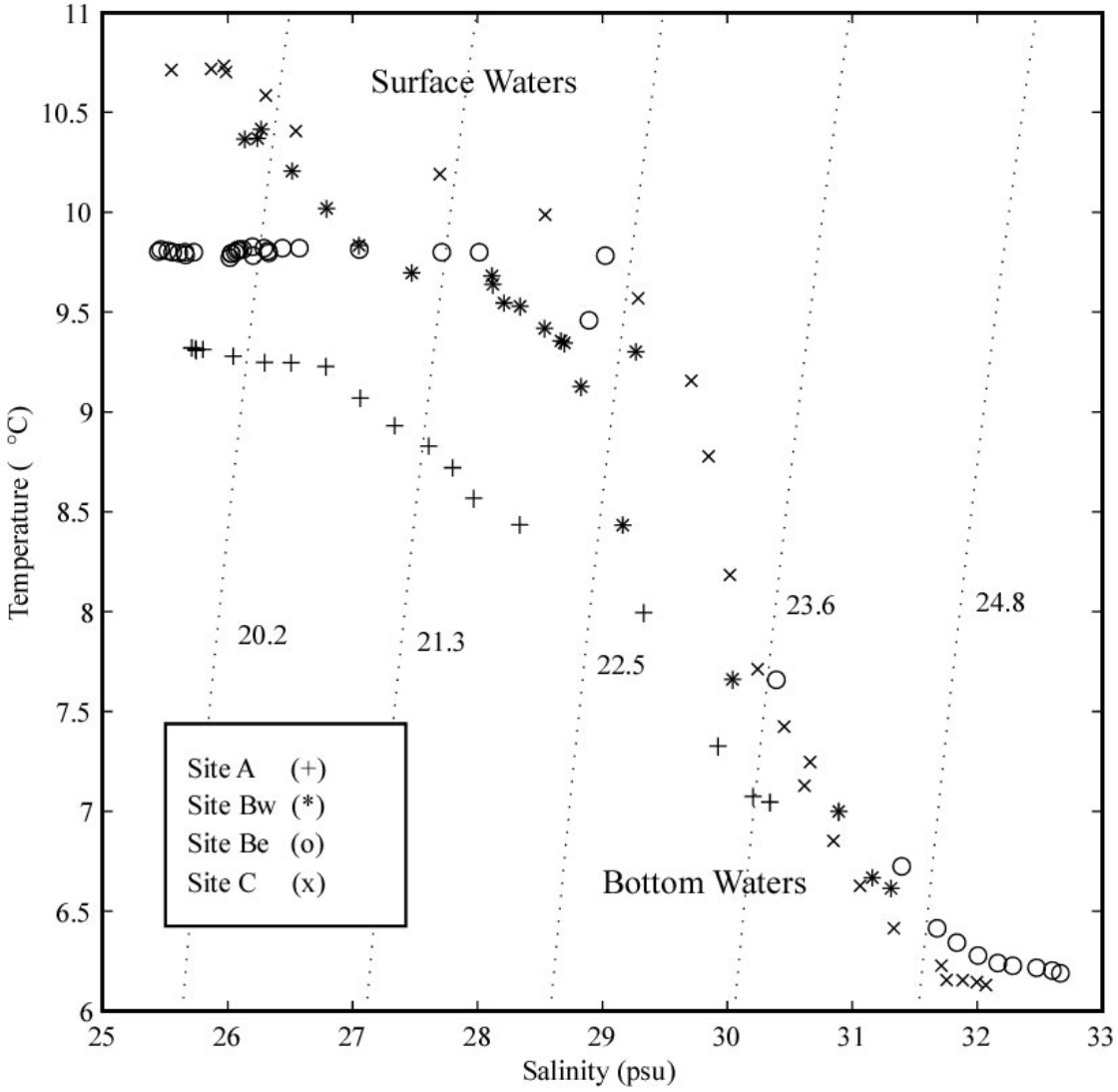

Figure 3-21. T/S plot of CTD data collected on 1 May 2001. Dotted lines in the background represent lines of constant density (isopycnals), which increase from left to right.

Data is also plotted as vertical profiles in Figures 3-22 and 3-23 for 5 April and 1 May, respectively. Significant saline stratification is noted in April, with as much as 10 PSU difference from surface to bottom. Temperature is still well mixed in April, but begins to stratify by the beginning of May. The pronounced difference in salinity from surface to bottom begins to subside by May, as the Spring rains tail off.

CTD transects were conducted from near-shore to offshore on 1 May, 3 May, and 4 June in an attempt to assess freshwater discharge from the NY/NJHE. The locations of individual sample points along the transects are shown in Figure 3-24, and contour plots of these transects are presented in Figures 3-25 to 3-27. The transect on 1 May (Figure 3-25) showed fairly similar water properties from near-shore to offshore, with consistent density increases with depth. A small region of slightly warmer and fresher water was noted offshore near the surface. (The sudden changes in water properties indicated near the shoreline [to the left of the diagram] were an artifact of the contouring process at an area where the depth changed rapidly.) A similar transect was made two days later (Figure 3-26) and similar water properties were noted, with the exception of some surface warming near shore. In addition, a trend toward a more well-defined pycnocline was noted from a 5–10 m depth near-shore, deepening to 7–12 m depth offshore. By 4 June (Figure 3-27), saline stratification had decreased and thermal stratification had increased, the net result being that density stratification was less pronounced than a month earlier.

Moored CT Data

Two continuously recording conductivity-temperature devices were deployed at near-surface and near-bottom levels to record temperature and salinity at Site Bw during both deployments. The devices recorded changes in the water column properties associated with seasonal warming, as well as freshwater input to the system, and could be correlated to changes noted in current velocity records. The C/T data is presented in two formats: 1.) as a time-series of near bottom and surface, temperature and salinity (Figure 3-28), and 2.) as T/S plots (as for the vertical CTD hydrocast data) in Figure 3-29.

Large changes in both temperature and salinity were noted at both the surface and near-bottom, particularly in April. Surface salinity varied from a minimum of ~12 PSU to a maximum of ~30 PSU, over the course of only one to two days. Near-bottom salinity changed less dramatically, ranging from ~31 to ~24 psu. Surface temperatures ranged from ~5° C to ~ 12° C and near-bottom temperatures ranged from ~4.5° C to 9° C. Ranges in salinities at both surface and near-bottom were smaller in May. Temperatures were warmer in May at both levels and increased gradually as the season progressed into summer. Periodic large changes within short periods of time also were noted (e.g. 26-29 April), and appeared to be associated with tidal influences. Large drops in salinity were often associated with increases in temperature, and vice versa, illustrating the difference between freshwater influxes and incoming offshore waters. For instance, a peak in the river discharge noted at the Passaic River from 11 to 14 April (Figure 3-7) corresponded to a decrease in surface salinities (of approximately 11 PSU) and an increase in the average temperature (of approximately 3° C) from 12 to 16 April.

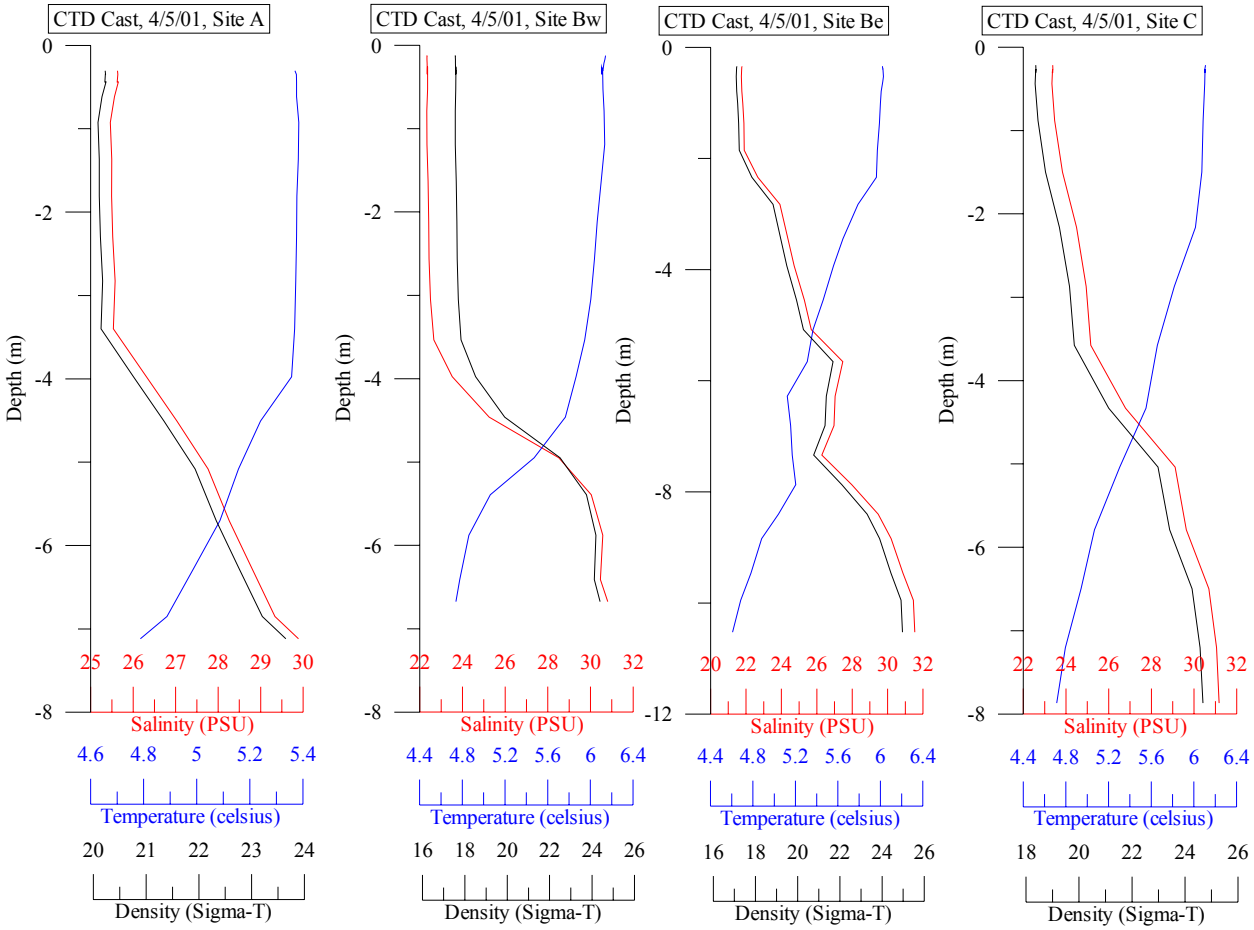

Figure 3-22. Vertical plots of CTD casts collected on 5 April 2001. Salinity is plotted in Practical Salinity Units, Temperature in Degrees Celsius, and Density in Sigma-T Units.

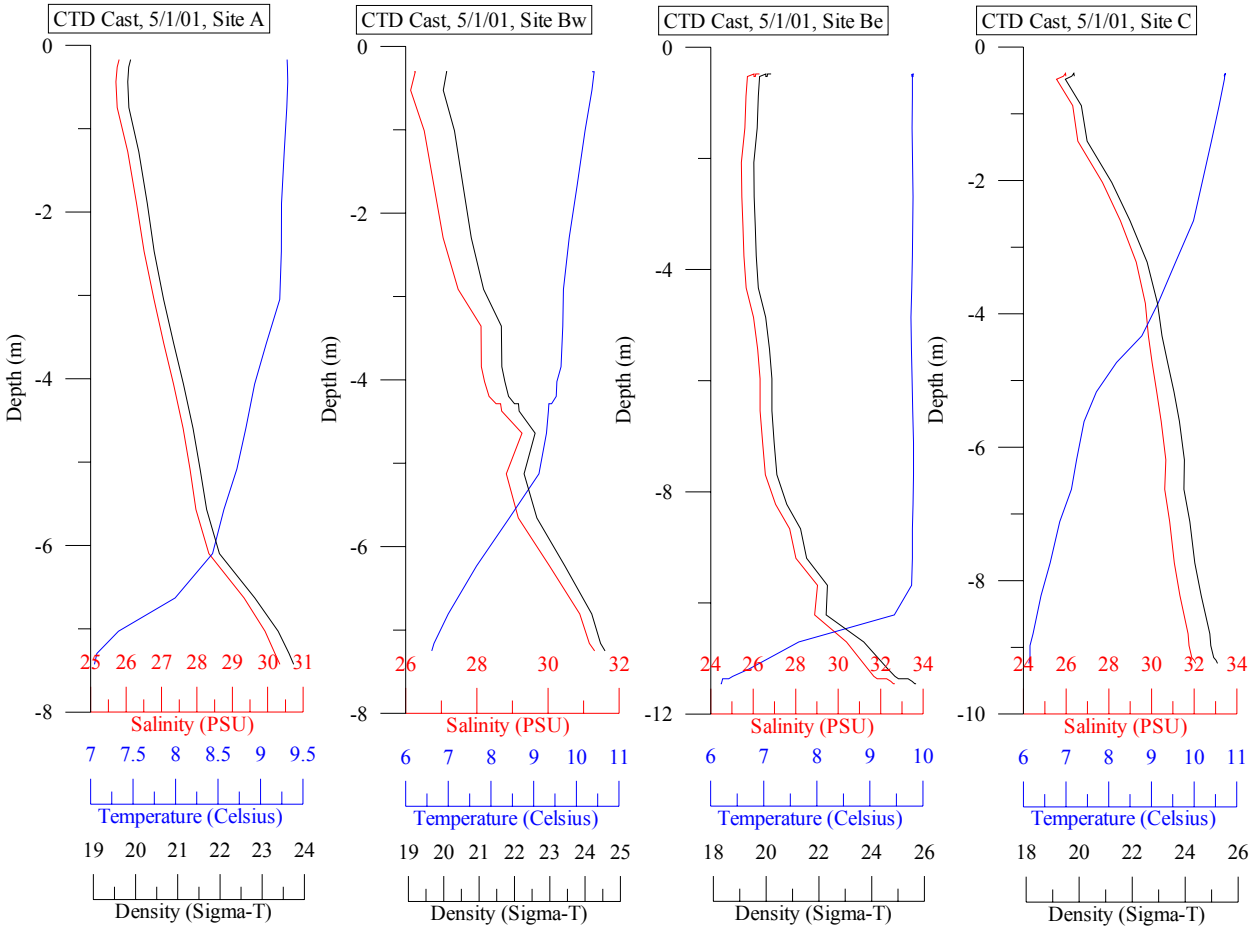

Figure 3-23. Vertical plots of CTD casts collected on 1 May 2001. Salinity is plotted in Practical Salinity Units, Temperature in Degrees Celsius, and Density in Sigma-T Units.

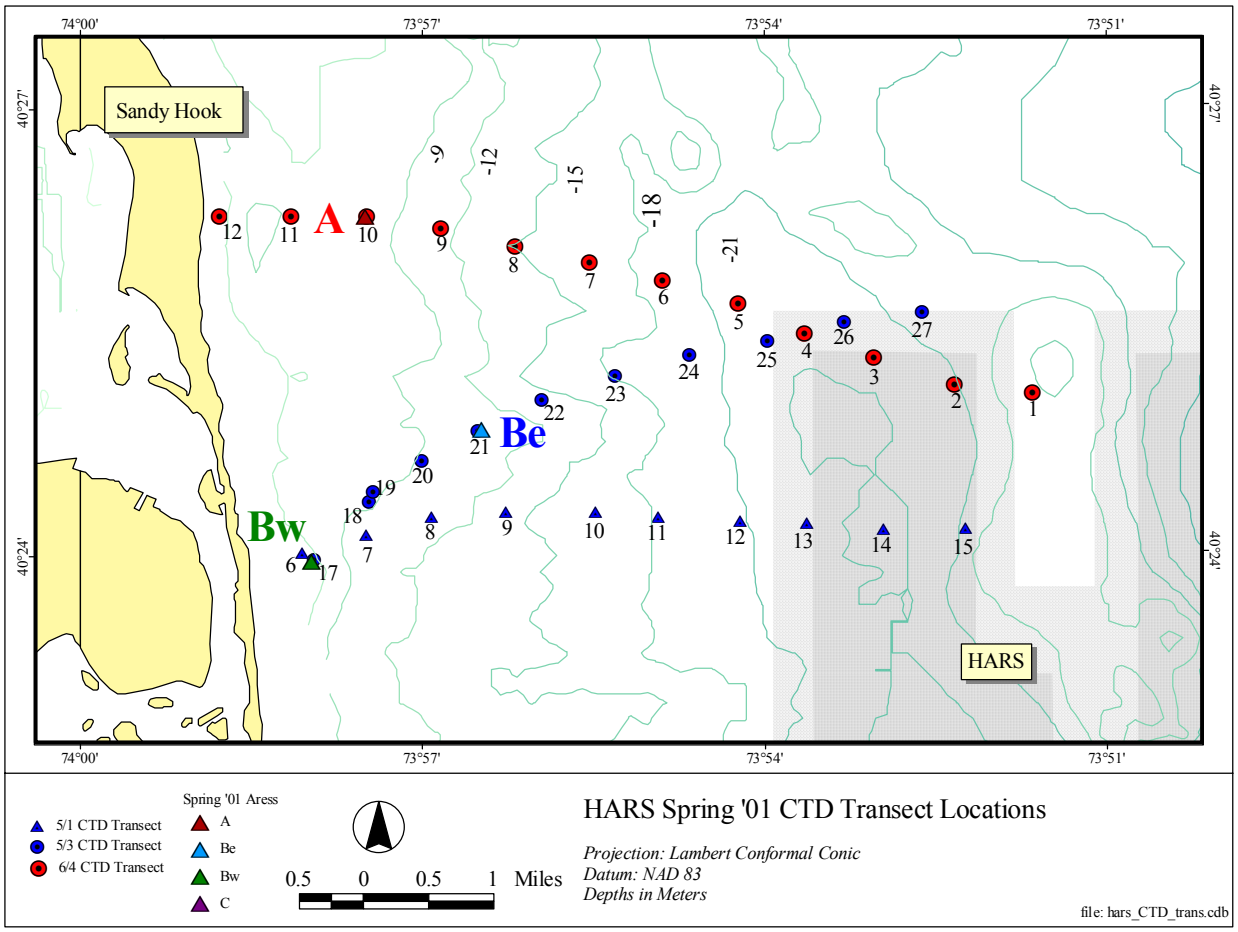

Figure 3-24. Transects from near-shore to offshore with vertical CTD hydrocast locations on 1 May, 3 May, and 4 June 2001.

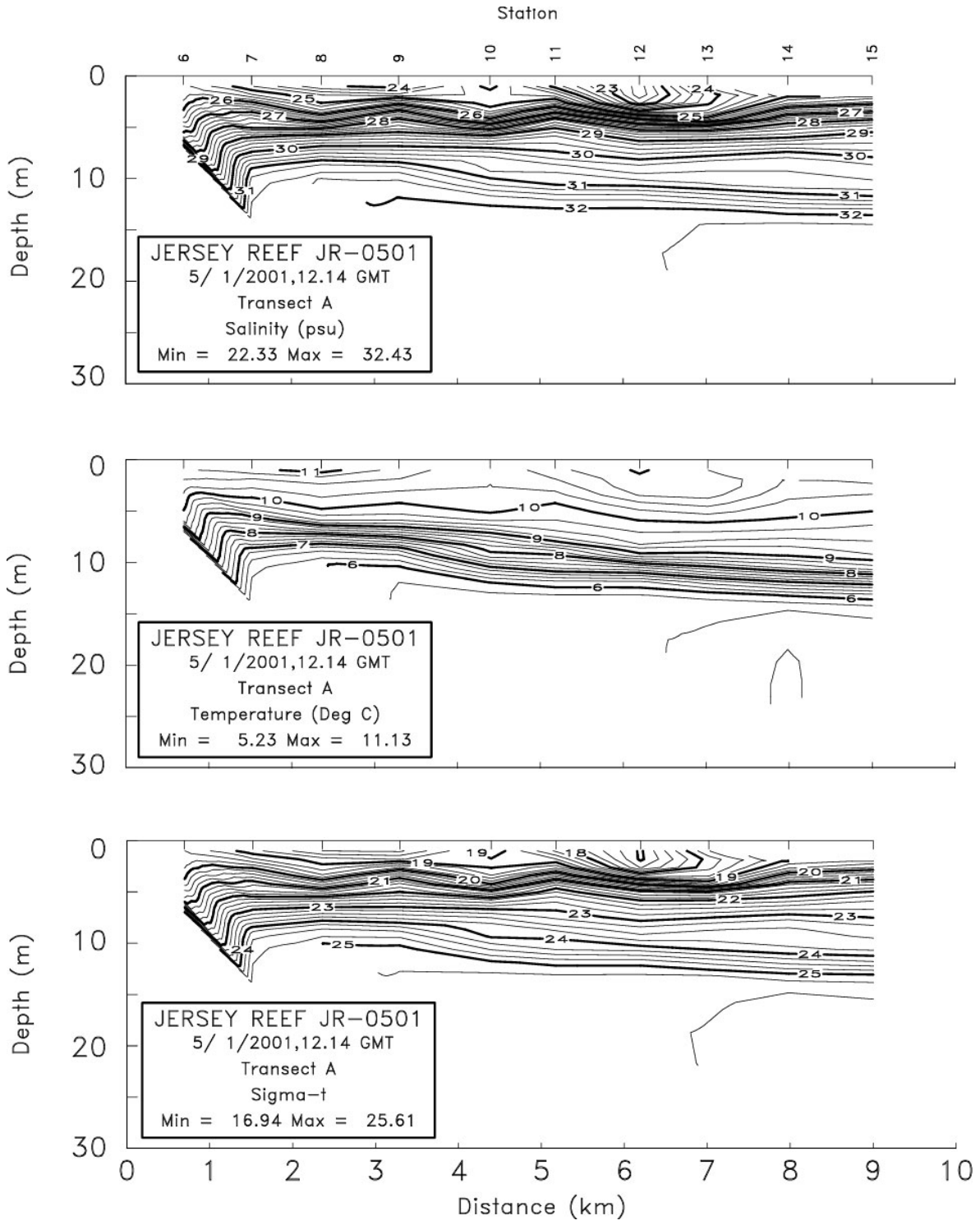

Figure 3-25. CTD transect taken on 1 May 2001, with individual temperature, salinity, and density contour plots. As noted, density is in Sigma-T units.

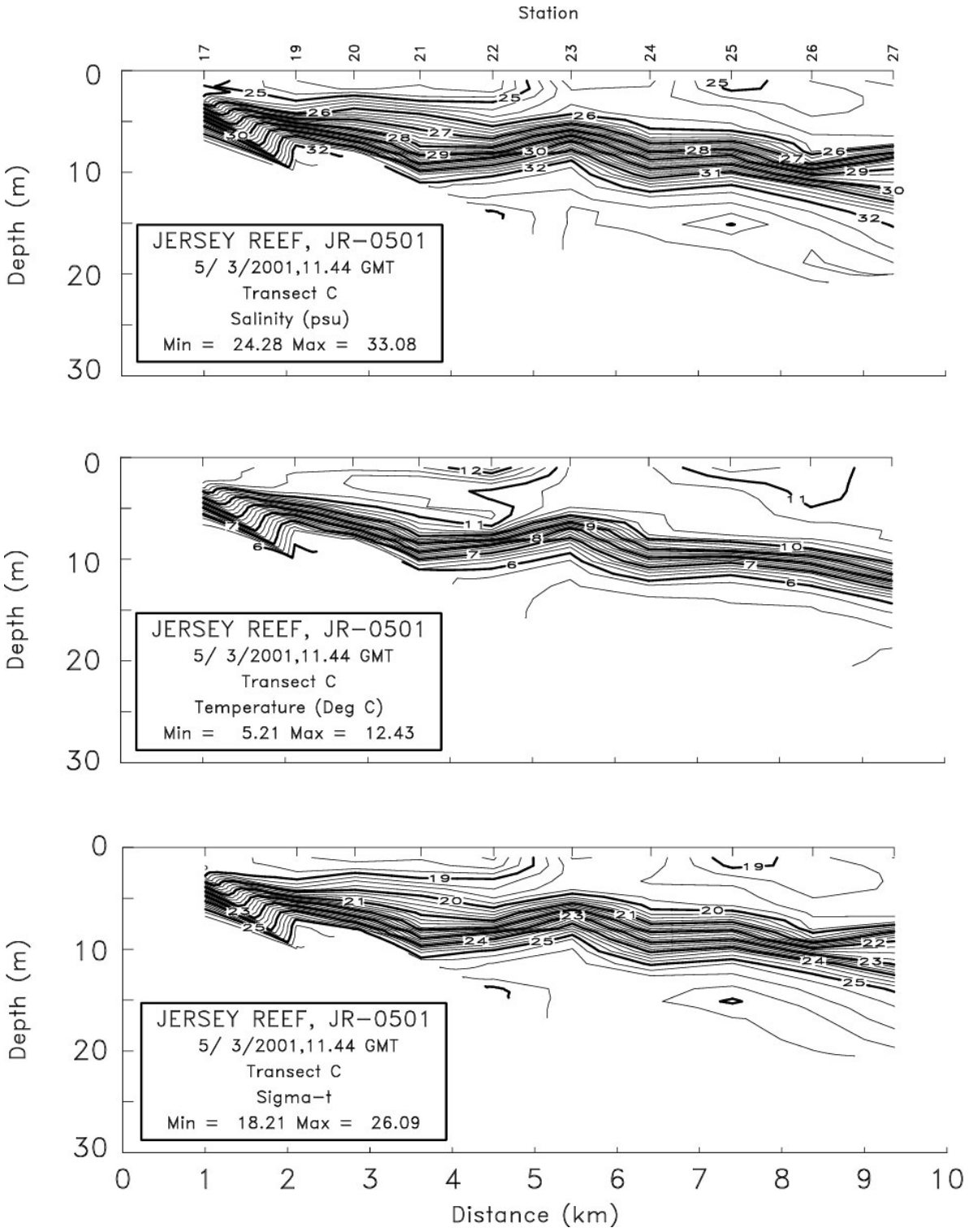

Figure 3-26. CTD transect taken on 3 May 2001, with individual temperature, salinity, and density contour plots. As noted, density is in Sigma-T units.

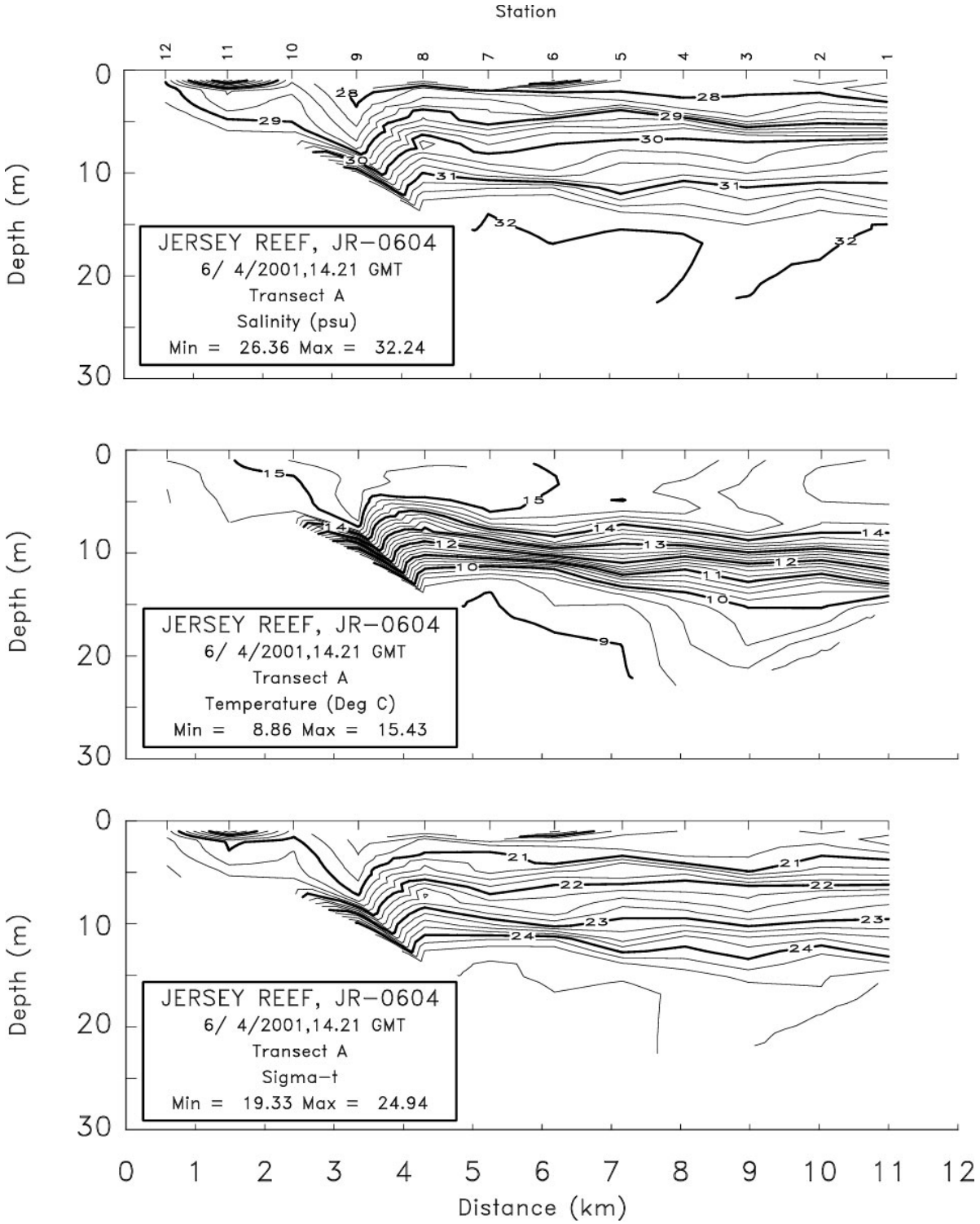

Figure 3-27. CTD transect taken on 4 June 2001, with individual temperature, salinity, and density contour plots. As noted, density is in Sigma-T units.

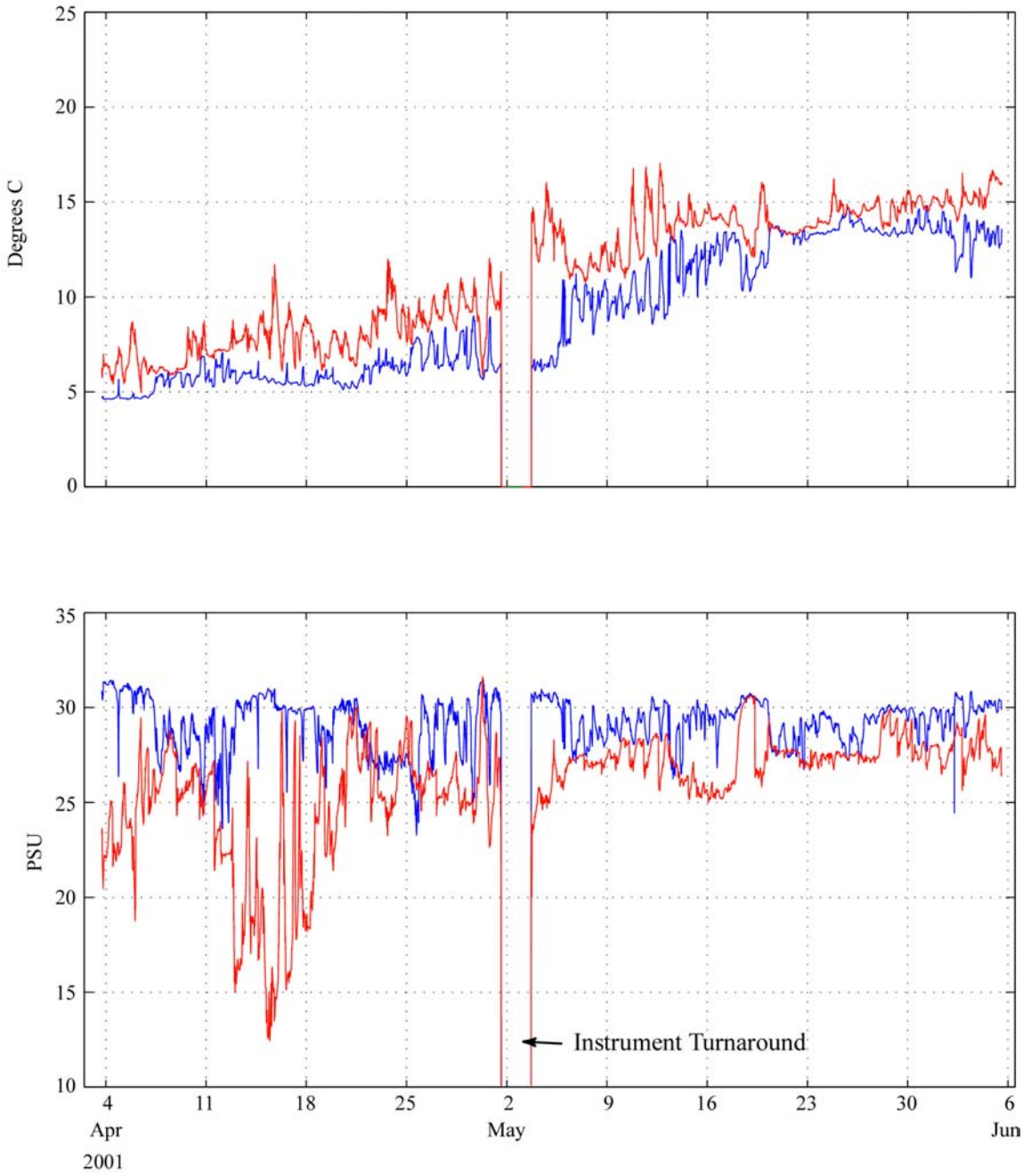

Figure 3-28. Time series of salinity (lower tier) and temperature (upper tier) noted at the near surface (0 m depth; red) and near bottom (7 m depth; blue) at Site Bw, spring 2001. Significant decreases in surface salinities as on 15-16 April correspond to higher river discharge.

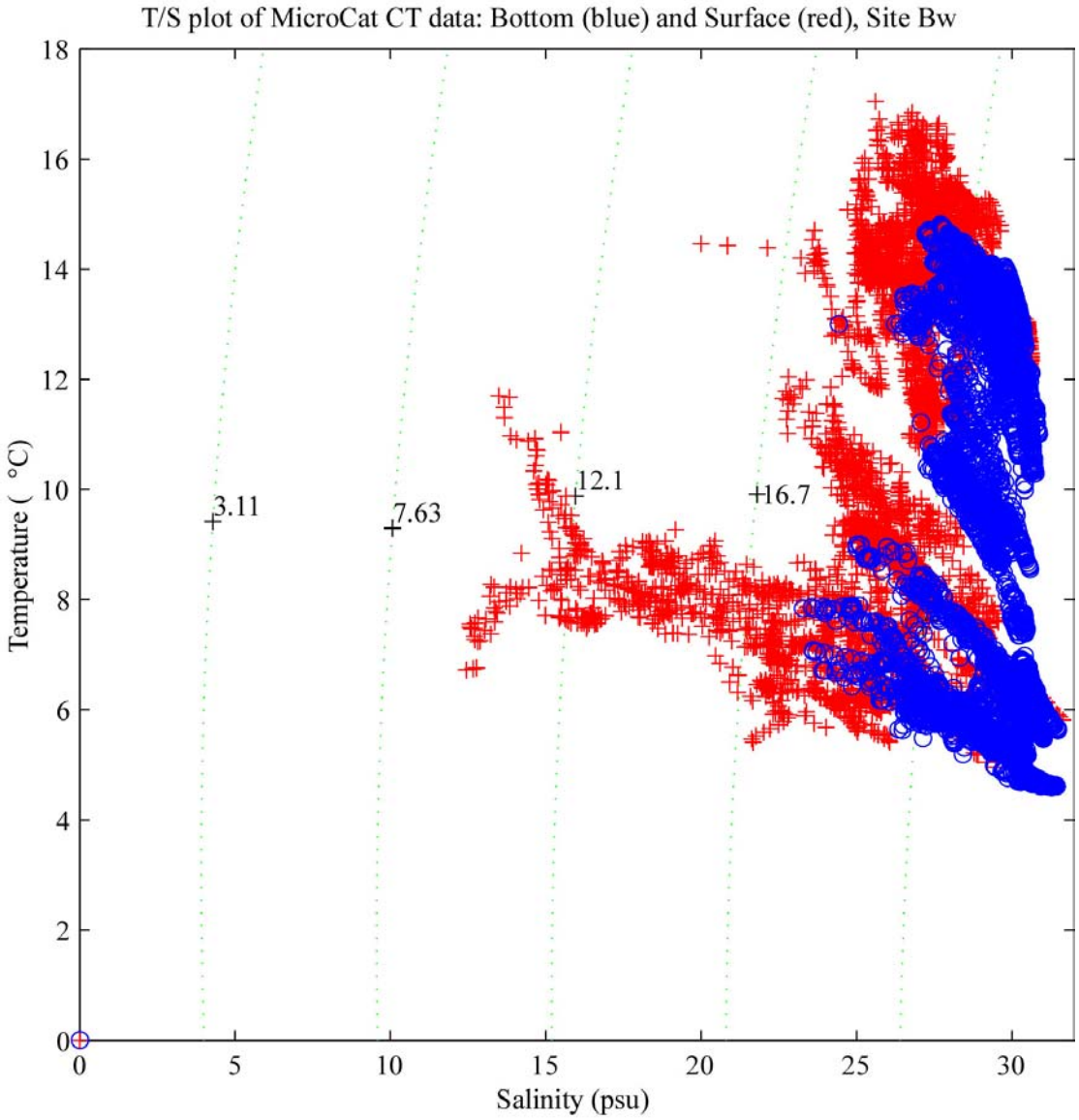

Figure 3-29. Temperature and salinity data plotted as a T/S diagram for MicroCat CT recorders at Site Bw, spring 2001. Blue circles represent bottom T/S data, whereas red crosses represent surface T/S data. Dotted lines represent isopycnals or lines of constant density, and the numbers represent density values in Sigma-T units.

Plotting the temperature against salinity gives a feeling for the constantly changing water properties along the shoreline due to freshwater input in the spring (Figure 3-29). Surface waters are represented by red crosses and bottom waters are represented by blue circles. As might be expected, surface waters show considerably more variability in both temperature and salinity, as solar heating and freshwater input have a greater effect on the T/S properties of the surface waters.

Near-bottom and Surface Temperature

Near-bottom water temperature was recorded by the ADCPs at Sites Be and Bw, and the Aquadopp at Site C, and surface water temperature was recorded by thermistors attached to the surface buoy chain at ARESS sites A, Be, and C. Near bottom and surface temperature and salinity were also recorded at Site Bw, described in the next section. Figure 3-30 shows surface and near-bottom temperatures for all four sites. Near-bottom temperature showed a gradual increase over the spring measurement program, starting at approximately 5° C at both sites in April, and reaching a maximum of approximately 12° C in mid-May. There was not a significant difference in bottom temperature between the three measurement sites, though Site Be showed more short-term variability due to the influence of intruding offshore waters driven by tidal flow.

Surface temperature also showed a generally monotonic increase over the course of the deployments (Figure 3-30). Some semi-diurnal as well as lower frequency variability was noted at all three sites and no significant differences were noted from one site to the next. The water column showed some thermal stratification even before the summer (as in the first week of May), which was susceptible to overturning by late spring storms (as on 20 May).

Drogue Studies

A surface and a mid-depth water-following drogue were deployed and tracked by the survey vessel on 24 April and 4 June 2001. The drogues were deployed from Site A on 24 April at 13:20 GMT (one hour before high tide), and were tracked for approximately 6 hours (Figure 3-31). Over the course of the deployment a change in the tide occurred, which was clearly indicated by the clockwise rotational track of the drogues. Initially the surface drogue traveled farther northward than the mid-depth drogue, but ultimately the two ended up very near each other upon recovery. This differential noted between depth levels is representative of the vertical shear in water column currents typically observed on the continental shelf. In addition to reduced currents closer to the bottom due to friction, there is also typically a phase delay in the tidal currents from one depth level to another.

On 4 June the total time of drogue deployments was almost 5 hours, and the total excursion was considerably less than on 24 April (Figure 3-32). The two drogues started in a southward direction together, the surface drogue began to change direction just before recovery in what appeared to be a clockwise rotation, following the mid-depth drogue, which had already changed direction toward the north in what appeared to be a counterclockwise rotation.

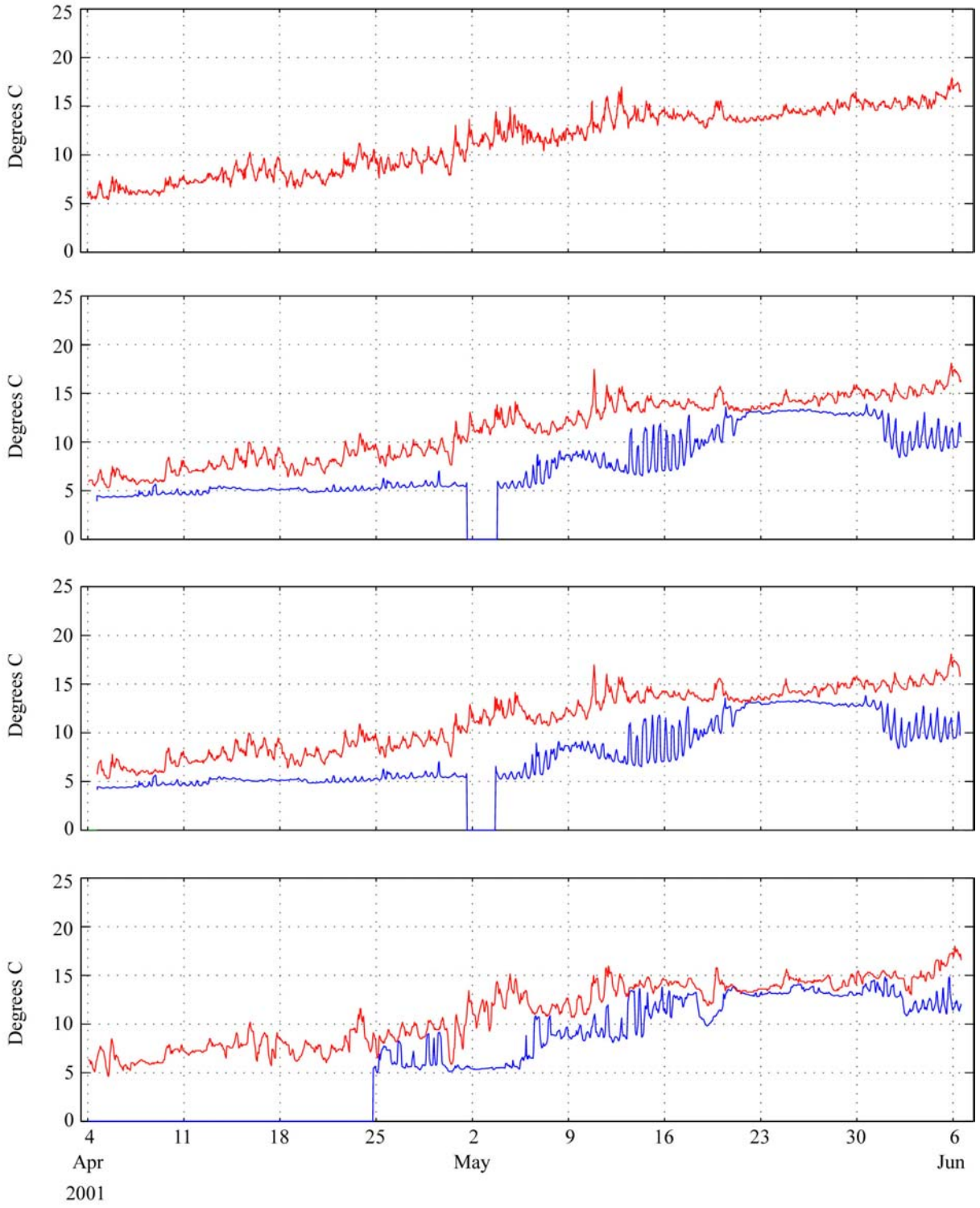

Figure 3-30. Time series of surface (red) and near-bottom (blue) temperature at all four sites (where data was available), spring 2001 deployment period. Surface temperature at Sites A, Be and C was recorded by Tidbit thermistors, whereas surface temperature at Site Bw was recorded by Seabird Microcat CT recorder.

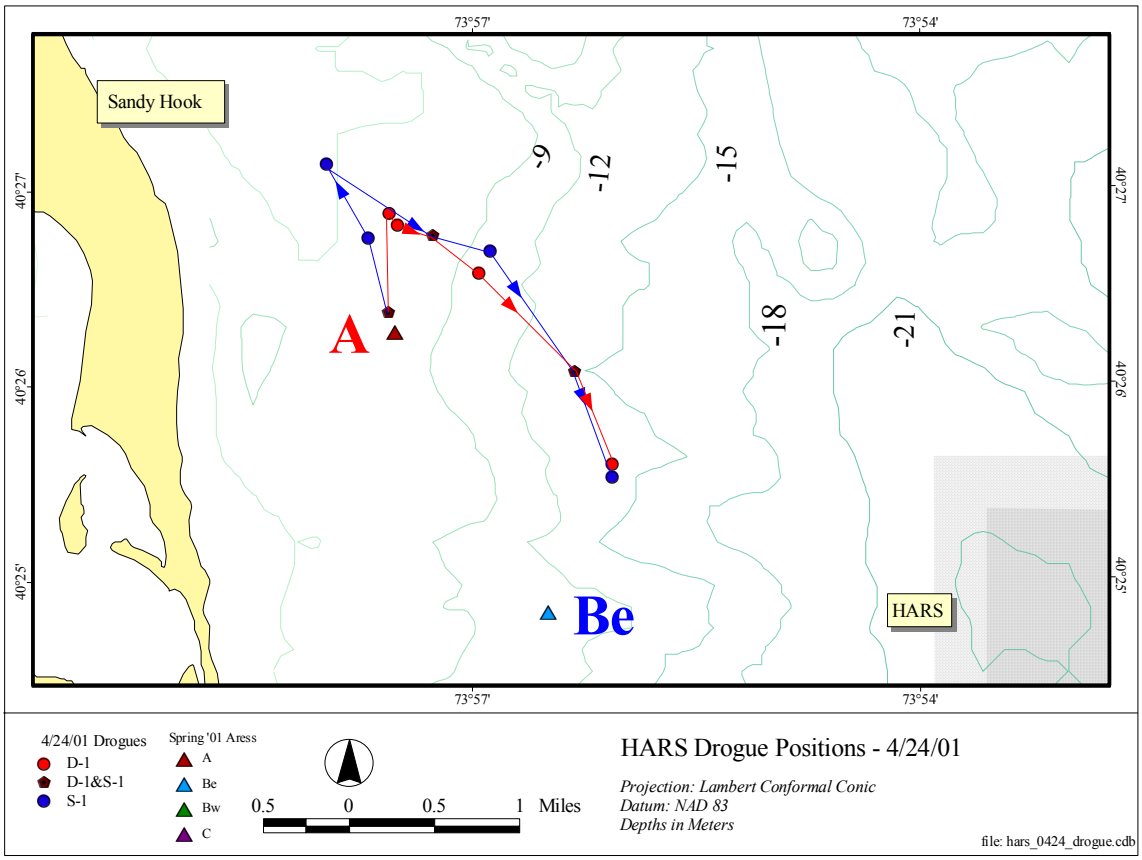

Figure 3-31. Drogue positions during 24 April deployment. Drogues were tracked for approximately 5 hours. Blue line represents surface drogue track and red line represents deep drogue track.

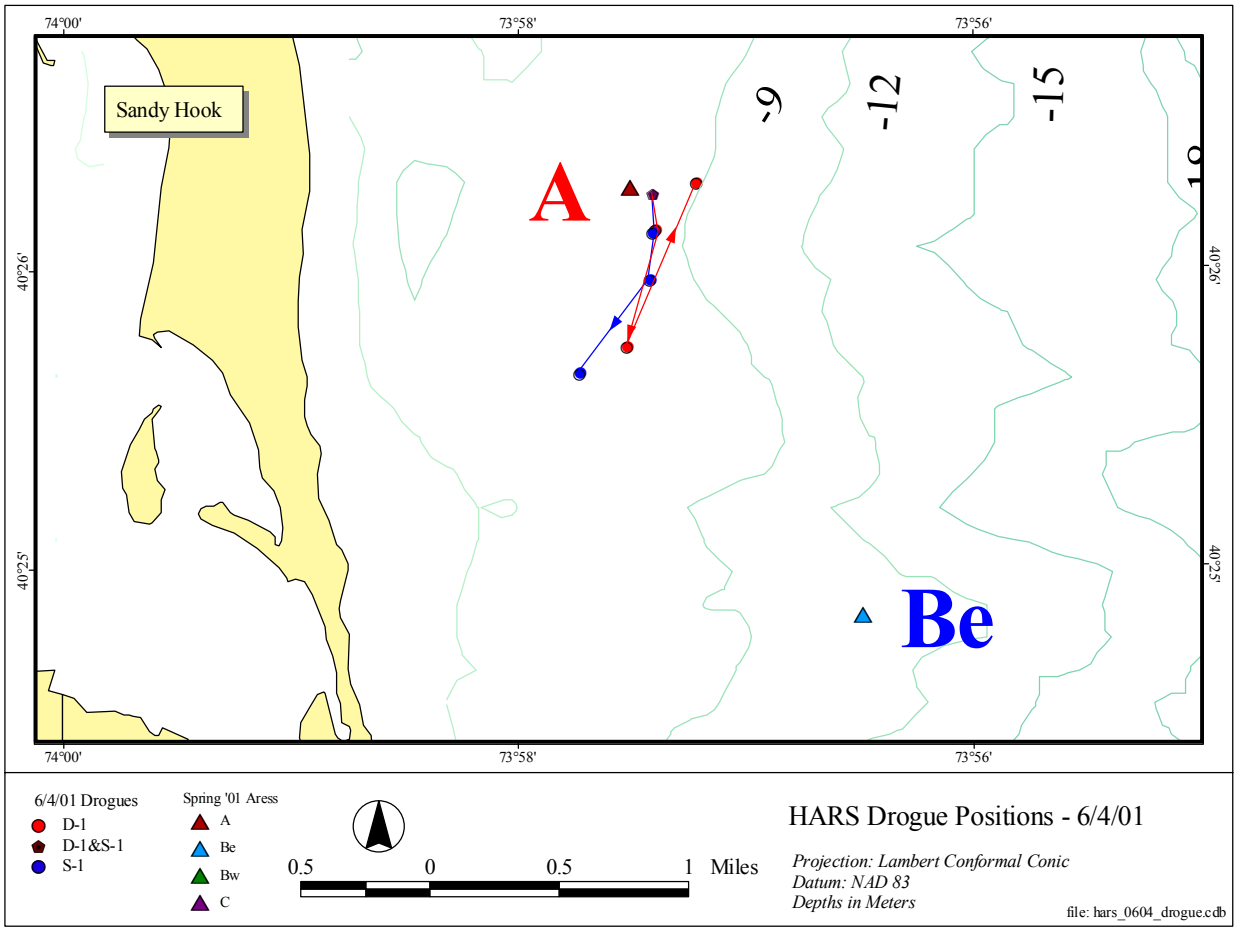

Figure 3-32. Drogue positions during 4 June deployment. Drogues were tracked for approximately 3 hours. Blue line represents surface drogue track and red line represents deep drogue track.

3.2.2 Time Series Observations

Meteorological, Waves, and River Flow Data

As with the fall measurement program, wind data were downloaded from the Ambrose Light Tower meteorological station for the spring 2001 deployment period, and waves were recorded by the ARESS array located at Site Be. The wave data are presented as significant wave height, or the average of the highest one-third of the waves observed during the measurement period. Data from the April deployment are presented in Figure 3-33; data for the May deployment are presented in Figure A-14. Winds in the spring were similar to the first fall measurement period (Deployment 1), with only five events exceeding 15 m/s in the two months of observations. Direction for the stronger winds events varied from the northwest in April to the east and southeast in May. There were no wave events over 2 m during the entire spring measurement program. Those periods when waves did approach 2 m were typically associated with winds from the southeast, east, or northeast.

A plot of the river discharge data from the Passaic River USGS gauge was provided in Figure 3-7. Based on these data, it appears that the spring measurement program began toward the end of the highest river discharge period for the season. Throughout the course of the spring measurement program, river discharge flows remained quite low, but increased rapidly at the tail end of the program.

Water Column Currents

For the spring deployment period the ADCPs were configured to record velocities in 0.5 m vertical bins. As data collection did not begin until 1.5 m above the instrument (itself approximately 0.5 m off the seafloor), the first data bin ranges from 2 to 2.5 m. Since a velocity value represents the center of the vertical bin, the first data bin represents 2.25 m off the seafloor. At Site Be reliable data were collected in 16 bins, ranging from heights above the seafloor of 2.25 m to 10.25 m; this equated to near-bottom, mid-depth, and near-surface water depths of 10.75, 7.25 and 3.25 m respectively. At Site Bw in 7.5 m of water, 7 bins of reliable data were collected, corresponding to near-bottom, mid-depth, and near-surface water depths of 5.25, 3.75 and 2.25 m depth. Examples of the time series currents are presented for the April deployment in Figures 3-34 and 3-35; data for the May deployment are presented in Figures A-15 and A-16.

In general, currents appeared to be weaker near-shore at Site Bw than at Site Be, with the exception of a few events, particularly that of 18 April, when velocities approached 1 m/s (~2 kts) near the surface (Figure 3-34). Unlike some events noted at Site Be farther offshore, the major events at Bw affected the entire water column. The current direction at Site Bw did not have as consistent a signature as offshore (particularly at deeper depths), but was still predominantly either northward or southward at all depths. Velocities were somewhat reduced in May at all water levels and the tidal currents were stronger at the beginning and end of both deployment periods. This periodic increase in tidal velocities could be due to the spring-neap modulation of the semidiurnal tide, however, without a complete harmonic analysis this cannot be stated with certainty.

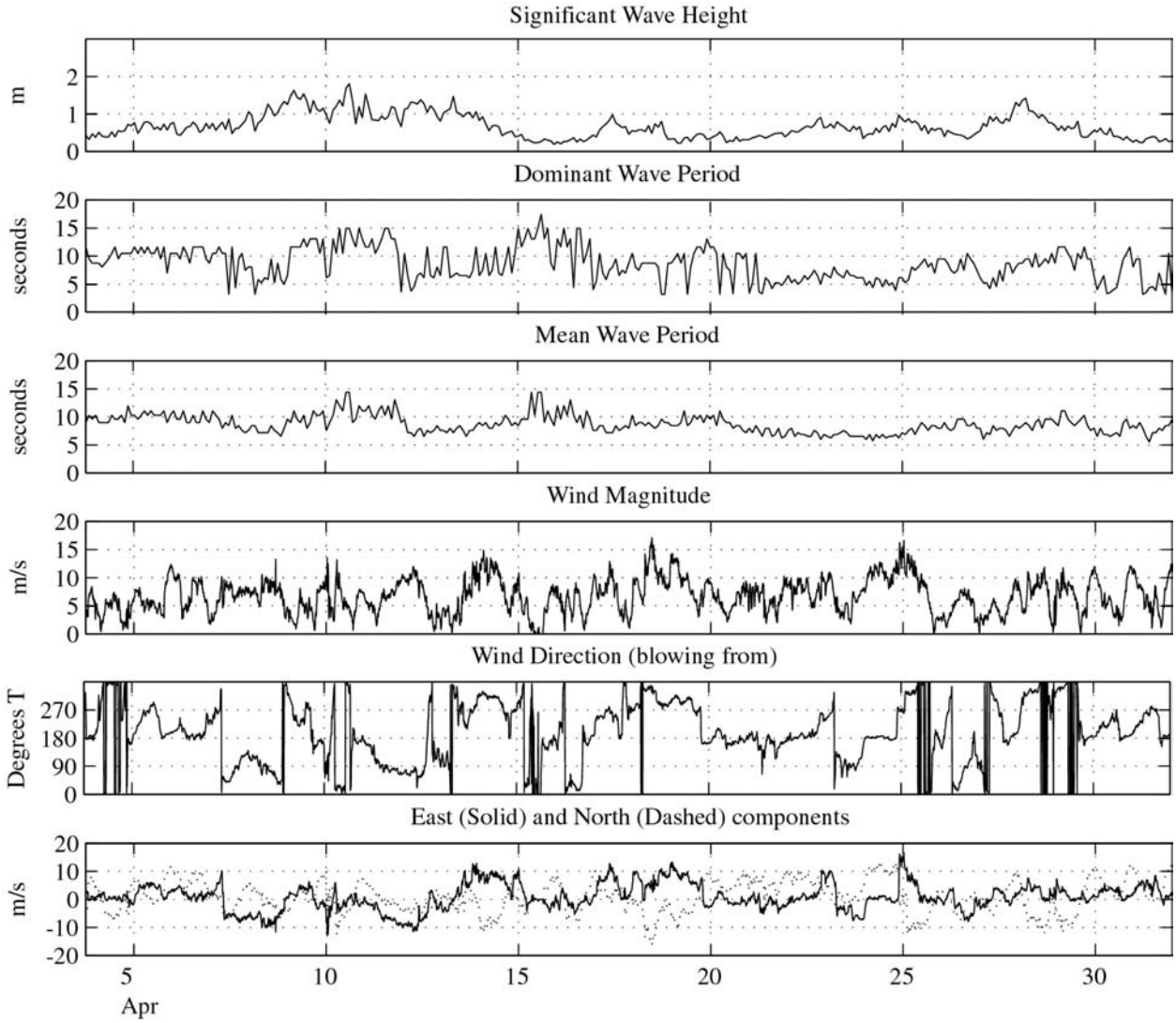

Figure 3-33. Time series of wave and wind data from Deployment 4, spring 2001. Wave data was derived from a bottom mounted pressure sensor at Site Be, presented as significant wave height, and wind data was downloaded from the NOAA Ambrose Light Tower station.

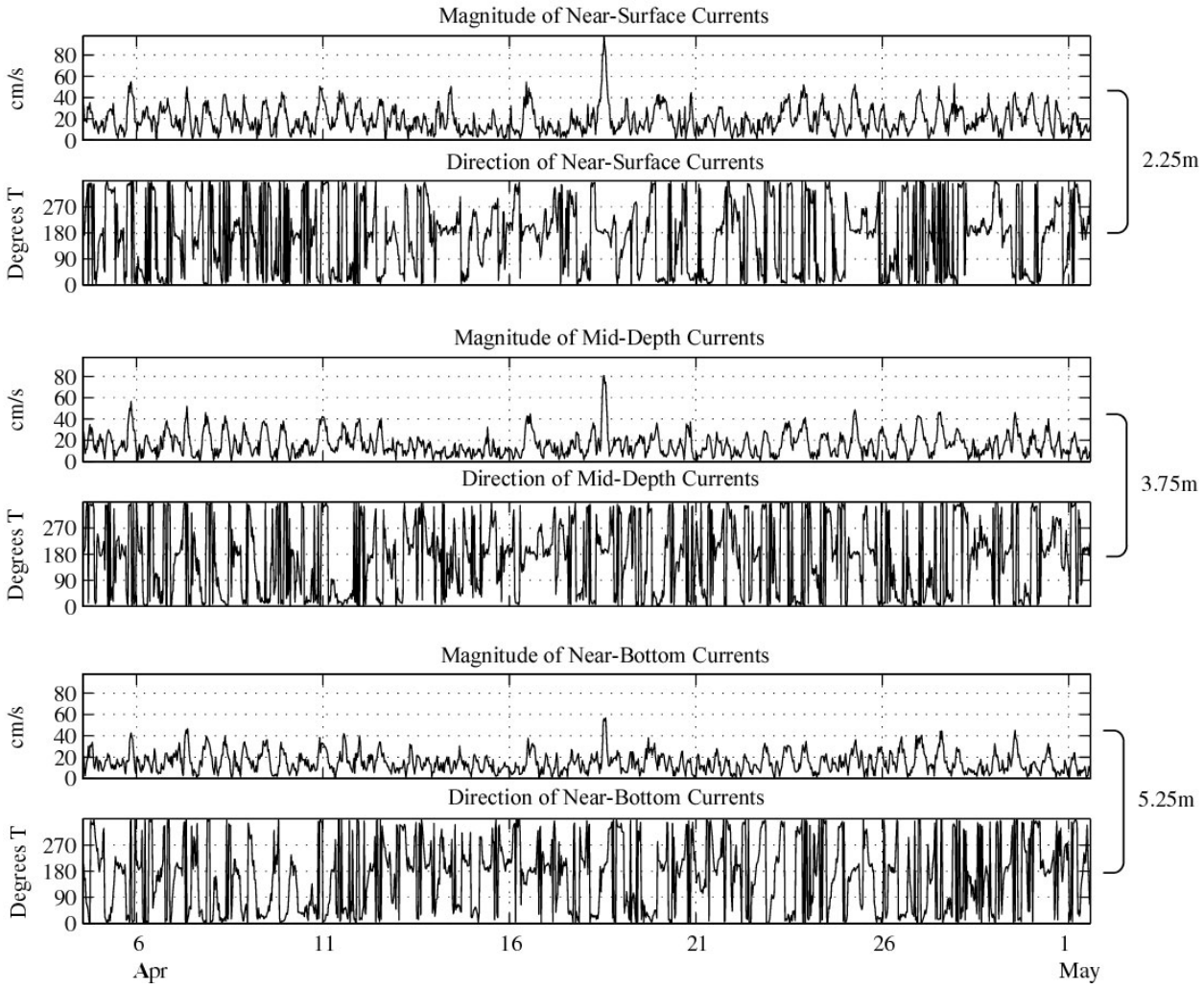

Figure 3-34. Time series of current magnitude and direction acquired by ADCP from three depth levels, Site Bw, Deployment 4, spring 2001. Values to the right of plots indicate measurement depth.

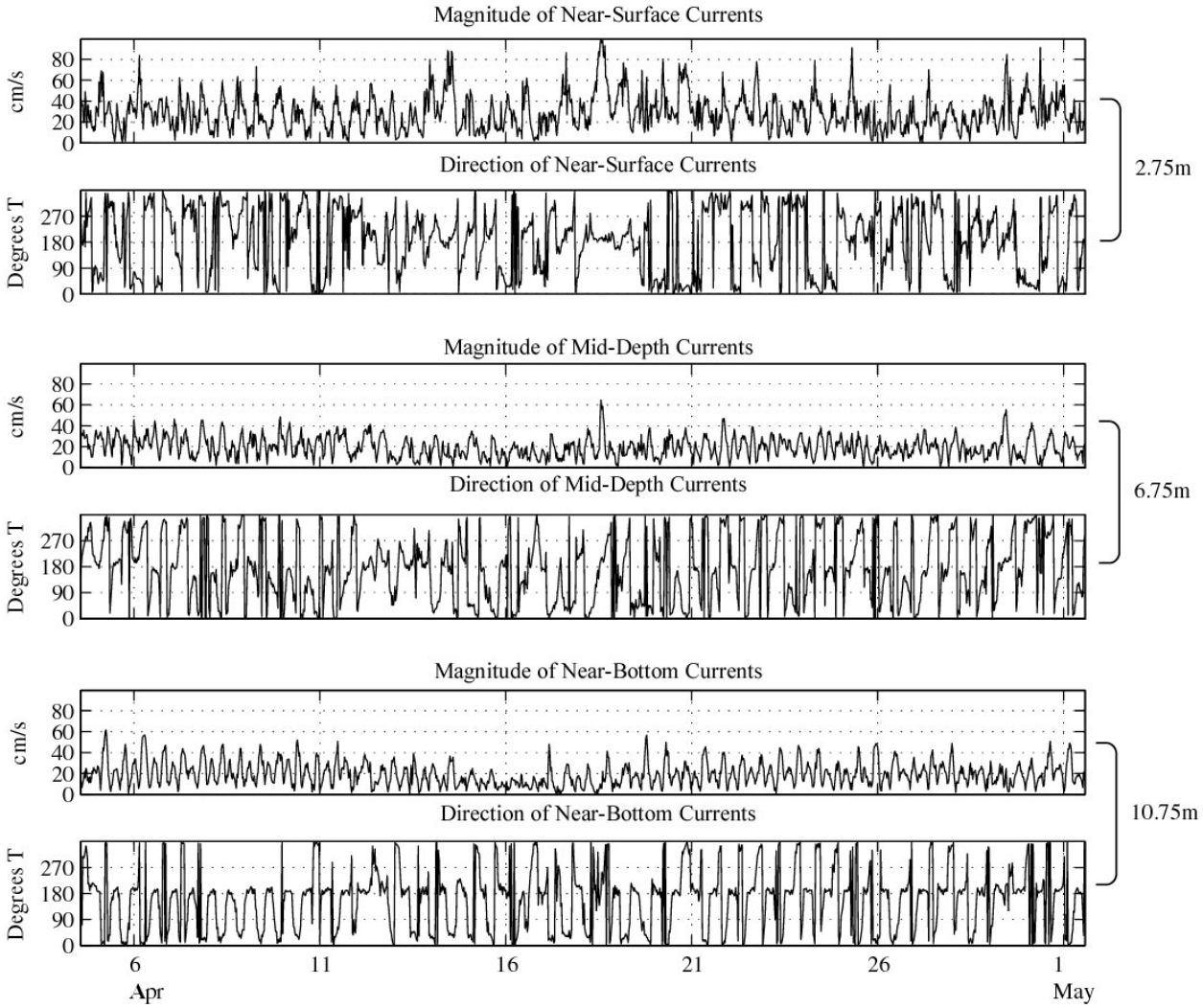

Figure 3-35. Time series of current magnitude and direction acquired by ADCP from three depth levels, Site Be, Deployment 4, spring 2001. Values to the right of plots indicate measurement depth.

Velocities offshore at Site Be were generally higher than inshore, with several large events (velocities greater than 60 cm/s) noted at all depths (Figure 3-35). Although the semi-diurnal tide was the prevalent signal, it was interrupted significantly by these larger events, particularly near the surface. For instance, on 18 April a constant flow to the south persisted for more than one day through multiple tidal cycles. Currents were far more consistent at greater depths, with the tidal influences dominating the record.

Near-bottom Currents

Of the four instrument arrays, three (A, Bw, and Be) were equipped with ARESS velocity and OBS turbidity sensors, and one (C) was equipped with a Nortek Aquadopp acoustic Doppler current meter and one OBS sensor. This single deployment at Site C coincided with the end of Deployment 4 and all of Deployment 5 for the other sites (Table 2-3). Data from the April deployment are presented for Sites A, Bw, and Be, respectively in Figures 3-36 to 3-38; data for the May deployment are presented in Figures A-17 through A-19.

At Site A to the north, near-bottom currents were fairly weak through April and May, with tidal velocities typically around 20 cm/s, and peak events near 40 cm/s (Figure 3-36). Overall, tidal currents were somewhat stronger at the beginning and end of the record; given the one-month deployment period, this difference in current magnitude was most likely due to the spring-neap modulation of the semi-diurnal tide. Currents were weaker at the lower sensor with tidal velocities from 10 to 15 cm/s, and peaks of ~30 cm/s. Direction data from both sensors showed the currents to be primarily rotary, sweeping counterclockwise through the entire compass rose, and typically not persisting in one direction for any length of time.

Farther southward at Site Bw, near-bottom currents were even weaker, with tidal currents of 10 to 15 cm/s and peaks of 25 to 30 cm/s in the upper sensor, and peaks of 15 to 20 cm/s in the lower sensor (Figure 3-37). Current direction was primarily bi-directional, though many deviations from this pattern were noted; for instance, from 8 to 9 May the direction appeared more rotary (Figure A-18). As noted at Site A, currents were stronger at the beginning and end of the deployment.

Currents increased in magnitude farther offshore at Site Be, with higher peak values (>50 cm/s), and a higher background mean (Figures 3-38 and A-19). A significant diurnal inequality was noted between successive tidal cycles and, as at the other sites, tidal velocities were greater at the beginning and ends of the record. Current direction was primarily bi-directional, switching between northward and southward currents.

Only one somewhat longer deployment was made at Site C to the south along the NJ shore (Figure 3-39). The Aquadopp instrument was set approximately 1 m off the seafloor and recorded current data at that level. Near-bottom currents were weaker here than at the northern sites, with average tidal velocities ranging from 5 to 10 cm/s and observed peak velocities of 15 to 20 cm/s. Again, current direction was primarily bi-directional in a northward and southward direction.

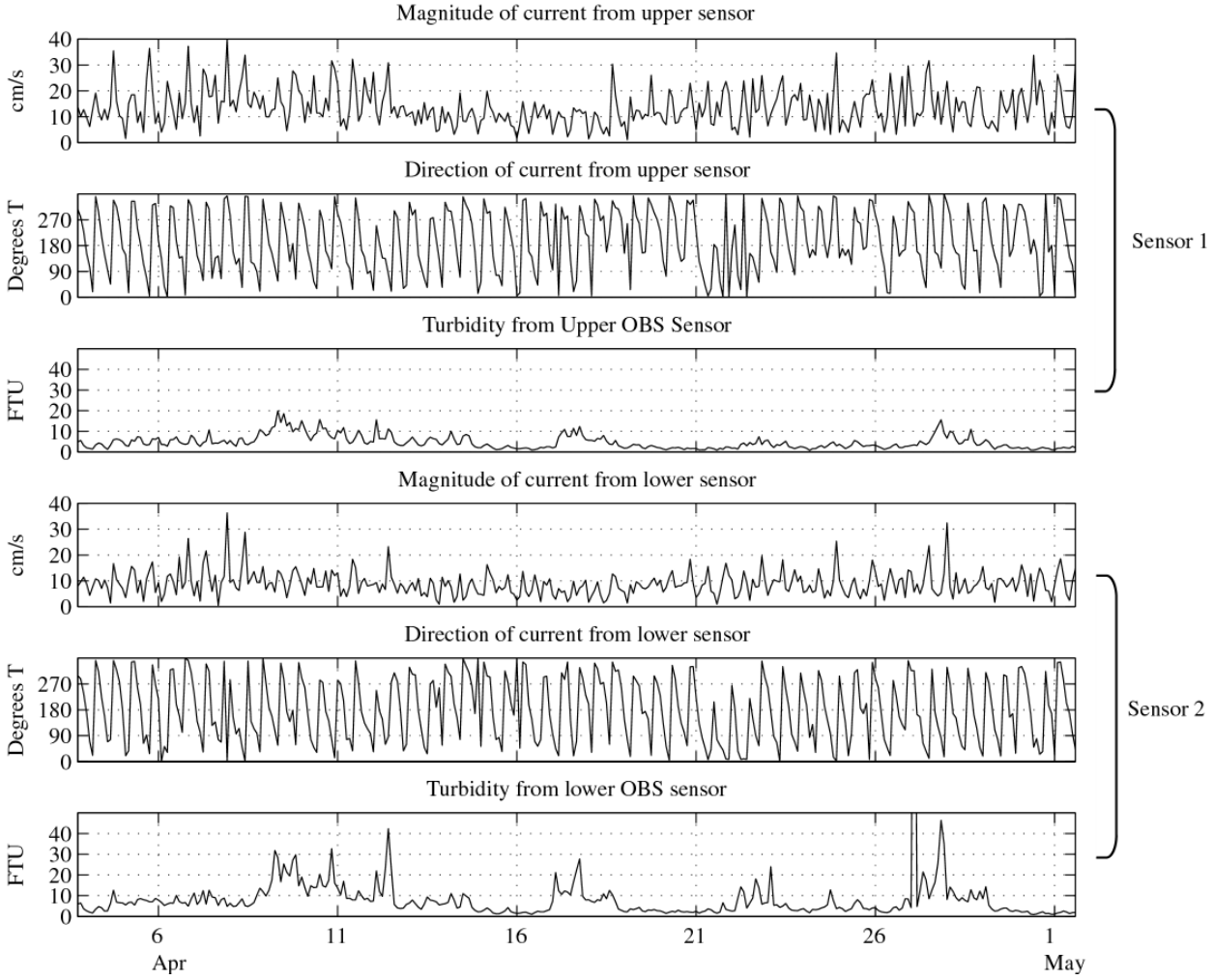

Figure 3-36. Time series of near-bottom current speed and direction and turbidity from two depth levels; 1.52 m (Sensor 1) and 0.76 m (Sensor 2), Site A, Deployment 4, spring 2001.

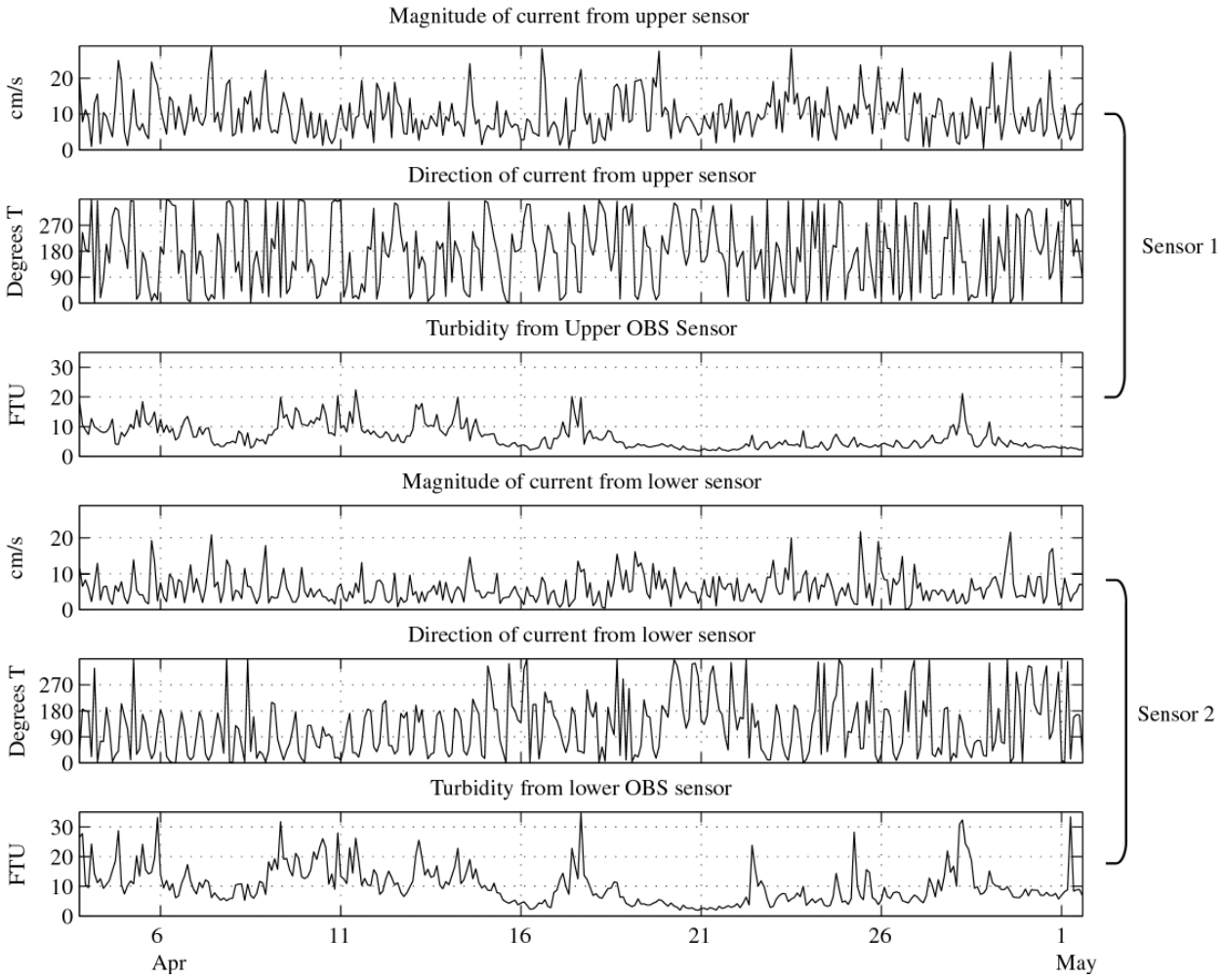

Figure 3-37. Time series of near-bottom current speed and direction and turbidity from two depth levels; 1.52 m (Sensor 1) and 0.76 m (Sensor 2), Site Bw, Deployment 4, spring 2001.

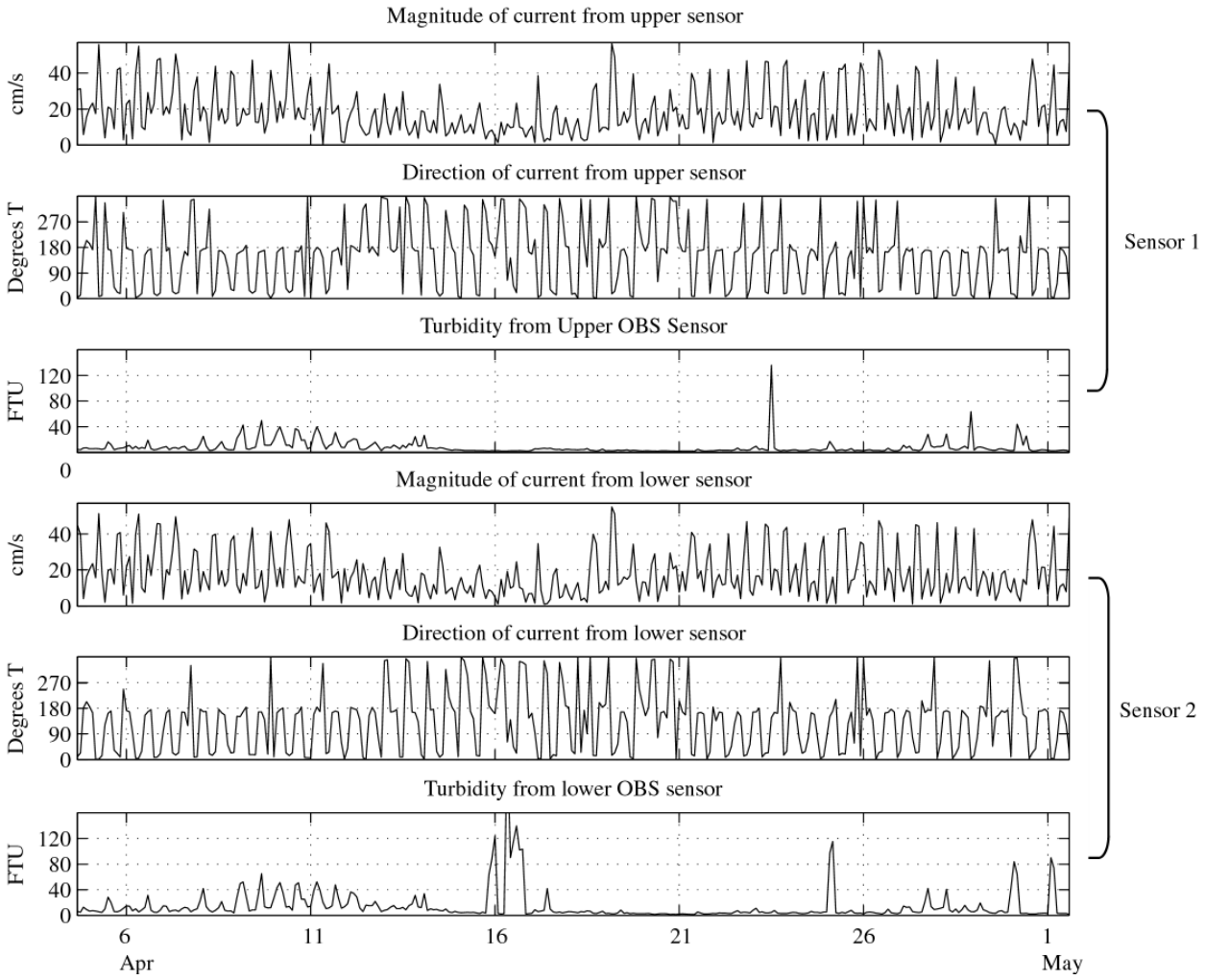

Figure 3-38. Time series of near-bottom current speed and direction and turbidity from two depth levels; 1.52 m (Sensor 1) and 0.76 m (Sensor 2), Site Be, Deployment 4, spring 2001.

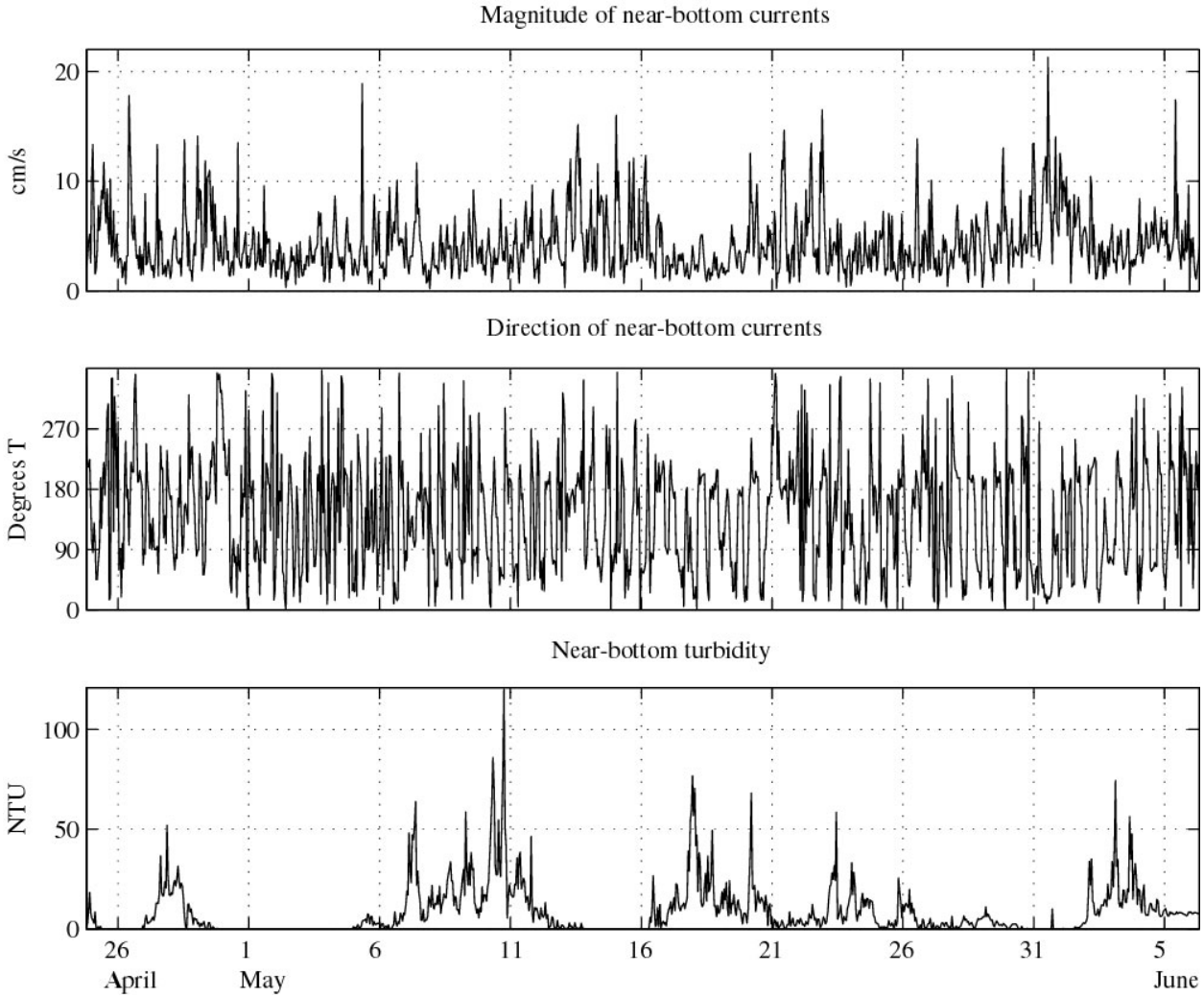

Figure 3-39. Time series of near-bottom current speed and direction and turbidity from two depth levels; 1.52 m (Sensor 1) and 0.76 m (Sensor 2), Site C, Deployment 4, spring 2001.

Near-bottom Turbidity

Turbidity data were acquired at all four sites, from two different levels at the three northern sites (A, Be, and Bw) and from one level at the southernmost site (C); the turbidity sensor levels corresponded with the current meter levels at each array. Turbidity values were generally low at Site A (on the order of 0 to 10 FTU), with small events that persisted for one to three days (with near-bottom levels at 30 to 40 FTU) (Figure 3-36). One large spike (>100 FTU) was recorded in the lower sensor on 27 April; because the upper sensor did not show a response at this time, nor was there any corresponding event at the other sites, this turbidity spike was attributed to solid matter interfering with the sensor. Similar turbidity results were noted in May for the upper and lower sensors (Figure A-17), with three events that exceeded 50 FTU, and overall low background values.

Turbidity at Site Bw in April also showed consistently low background values (5-15 FTU) with several small peaks noted in both sensors (typical values of 20-35 FTU in the lower sensor and 15-20 FTU in the upper sensor) (Figure 3-37). Similar results were recorded in May, with the exception of two spikes in the lower sensor on May 17, which again were again attributed to short-term fouling at the sensor (Figure A-19). Offshore at Site Be, similar low background turbidity values were observed. Turbidity events were somewhat greater in magnitude, with several exceeding 40 FTU and a couple in the lower sensor exceeding 80 FTU (Figure 3-38). Once again, isolated high turbidity events were noted on 16 April in the lower sensor and on 23 April in the upper sensor, and were most likely the result of sensor interference from solid matter. At this site, there were periodic increases in turbidity that appeared to be closely correlated with the tidal cycle (e.g., 8 to 13 April).

Farther to the south at Site C, the turbidity events in May (Figure 3-39) were generally greater in magnitude and persisted for longer periods than at other sites; the timing of these events corresponded well with events noted at the other sites. As stated earlier, a turbidity sensor of a different manufacturer was used at this site, and values are reported in Nepholometric Turbidity Units (NTU). Although FTUs and NTUs can be used interchangeably, if the turbidity sensors have not been calibrated to a consistent standard, then a direct comparison between sensors may not provide consistent results. It is likely that the difference in magnitudes between Site C and the other sites can be attributed to the difference in calibration standards.

3.2.3 Long-Term Mean and Statistics

Water Column Current Statistics – Vertical Means

Statistics of currents measured throughout the water column at Sites Bw and Be for both spring deployments are presented in Tables 3-6 and 3-7; mean speed and direction, and vector magnitude for the entire water column are plotted in Figure 3-40 for the April deployment. At Site Bw, situated near-shore and westward from Site Be, mean vector magnitudes were greater, showing a fairly consistent profile with magnitudes slightly higher at mid-depth than at the near-surface. Mean current direction was northward at all depths. In May (Table 3-6) mean speeds and vector magnitudes decreased noticeably throughout the water column, although northward flow dominated.

Table 3-6.

Statistics of ADCP data collected at Site Bw during the spring 2001 deployment period

Deployment Number and dates	Depth Level (m)	Mean Vector Magnitude (cm/s)	Mean Direction	Mean Speed (cm/s)	Max Speed (cm/s)	Percentage of Observations in Speed ranges below								
						0-10	10-20	20-30	30-40	40-50	50-60	60-70	70-80	80-90
FOUR 4/3/2001 to 5/1/2001	2.25	5.7	359.2	19.3	98	24.3	34.9	22.3	12.7	4.3	1.0	0.1	0.0	0.4
	3.75	6.3	1.4	16.4	80.8	32.3	36.7	18.8	8.7	2.8	0.3	0.1	0.2	0.1
	5.25	4.8	11.5	15.1	56.9	34.8	37.7	19.6	6.6	1.1	0.3	0.0	0.0	0.0
FIVE 5/3/2001 to 6/5/2001	2.25	3.6	333.2	17	53.7	27.2	38.8	23.1	8.6	2.0	0.3	0.0	0.0	0.0
	3.75	4.1	351.3	15.4	51.2	33.6	38.1	20.5	6.5	1.2	0.1	0.0	0.0	0.0
	5.25	4.1	11.3	14.6	56.9	33.3	43.1	18.1	4.9	0.6	0.1	0.0	0.0	0.0

Table 3-7.

Statistics of ADCP data collected at Site Be during the spring 2001 deployment period

Deployment Number and dates	Depth Level (m)	Mean Vector Magnitude (cm/s)	Mean Direction	Mean Speed (cm/s)	Max Speed (cm/s)	Percentage of Observations in Speed ranges below								
						0-10	10-20	20-30	30-40	40-50	50-60	60-70	70-80	80-90
FOUR 4/3/2001 to 5/1/2001	2.75	3.4	307.1	29	99.3	10.9	23.2	23.1	20.8	11.0	5.6	2.7	1.2	1.5
	6.75	2.3	13	19.7	64.5	17.8	35.3	30.4	14.1	1.9	0.4	0.1	0.0	0.0
	10.75	1.7	46.4	19.6	61.6	21.6	34.6	26.6	10.7	5.3	1.0	0.1	0.0	0.0
FIVE 5/3/2001 to 6/5/2001	2.75	6.8	258.8	23.8	72.7	11.2	31.1	29.4	17.5	8.4	2.0	0.2	0.1	0.0
	6.75	1.5	269.2	17.7	60.2	24.4	38.5	25.4	10.1	1.5	0.1	0.1	0.0	0.0
	10.75	4.4	20.8	19.5	61.2	22.0	36.7	23.5	10.8	6.0	1.0	0.1	0.0	0.0

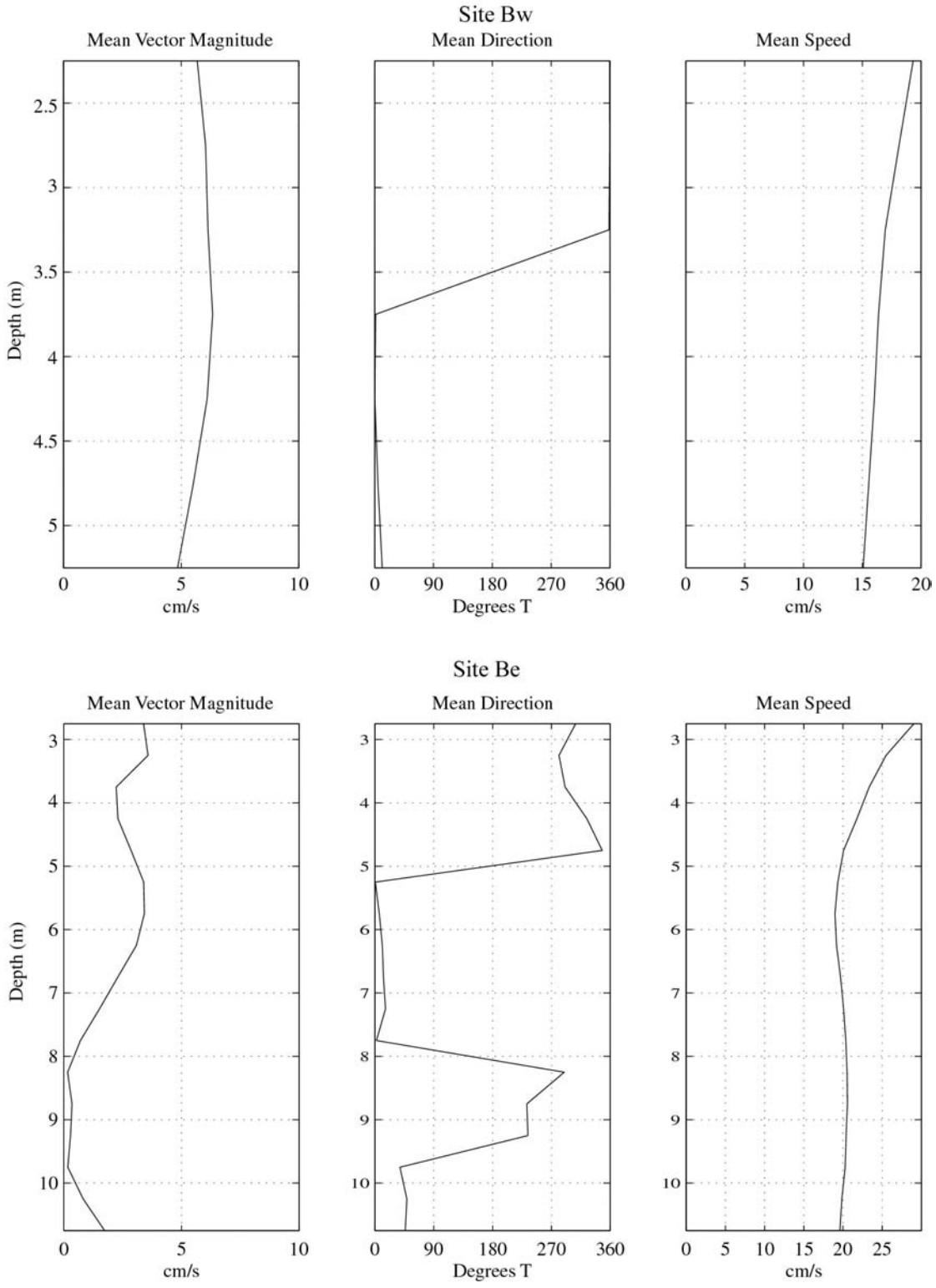

Figure 3-40. Vertical profiles of mean vector magnitude and direction and mean speed for Deployment 4, spring 2001, from ADCP data at Sites Bw and Be.

Mean vector magnitudes at Site Be were lower in spring than at Site 1(co-located with Site Be; Figure 2-1) in the fall, and increased slightly from the April (Deployment 4) to the May deployment. From near-surface to bottom, magnitudes gradually decreased to a minimum at mid-depth and increased slightly again to the bottom in April (Figure 3-40, lower plots). The mean direction for April showed a northwestward flow at the near-surface, a northward flow through the mid-depth, southwestward flow below, and a northeastward flow near the bottom.

Mean speeds showed a consistently decreasing profile with depth at Site Bw, ranging from ~19 cm/s at the near-surface to 15 cm/s at the near-bottom in April (Figure 3-40); these values decreased to a range of 17 to ~14.5 cm/s in May (Table 3-6). Maximum speeds of almost 1 m/s were reached at the near-surface in April and decreased consistently with depth to a maximum of ~57 cm/s at the near-bottom. In May, maximum speeds dropped considerably at the near-surface and mid-depth levels to ~54 and 51 cm/s respectively, but remained at ~57 cm/s at the near-bottom (Table 3-6). Higher mean speeds were recorded offshore at Site Be, ranging from 29 cm/s at the near-surface to ~20 cm/s at the near-bottom (Table 3-7). Near-surface and mid-depth mean speeds dropped in May, with a water column minimum of ~18 cm/s noted at mid-depth. Maximum speeds at Site Be also reached 1 m/s at the near-surface in April and decreased to ~62 cm/s at the near-bottom. Maximum speeds were lower at the near surface in May (at approximately 73 cm/s), but were still higher than those observed at Site Bw. May mid-depth and near-bottom maxima were similar to the values observed in April.

Water Column Current Histograms

Inspection of histogram plots of current velocities at Site Bw for April showed that the highest number of observations were in the 10-20 cm/s range at all depths (Table 3-6). Near-surface currents showed higher percentages in the higher ranges, whereas near-bottom showed higher percentages in the lower ranges. The analysis for the May data showed similar results, though fewer observations were made in the higher ranges at near-surface. Statistics for Site Be showed that observations were more evenly distributed between the first few velocity ranges in April, particularly at the near-surface (Table 3-7). Higher percentages of observations were noted in the higher velocity ranges at the offshore (Be) site than at the near-shore (Bw) site. Similar results were observed in May, though a higher percentage of observations were noted in the lower ranges than in April.

Histogram plots of current direction data on rose diagrams illustrate the bi-directional nature of currents near the shore at Site Bw (Figure 3-41). In both April and May, the majority of observations were directed toward the north or south at all depths, with a slightly higher percentage to the north. Farther offshore at Site Be, current directions were more random at the near-surface, with all directions almost equally represented during April (Figure 3-42). Mid-depth and near-bottom currents were more bi-directional, as at Site Bw, with a prevalence of southward currents at the near-bottom. Similar results were noted in May, however, a prevalence of westward to southward currents was noted in the near-surface.

Near-bottom Current Means

Results of statistical analysis from the ARESS arrays deployed in the spring of 2001 are presented in Tables 3-8 to 3-11. In general, currents were stronger in the spring than in the fall (Tables 3-3 to 3-5), with higher mean speeds and maximum speeds. Mean vector magnitudes at

Table 3-8.

Statistics of near-bottom currents as recorded by ARESS at Site A during the spring 2001 deployment period

Deployment Number and dates	Sensor Level (cm)	Mean Vector Magnitude (cm/s)	Mean Direction	Mean Speed (cm/s)	Max Speed (cm/s)	Percentage of Observations in Speed ranges					
						0-10	10-20	20-30	30-40	40-50	50-60
Four 4/3-5/1/2000	152	3.1	0.0	13.5	39.8	34.9	48.1	13.1	3.9	0.0	0.0
	76	2.4	0.1	8.9	36.3	66.6	31.0	1.8	0.6	0.0	0.0
Five 5/3-6/6/2000	152	4.0	0.0	14.2	43.6	32.2	47.7	16.8	3.0	0.3	0.0
	76	3.2	6.2	8.7	32.4	68.1	28.4	3.3	0.3	0.0	0.0

Table 3-9.

Statistics of near-bottom currents as recorded by ARESS at Site Bw during the spring 2001 deployment period

Deployment Number and dates	Sensor Level (cm)	Mean Vector Magnitude (cm/s)	Mean Direction	Mean Speed (cm/s)	Max Speed (cm/s)	Percentage of Observations in Speed ranges					
						0-10	10-20	20-30	30-40	40-50	50-60
Four 4/3-5/1/2000	152	3.0	0.4	9.7	28.7	57.3	37.0	5.7	0.0	0.0	0.0
	76	2.4	0.9	6.0	21.8	86.3	12.5	1.2	0.0	0.0	0.0
Five 5/3-6/5/2000	152	2.5	0.7	8.3	26.6	68.9	27.5	3.6	0.0	0.0	0.0
	76	1.8	0.4	4.8	19.8	88.3	11.7	0.0	0.0	0.0	0.0

Table 3-10.

Statistics of near-bottom currents as recorded by ARESS at Site Be during the spring 2001 deployment period

Deployment Number and dates	Sensor Level (cm)	Mean Vector Magnitude (cm/s)	Mean Direction	Mean Speed (cm/s)	Max Speed (cm/s)	Percentage of Observations in Speed ranges					
						0-10	10-20	20-30	30-40	40-50	50-60
Four 4/4-5/1/2000	152	5.8	0.6	18.3	56.3	31.5	33.6	16.4	7.4	9.3	1.9
	76	7.0	0.6	17.9	54.9	34.0	34.0	13.0	8.3	9.6	1.2
Five 4/3-6/6/2000	152	6.0	0.4	13.7	48.7	48.7	29.9	7.7	7.7	6.0	0.0
	76	6.2	0.4	12.0	41.8	59.8	18.8	10.3	7.7	3.4	0.0

Table 3-11.

Statistics of near-bottom currents as recorded by ARESS at Site C during the spring 2001 deployment period

Deployment Number and dates	Sensor Level (cm)	Mean Vector Magnitude (cm/s)	Mean Direction	Mean Speed (cm/s)	Max Speed (cm/s)	Percentage of Observations in Speed ranges					
						0-10	10-20	20-30	30-40	40-50	50-60
Four 4/24-6/6/2000	100	1.3	2.2	4.3	21.3	94.4	5.5	0.1	0.0	0.0	0.0

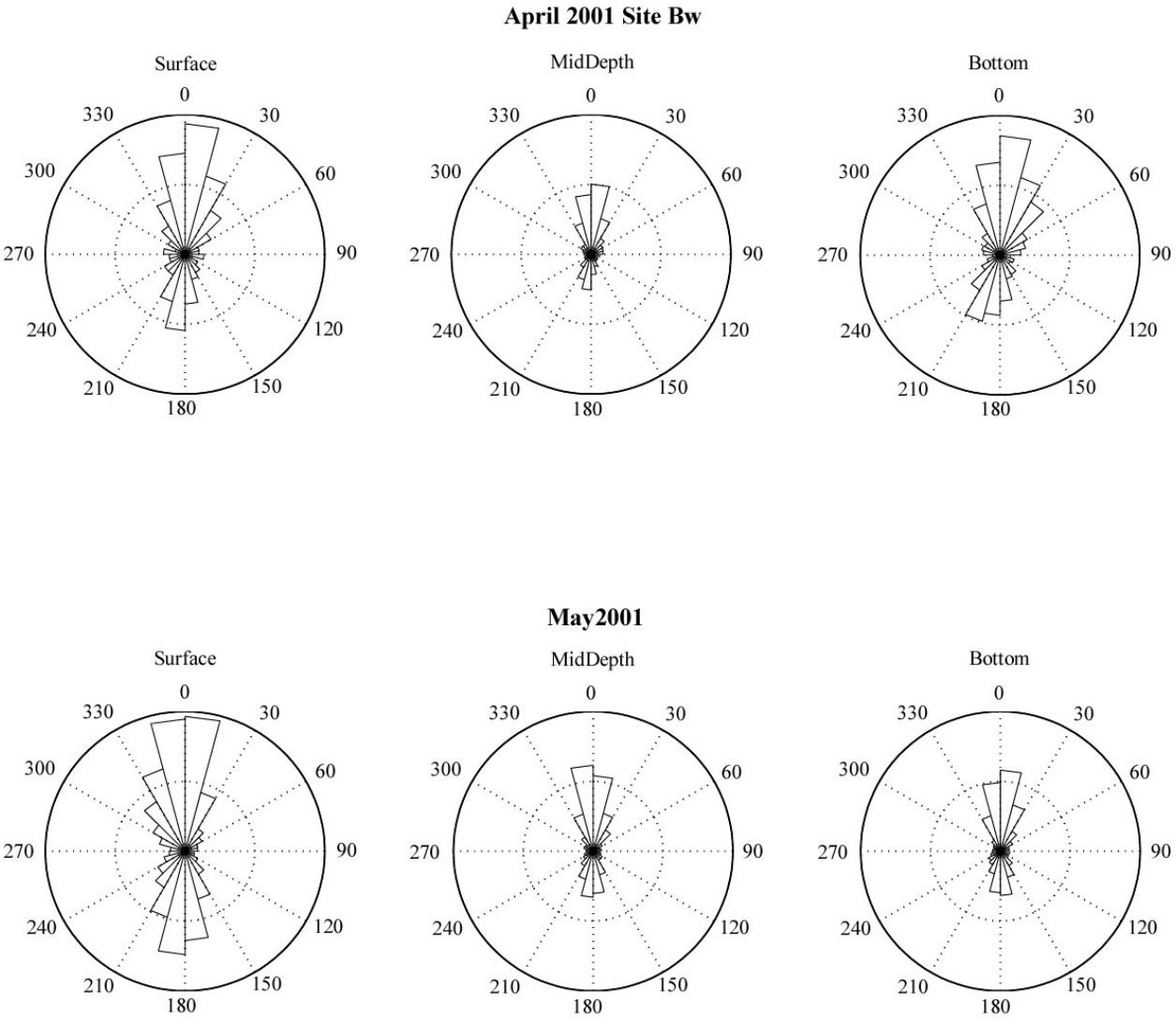

Figure 3-41. Rose histograms of current meter data from ADCP at three depth levels for the spring 2001 deployment period at Site Bw.

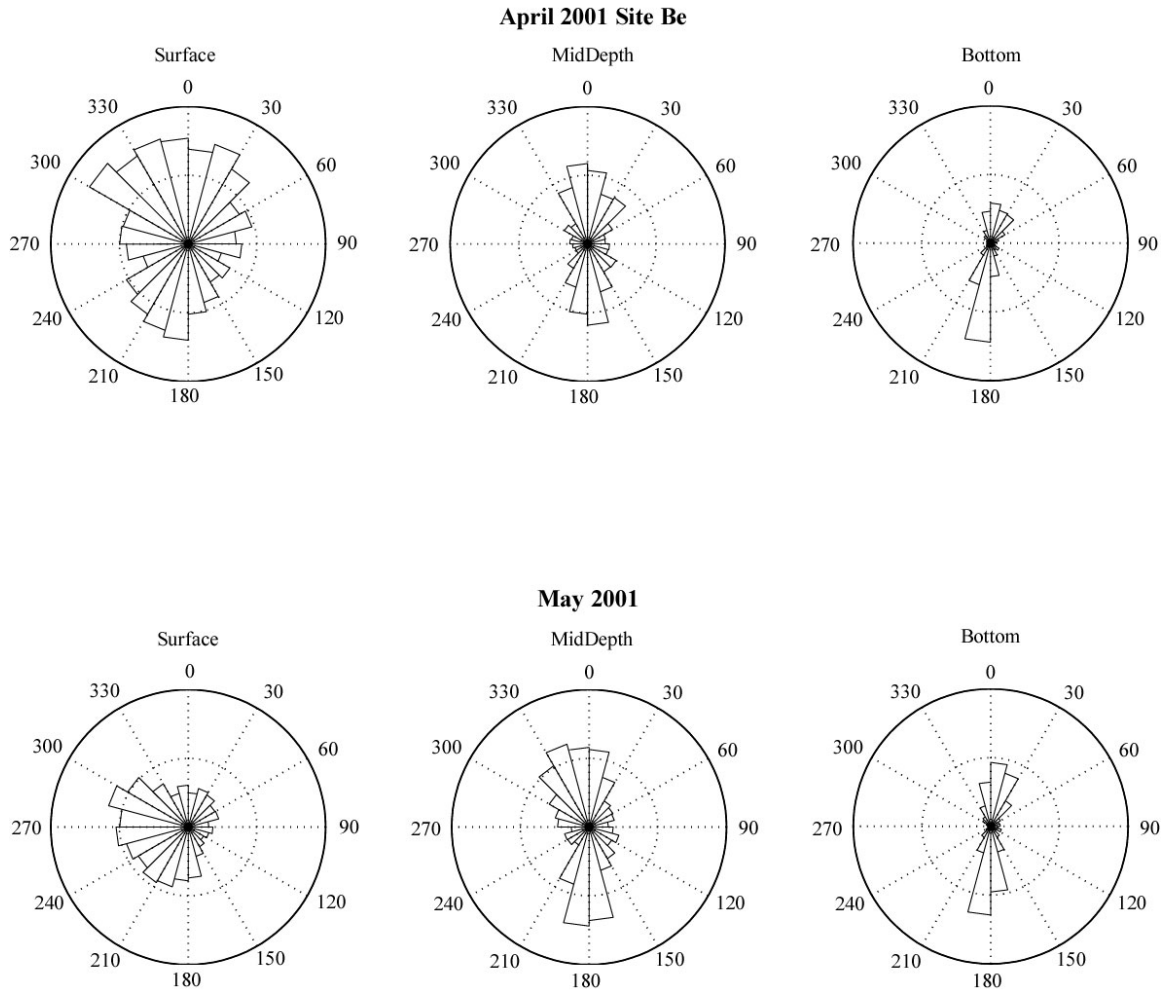

Figure 3-42. Rose histograms of current meter data from ADCP at three depth levels for the spring 2001 deployment period at Site Be.

Site A were weak (below 5 cm/s) at both levels for each deployment, and direction was predominantly to the north. This same general regime also held true for the other two alongshore sites (Sites Bw and C). Site Be showed slightly higher mean vector magnitudes, at 6 to 7 cm/s, and direction was still northward for both sensor levels at each deployment.

Mean speeds were considerably higher in the upper sensor at Site A than the lower sensor (approximately 14 cm/s versus 9 cm/s; Table 3-8). Maximum speeds recorded during each deployment were similar, varying from ~32 to ~44 cm/s. At Site Bw (Table 3-9), both mean and maximum speeds were lower than at Site A: from 5 to 9 cm/s for mean and from 20 to 29 cm/s for maximum. The lowest mean and maximum speeds were recorded at Site C (Table 3-11) to the south (below 5 cm/s for mean and ~21 cm/s for maxima). The highest near-bottom mean speeds were recorded offshore at Site Be (12 to 18 cm/s; Table 3-10). Maximum speeds at Site Be ranged from 42 to 55 cm/s.

Near-bottom Current Histograms

Statistics of near-bottom current data illustrate a difference between upper and lower sensors at Site A. While the upper sensor indicated almost half of the observations in the 10 to 20 cm/s range, the lower sensor showed more than 2/3 of observations in the 0 to 10 cm/s range for each deployment (Table 3-8). This difference was noted at Site Bw as well, however, even higher percentages were noted in the 0 to 10 cm/s range for each sensor in each deployment (Table 3-9). Over 94 percent of the observations at Site C were within the lower range (Table 3-11). Offshore at Site Be, where currents were consistently the strongest, higher percentages were indicated in the higher ranges (Table 3-10).

Rose histograms of current direction for near-bottom velocities are plotted in Figure 3-43. The lower sensor at Site A showed primarily a bi-directional current structure in the northwest and southeast directions, aligned with the coastline at this deployment location. Site Bw showed the bi-directional nature as well, aligned in a more north-south orientation with a dominance of northward flow. A deviation from the bi-directional current structure at Sites A and Bw was noted at Site C, where flow tended to be either eastward, or southward. Offshore at Site Be, near-bottom currents were predominantly northward or south-southeastward, with a dominance of southward currents noted for each deployment.

3.2.4 Event-Based Processes

Water Column Low-pass Filtered Currents

As with the fall 2000 data, the spring ADCP velocity data were passed through a 30-hr low-pass filter to remove the tidal signal and to facilitate the interpretation of lower frequency events. Vector plots of the average data for deployment are presented in Figures 3-44 and 3-45 for Sites Bw and Be, respectively. Near shore at Site Bw, low-frequency currents tended to be bi-directional in the northward or southward direction, even at timescales greater than the dominant tidal cycles. Based on these data, the entire water column response appeared to be relatively uniform at this time of year at this site. Events in the near-surface typically showed a similar response at depth, although not always equal in magnitude. For instance, on April 23 low-passed, near-surface velocities exceeded 20 cm/s, while near-bottom velocities reached only

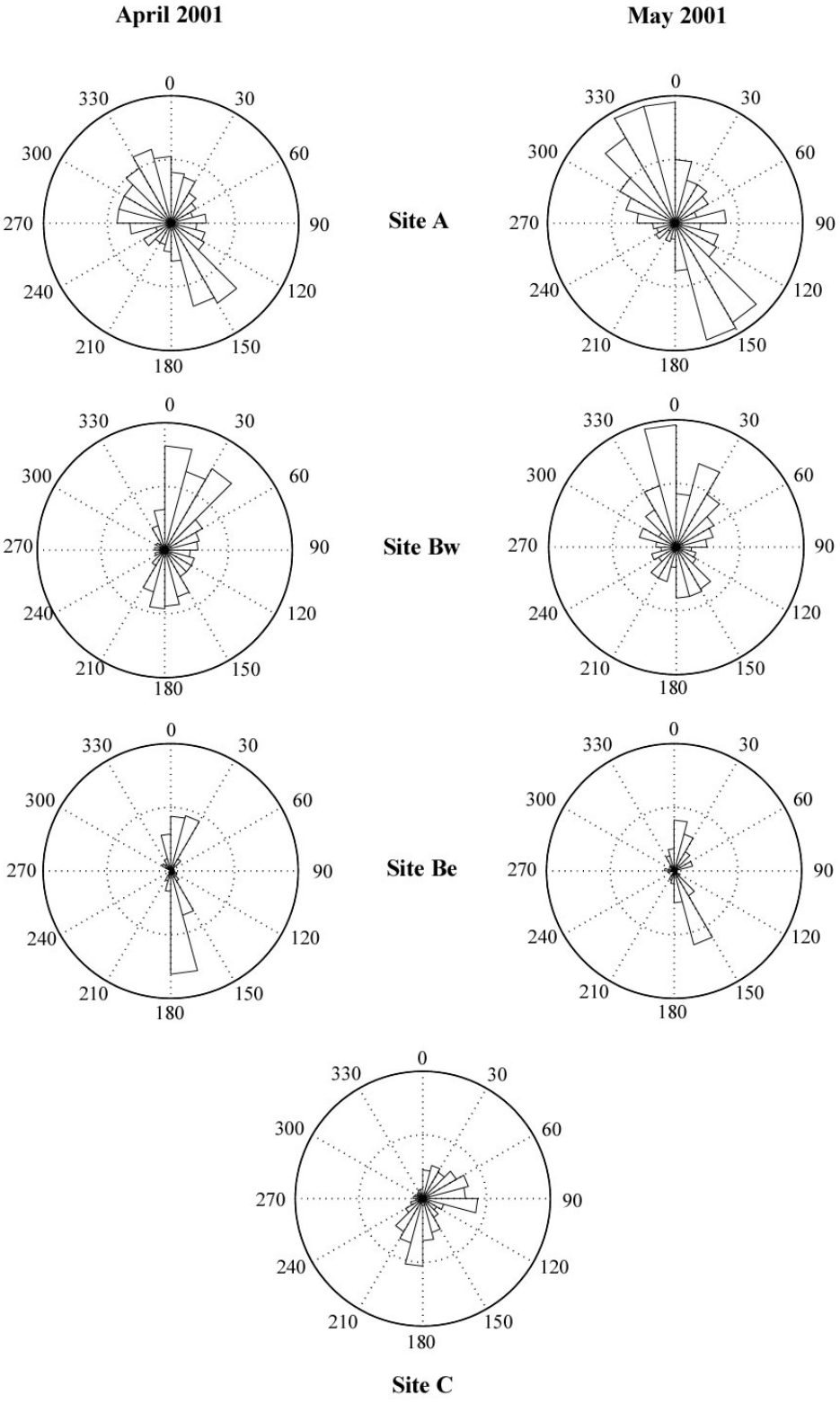

Figure 3-43. Rose histograms of near-bottom current meter data from ARESS at the lower depth level (0.76 m) for the spring 2001 deployment period at all Sites.

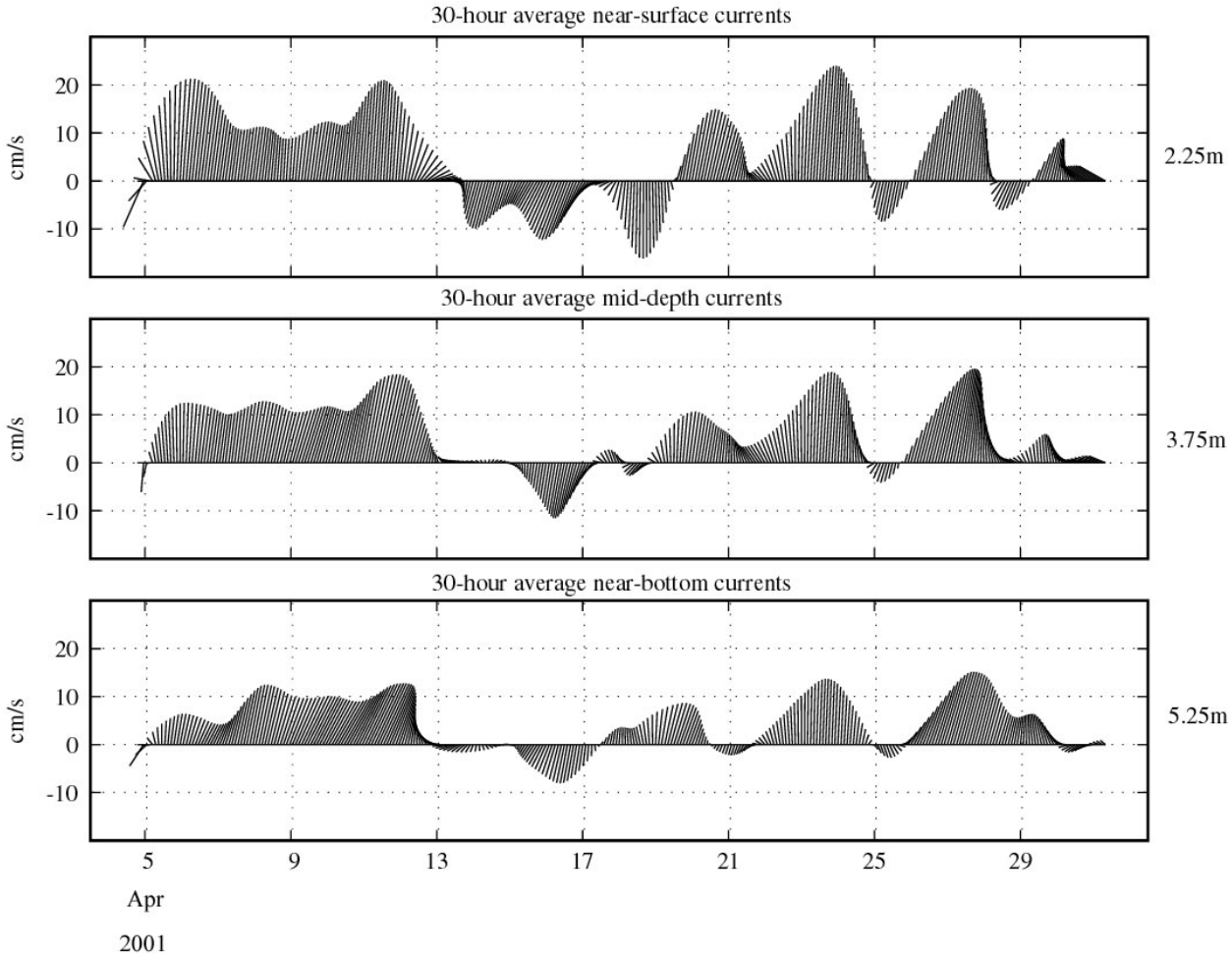

Figure 3-44. Time series vector plots of 30-hr LPF ADCP data from three depth levels for the spring 2001 deployment period at Site Bw. Values to the right of plots indicate measurement depth.

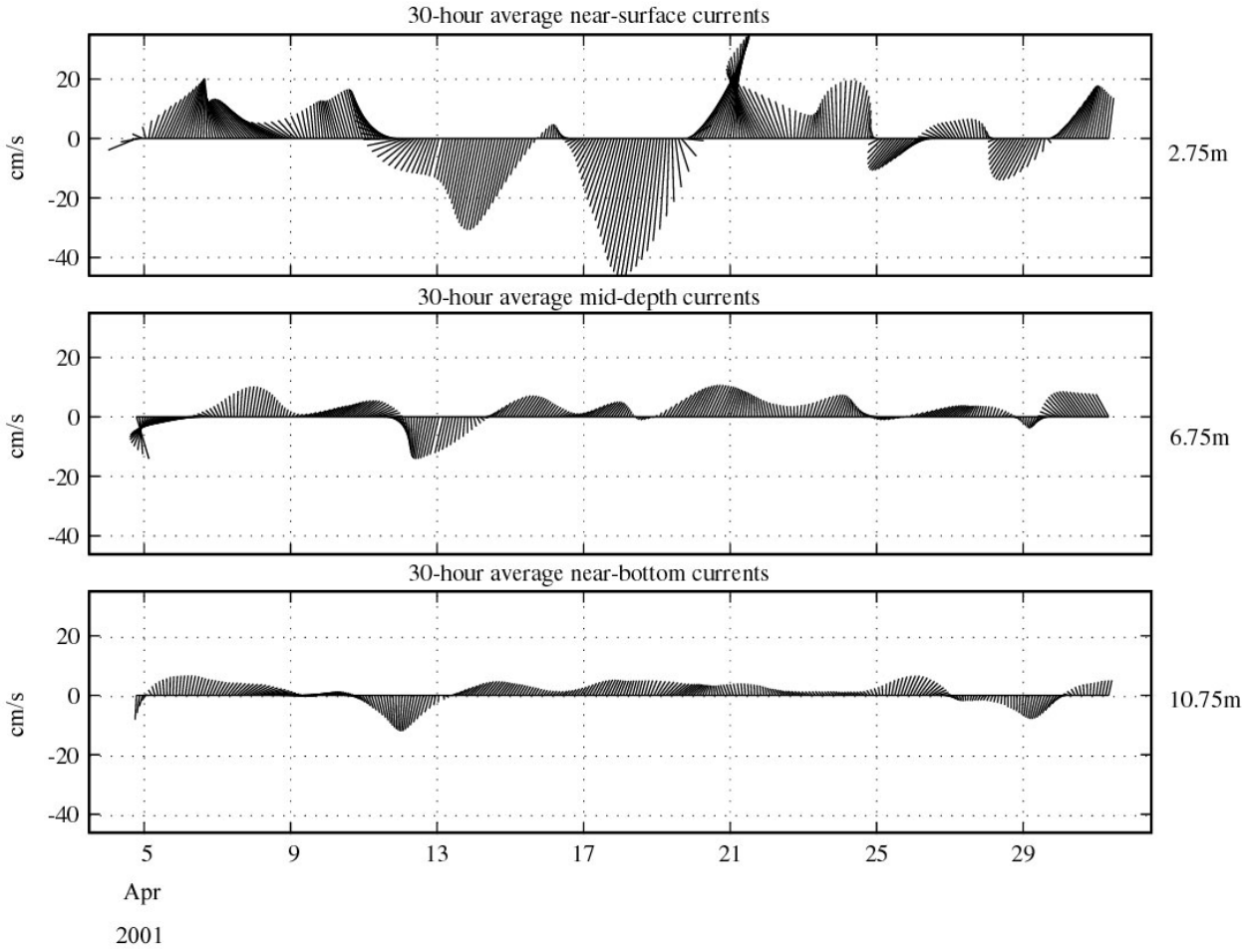

Figure 3-45. Time series vector plots of 30-hr LPF ADCP data from three depth levels for the spring 2001 deployment period at Site Be. Values to the right of plots indicate measurement depth. Values to the right of plots indicate measurement depth.

14 cm/s (Figure 3-44). Strong southward flow around 16 April was observed at all depths and corresponded well with higher river discharges noted at the Passaic River.

Offshore at Site Be, low-frequency currents were oriented primarily northward and southward, but skewed slightly to the northeast and southwest (Figure 3-45). Near-bottom velocities were considerably less than at near-surface, particularly for large events. A strong southward event beginning 12 April was noted at all depths, and was most likely associated with the stronger winds and freshwater discharge at that time. On 18 to 19 April, a large southward event (low-passed velocities exceeding 40 cm/s near-surface) was not manifested at depth. A different response was noted in the second week of May, where sustained southwestward currents at the near-surface appeared to have induced a northward response at the near-bottom.

Near-bottom Low-pass Filtered Currents

Filtering the data to remove tidal and high-frequency processes demonstrated the weak, low-frequency northward trend of the near-bottom currents at Site A (Figure 3-46). Most low-frequency events resulted in average northward velocities of less than 10 cm/s in both April and May. Farther down shore at Site Bw, average currents were still predominantly northward, though some periods of weak southward currents were noted. Comparing the near-bottom currents from ARESS at this site with the lowest bin of ADCP data (which corresponds to 2.25m above the seafloor, Figure 3-44), it can be noted that low-frequency currents in the mid-water column show more variability and are somewhat stronger than at the near bottom. In contrast to the sites to the north, Site C demonstrated primarily southward and eastward sub-tidal currents. This corresponds well with the rose histograms presented in the previous section, where the majority of current directions occurred to the east and south.

Offshore at Site Be, velocities were predominantly northward in both April and May, as noted at Sites A and Bw. Two small magnitude events to the southeastward on 13 and 29 April were the only periods where flow was not northward. As noted in previous sections, the average near-bottom current velocities were consistently greater at Site Be, with average velocities during some events exceeding 10 cm/s. In contrast to Site Bw, the low-frequency near-bottom currents as recorded by ARESS (Figure 3-46) show more variability than the lowest bin of current data from the ADCP (Figure 3-45).

3.2.5 Summary of Spring 2001 Results

- Winds and waves were considerably calmer in spring than in winter, with far fewer wind events exceeding 15 m/s and no waves over 2 m. As in the winter, periods of higher waves in spring were typically associated with winds blowing from the southeast, east, or northeast. Freshwater input to the system was actually less than in late winter and early spring, but one river discharge event did correspond to lower surface salinities noted at the near-shore Site Bw.

- As with the fall/winter data, the ADCP time series data revealed that the semi-diurnal tide was the most significant component of the current signal, and that the main flow was bi-directional in a northward and southward direction. The near-surface data appeared to be most affected by non-tidal current influences.

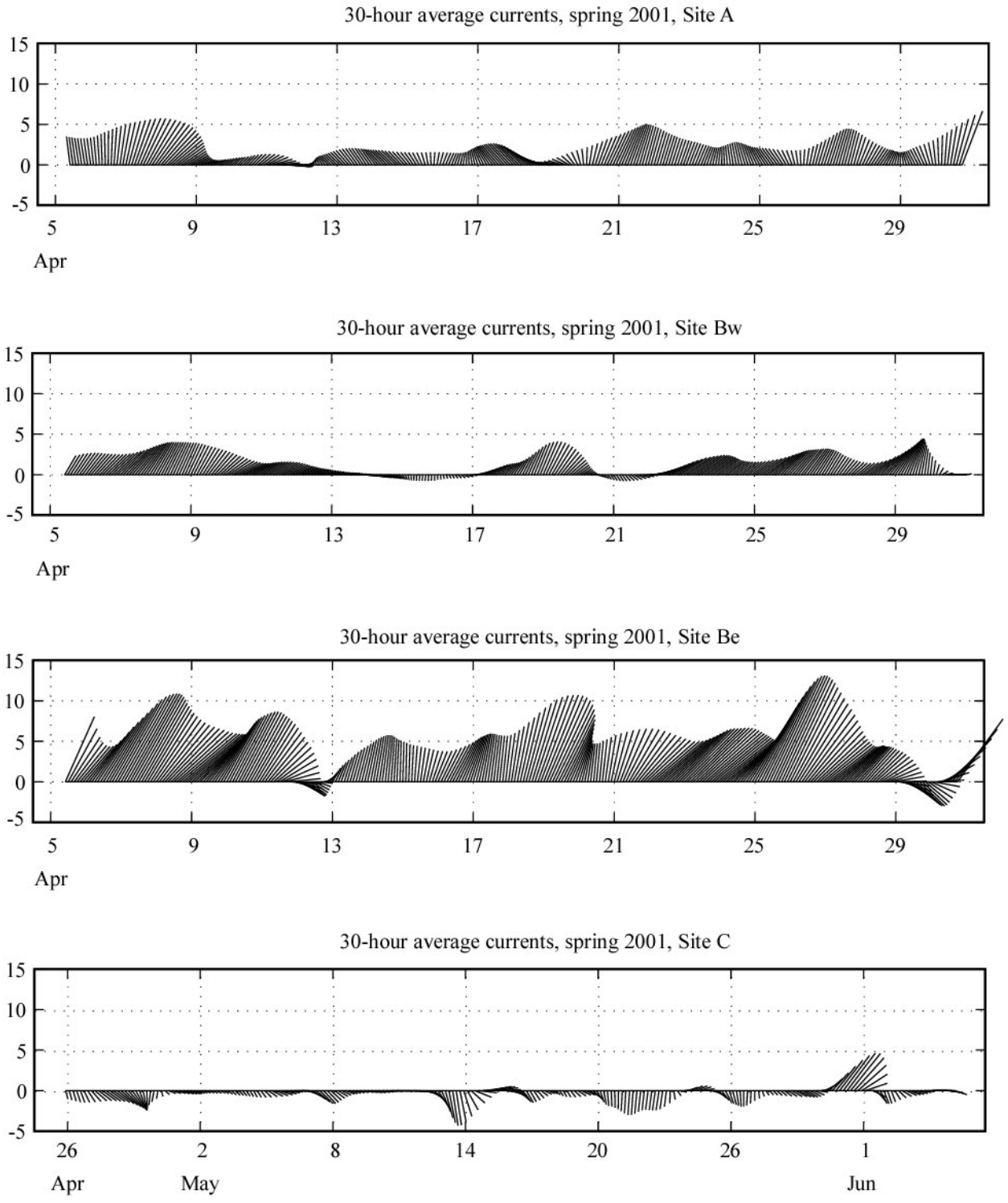

Figure 3-46. Time series vector plots of near-bottom currents from the lower sensor level (0.76 m off seafloor) for the spring 2001 deployment period at Site A (top tier), Site Bw (second tier), Site Be (third tier) and Site C (bottom tier).

- Near-bottom current meter data recorded at three sites along-shore and one site offshore demonstrated the differences between the two regimes. Near-bottom currents along the shoreline were weak and more scattered than even a few kilometers offshore, where strong northward and southward trends were observed.

- Turbidity data showed generally low background levels at all sites, with only a few small magnitude turbidity events (relative to the fall/winter program) noted during the period. Many of the smaller turbidity events noted in the spring were confined to the lower sensor and were typically short in duration.

- Mean water column speeds were greater at Site Be (coincident with Site 1) in spring than in fall, as were the maximum speeds. Histograms of current direction show the bi-directional nature of currents observed at most sites, with the exception of the near-surface at the offshore site, where more random directions were noted.

- Near-bottom currents were stronger in spring than in fall and early winter. Of the sites along the shore, Site A to the north demonstrated the highest mean and maximum speeds. Site Be offshore showed means and maxima that were higher still. Histograms of current direction reiterated the bi-directional nature of the currents in the study area, though the mean direction was consistently to the north.

- Examination of the ADCP velocity data in a sub-tidal context showed that low-period currents were primarily northward or southward throughout the water column. Strong velocity events generally occurred either northward or southward as well; however, at Site Be the strongest events were southward at near-surface and northward at near-bottom.

- Sub-tidal currents at near-bottom levels demonstrated primarily north to northeastward trends, with a few instances of southward currents that correlated with smaller storm events. Site C to the south demonstrated an entirely different current regime, with primarily southward and eastward near-bottom currents.

3.3 Supplemental Data—Fall/Winter 1999–2000

Due to difficulties with instrument recovery and performance, a complete dataset was not recovered from an oceanographic measurement program conducted in the fall/winter of 1999–2000 (11 November 1999 to 3 February 2000). Although four ARESS arrays were deployed during this program, only one complete set of useable data were obtained. Diving operations were necessary to recover three of the instrument arrays, and the fourth array was never recovered. Bottom trawl marks noted throughout this area during subsequent side-scan operations indicated that this array was likely lost due to fishing activity. Though this program provided insufficient data to enable a comprehensive oceanographic analysis, the data were used for comparisons against the 2000/2001 data.

Water Column Currents at HARS

An instrument array with an ARESS pod and an ADCP was deployed within the HARS in approximately 26.5 m of water (near Site 3 for fall/winter 2000 deployment period). Valid ADCP current data were acquired from 24.25 m to 3.25 m depth. The time series of current speed and direction from this deployment showed the dominance of the semi-diurnal tide (Figure 3-47). Maximum speeds of approximately 65 cm/s were noted in the surface layers, and approximately 40 cm/s in the near-bottom layers, for both deployments. Strong mean flows were noted in all layers (particularly during southward flows) that persisted for a few days at a time. Average currents were northward at depth, and either northward or southward at the near-surface. Plotting the 30-hour low-passed currents on vector plots showed that strong southward flows that occurred in the upper water column were most likely responsible for a northward response at depth (Figure 3-48).

A calculation of mean speeds and direction for various depth levels is presented in Table 3-12 for each deployment period (fall 1999 and winter 1999–2000). Mean vector magnitude showed stronger currents at depth, which increased from the fall to the winter deployment (from 7 to ~12 cm/s at the bottom). Mean direction at depth was southward in the surface layers, shifting gradually through west to a northward trend in the fall. A similar trend was noted in the winter, though the transition from southward to northward occurred higher in the water column and was much more abrupt. Though the mean vector magnitudes were greater at depth than at the surface, mean speed calculations for the fall showed higher speeds at the near-surface (~20 cm/s), and a gradual trend to lower speeds at the near-bottom (~13 cm/s). Mid-water column maximum current speeds ranged up to 40 cm/s, while the near-surface speeds ranged up to 73 cm/s in the fall. Winter maximums ranged from 40 cm/s at the near-bottom to 56 cm/s near the surface.

Near-bottom Currents and Turbidity at Site 1

Currents recorded by the ARESS array at Site 1 (which corresponds to Site 1 in the fall/winter 2000 deployment period) in mid-November 1999 showed generally strong currents (typically over 40 cm/s at the upper sensor and over 30 cm/s in the lower sensor). Maximum currents reached almost 80 cm/s several times in the upper sensor and one time in the lower sensor as well. Turbidity remained at generally low background levels for most of the measurement period, though short periods of increased turbidity were noted (Figure 3-49). Though wave pressure data were not acquired during this measurement program, a review of NOAA buoy wave data showed that these higher turbidity periods were associated with larger wave events. Turbidity events were generally stronger and more frequent in the winter than in the fall, with several events producing maximum turbidity values reaching over 150 FTU in the lower sensor. Low-frequency currents (30-hr low-pass filtered vector plots) were predominantly to the north for both deployments, with infrequent southward events also noted (Figure 3-50). Some northward events were reasonably strong for low-frequency flow, exceeding 25 cm/s in the upper sensor. Though sporadic eastward currents were noted during the transitions between northward and southward flow, westward currents were very rare.

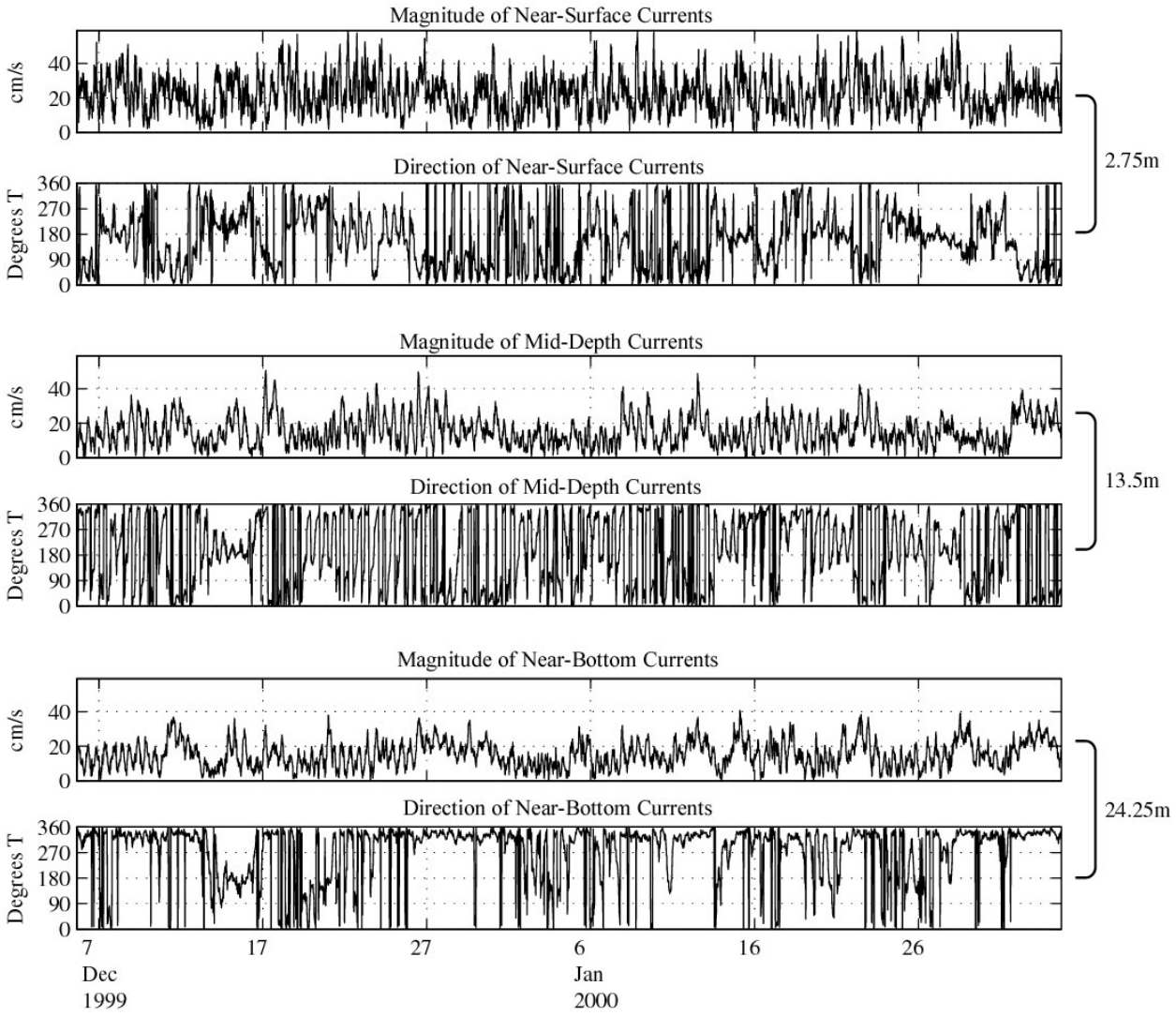

Figure 3-47. Time series of ADCP current magnitude and direction from three depth levels, at the HARS, winter 1999–2000 deployment. Values to the right of plots indicate measurement depth.

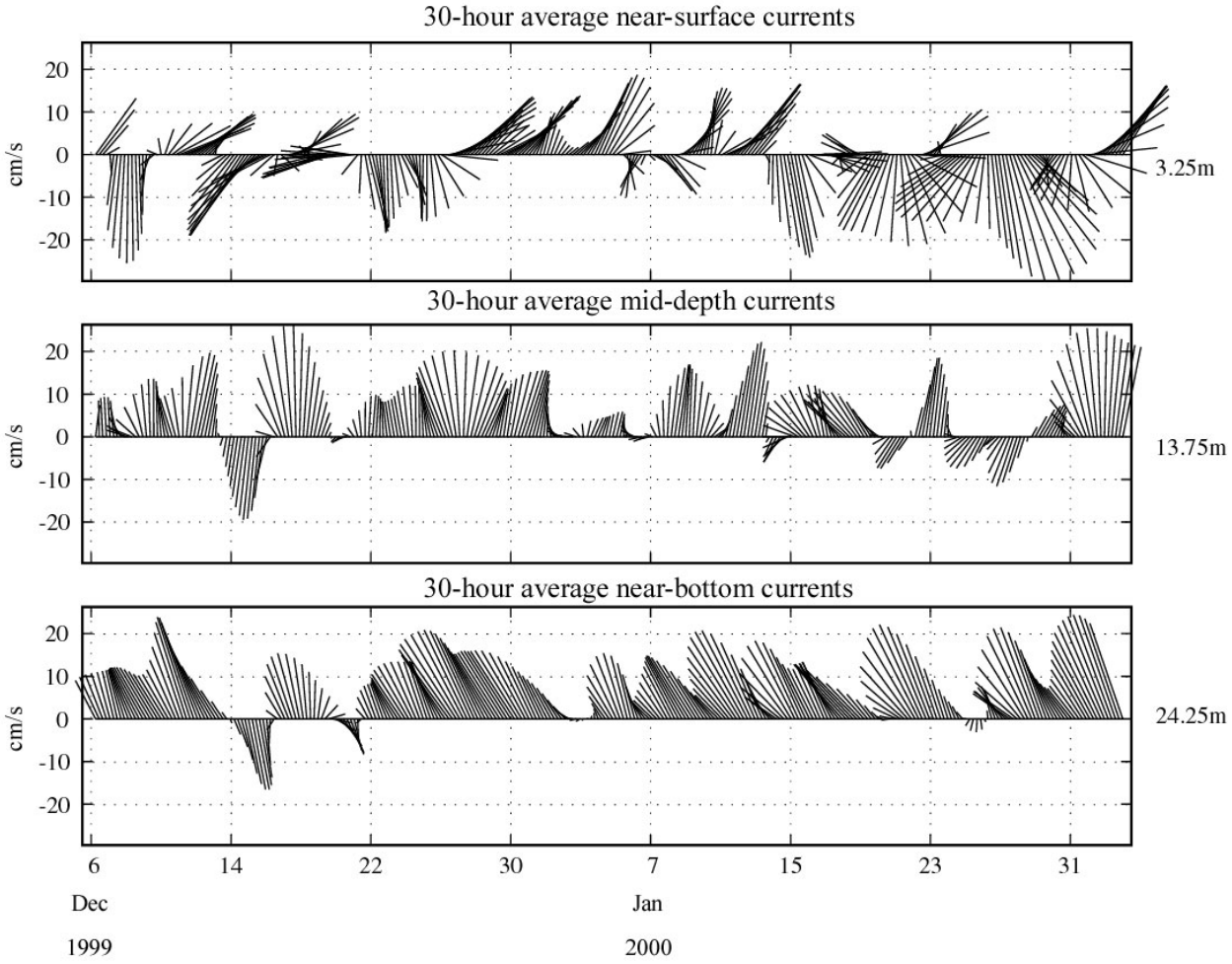

Figure 3-48. Time series vector plot of 30-hr LPF currents acquired by ADCP from three depth levels at the HARS, winter 1999–2000 deployment. Values to the right of plots indicate measurement depth.

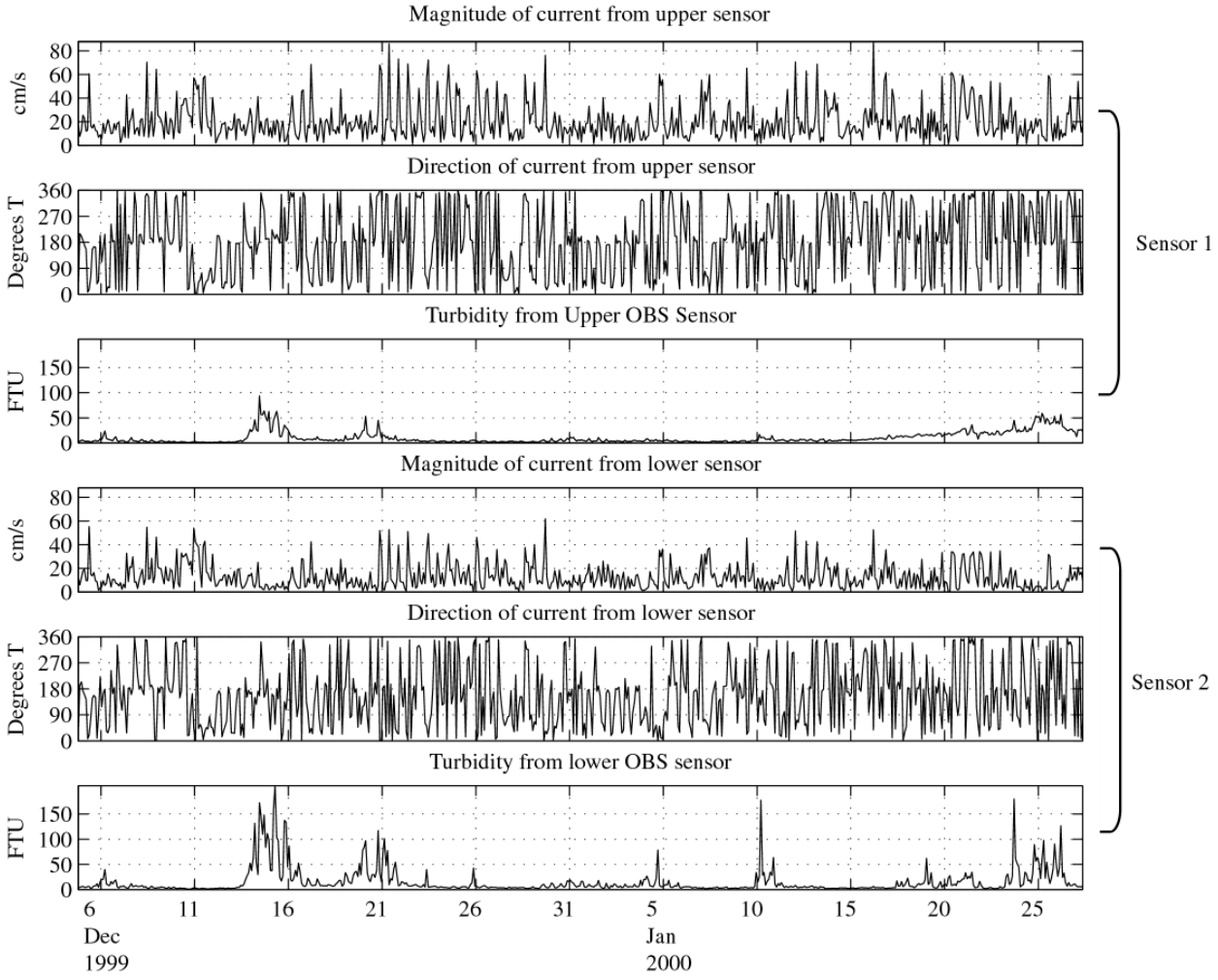

Figure 3-49. Time series of near-bottom current speed and direction and turbidity from two depth levels; 1.52 m (Sensor 1) and 0.76 m (Sensor 2), Site 1, winter 1999–2000 deployment.

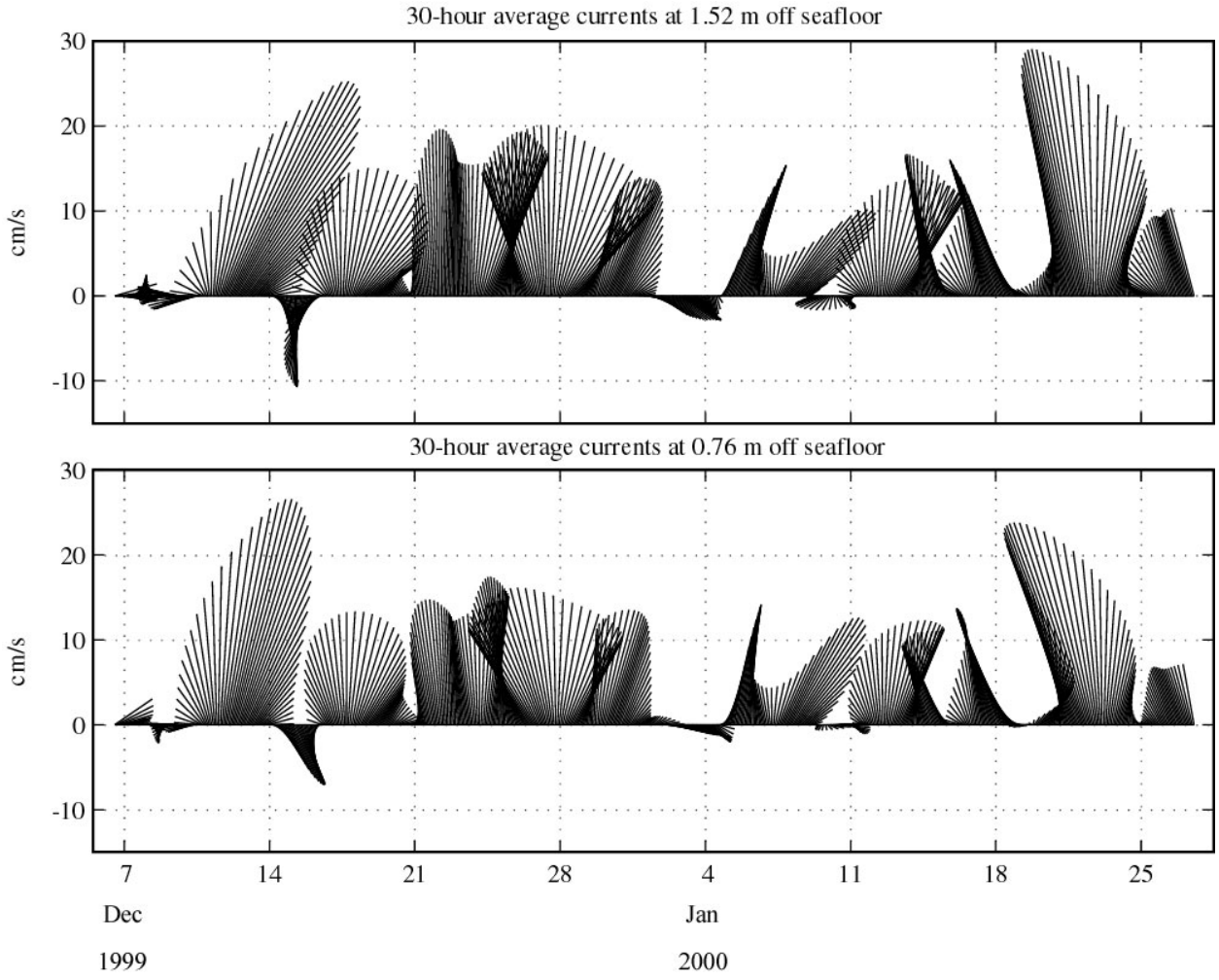

Figure 3-50. Time series vector plots of 30-hr LPF near bottom ARESS current meter data for two depth levels (1.52 m off seafloor—top tier; and 0.76 m off seafloor—bottom tier) for the winter 1999–2000 deployment at Site 1.

Table 3-12.

Statistics of ADCP data collected at Site 3 during the fall/winter 1999 deployment period

Deployment Dates	Depth Level (m)	Mean Vector Magnitude (cm/s)	Mean Direction	Mean Speed (cm/s)	Max Speed (cm/s)	Percentage of Observations in Speed ranges below								
						0-10	10-20	20-30	30-40	40-50	50-60	60-70	70-80	80-90
11/9/1999 to 12/4/1999	3.25	2.8	150.0	21.1	73.0	16.6	35.0	28.9	12.8	4.2	1.8	0.7	0.1	0.0
	13.75	4.1	356.6	14.6	37.2	30.8	45.6	21.1	2.5	0.0	0.0	0.0	0.0	0.0
	24.25	7.1	336.0	13.2	40.9	37.6	44.0	16.6	1.7	0.1	0.0	0.0	0.0	0.0
12/5/1999 to 2/3/2000	3.25	4.2	123.6	22.3	59.1	14.2	30.3	32.2	16.3	5.5	1.5	0.0	0.0	0.0
	13.75	7.3	353.0	15.4	50.6	30.2	42.4	21.3	5.2	0.9	0.0	0.0	0.0	0.0
	24.25	11.2	331.3	15.3	40.8	27.6	46.0	22.4	4.0	0.0	0.0	0.0	0.0	0.0

Summary of Fall/Winter 1999 Results

- During the abbreviated fall/winter 1999 measurement program, water column currents were bi-directional near the surface, flowing primarily northward or southward; lower in the water column, a more northward trend was noted. In general, currents were stronger near the surface, however, the long-term vector mean calculation showed currents to be stronger at depth, indicating a more consistent current flow in the lower water column.

- Near-bottom currents at Site 1 showed strong tidal flows in both fall and winter, as well as strong low-frequency currents oriented primarily northward. Turbidity events were consistently associated with southward currents in the near-bottom layers.

4.0 DISCUSSION

The following section addresses how the extensive data acquired during this oceanographic measurement program were interpreted to help meet the objectives of this study. As presented in the Introduction, the primary objectives of this study were to answer the following two questions: 1) What is the potential for transport of near-bottom waters (and any associated turbidity) from the HARS toward the New Jersey shoreline; and 2) What is the potential for outflow from the NY/NJHE to contribute turbid waters to the New Jersey coastal environment. The discussion in this section will focus primarily on the periods of observed elevated turbidity and address both the causes of the higher turbidity and also the likely sediment transport pathways during these periods.

4.1 Causes and Sources of Elevated Turbidity

As presented in the Results section above, one of the most consistent relationships observed within the oceanographic data was the strong correlation between wave height and turbidity. As observed in numerous instances during this measurement program, almost all significant increases in turbidity above the generally low background levels were associated with infrequent, large wave events. The strong correlation between wave height and increased turbidity levels implies that wave-induced sediment resuspension is a primary cause of increased turbidity in this area. This result is consistent with results from previous oceanographic studies [SAIC 1995, Harris 1999] conducted in and around the HARS that also indicated that large, storm-driven waves were capable of causing localized sediment resuspension.

Sediment resuspension is a complex process that is dependent upon many parameters that can vary greatly from one location to another (e.g., material grain size, cohesion of sediments, water depth, etc.). However, direct comparisons between the simultaneous wave, current, and turbidity data that were acquired during this study can provide a reliable, first-order estimate of resuspension magnitude. Figure 4-1 presents a depiction of some of the relevant wave, current, and turbidity data that were acquired around the period of the largest observed wave event over the entire 6-month monitoring program (26-27 November 2000). This figure provides the observed wind speed and direction (from Ambrose Tower), the significant wave height from Site 1, and the 30-hour low-pass filtered currents and turbidity from Site 3. (Because the current velocity values recorded during this study represent an average over a 2.5-minute data burst, those processes that occur on much shorter timescales, such as short period wave-induced oscillatory currents, cannot be extracted from the averaged values.)

The early portion of this record was characterized by moderately strong westerly winds, small significant wave heights, and low background turbidity levels. During the middle portion of the record, wind direction changed to the east, wind speed increased, and significant wave height quickly grew to almost 4 m. This rapid increase in significant wave height corresponded to an equally rapid increase in the turbidity level as well, most likely caused by bottom sediments being resuspended by orbital, wave-induced near-bottom currents. In the latter portions of the record, wind direction changed back to the west, significant wave height decreased below 1 m, and turbidity levels quickly returned to low background levels.

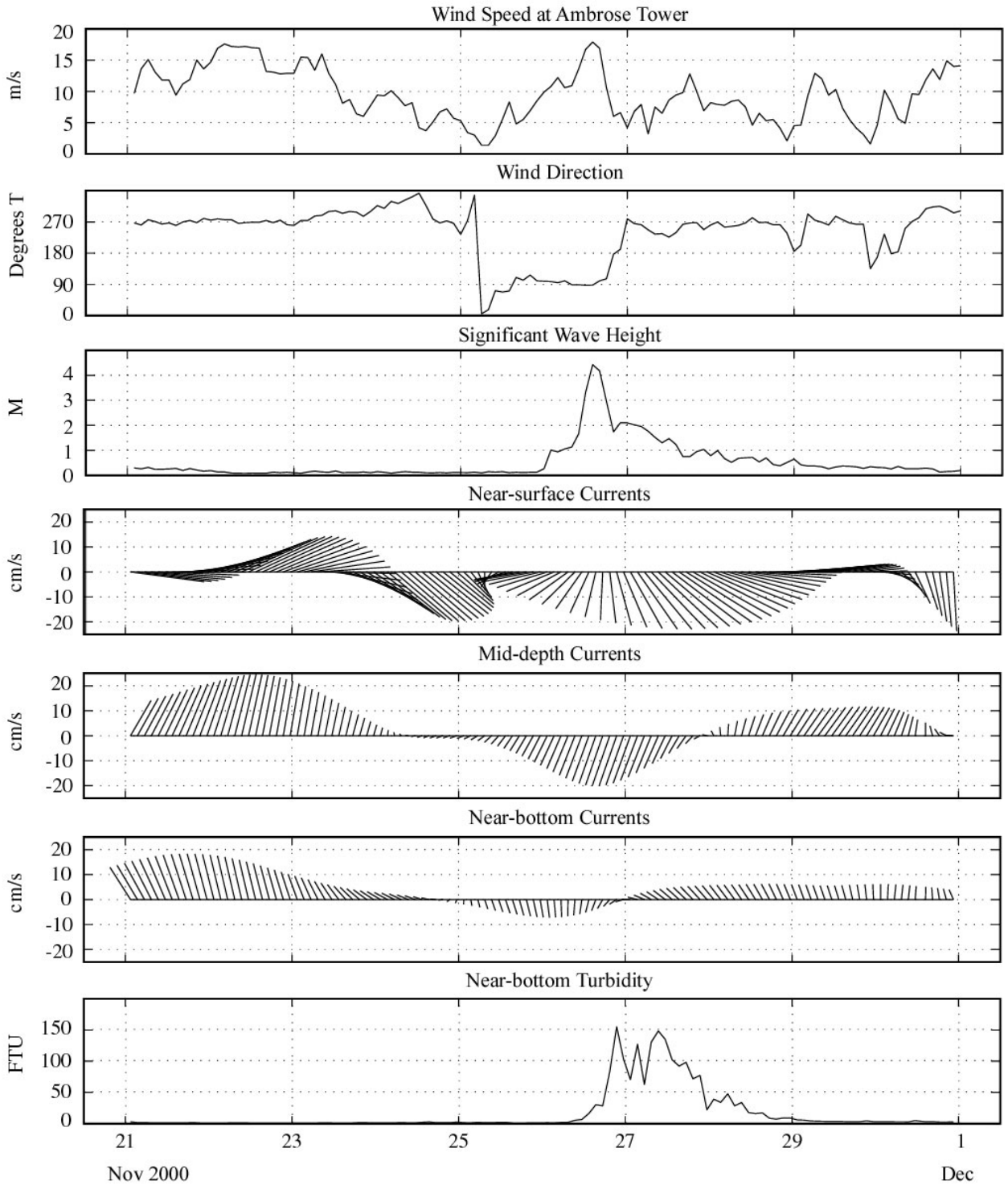

Figure 4-1. Environmental and oceanographic data during the largest wave event observed throughout the 6-month measurement program. Significant wave height was measured at Site 1, whereas currents and turbidity were measured at Site 3.

A similar response was noted during several somewhat smaller wave events over the course of this measurement program. The relatively rapid return to background turbidity levels that was consistently noted indicates that the source of the turbidity was most likely a coarser-grained sediment (e.g., sand) that quickly settled out of the water column following the decrease in wave height; finer grained sediments (e.g., silt) would tend to remain suspended for longer periods of time. Aggregates of fine-grained material would have a tendency to settle quickly as well, however, given that the seafloor sediments inshore of the HARS are rather uniform and comprised primarily of sand, it is to be expected that short-term turbidity increases in the inshore region to be due to the local coarse-grained sand, as aggregates of fine-grained material would not likely transport on such a short time basis. The sediment composition of the seafloor, together with the rapid turbidity response noted after the passage of large wave events, suggests that the observed increases in turbidity in the inshore region were most likely the result of local resuspension, rather than the transport of fine-grained sediment from another location. At Site 3, in the immediate vicinity of the HARS, it is possible that these temporary increases were due to the short-term tidal transport of material resuspended at the HARS, given that the peak in turbidity lagged a few hours behind the peak in wave height.

Because seafloor resuspension is directly dependent upon both wave height and water depth, smaller wave events have less potential to cause resuspension impacts in deeper waters. Figure 4-2 presents a depiction of some of the relevant wave and turbidity data that were acquired around a moderate wave event in mid-October 2000. This figure provides the observed wind speed and direction (from Ambrose Tower), the significant wave height from Site 1, and the turbidity values from Sites 1, 2, and 3. During this event, wind direction shifted quickly from the south to the east, wind speed increased to 10-12 m/s, and significant wave heights increased to just under 2m for approximately 2 days. As this figure shows, the turbidity response to this event was dependent upon the water depth at the measurement site. Site 3 (in 21 m of water) showed almost no turbidity impacts, Site 1 (in 16 m of water) showed somewhat higher turbidity levels for a portion of the event, and Site 2 (in 12 m of water) showed the most prominent and consistent turbidity increases. Thus, for larger wave events, resuspension occurs on a more regional basis, wheras for smaller ones, only the shallower regions will exhibit sediment resuspension.

Although outflow from the NY/NJHE system was also envisioned as a potential source and cause of increased turbidity during this study (particularly during the spring measurement phase), none of the data acquired during this study provided any conclusive evidence on these impacts. River discharge and flow data from the USGS river gauge on the Passaic River was used to make general characterizations about the volume of flow out of the NY/NJHE system (Figure 3-7). Based on the USGS data, it appeared that most of the spring oceanographic measurement program was acquired during a period of generally low river flow. Some of the higher flow data noted at the beginning of the spring measurement program did correspond well with lower salinities at the surface and strong southerly currents at all depth levels at the oceanographic moorings; however, no significant turbidity impacts were detected during this period. Although no significant turbidity increases at the oceanographic measurement stations could be attributed to outflow from the NY/NJHE system during the course of this study, the NY/NJHE is still considered a likely source for large suspended sediment increases in this area, particularly during any unusually high flow event.

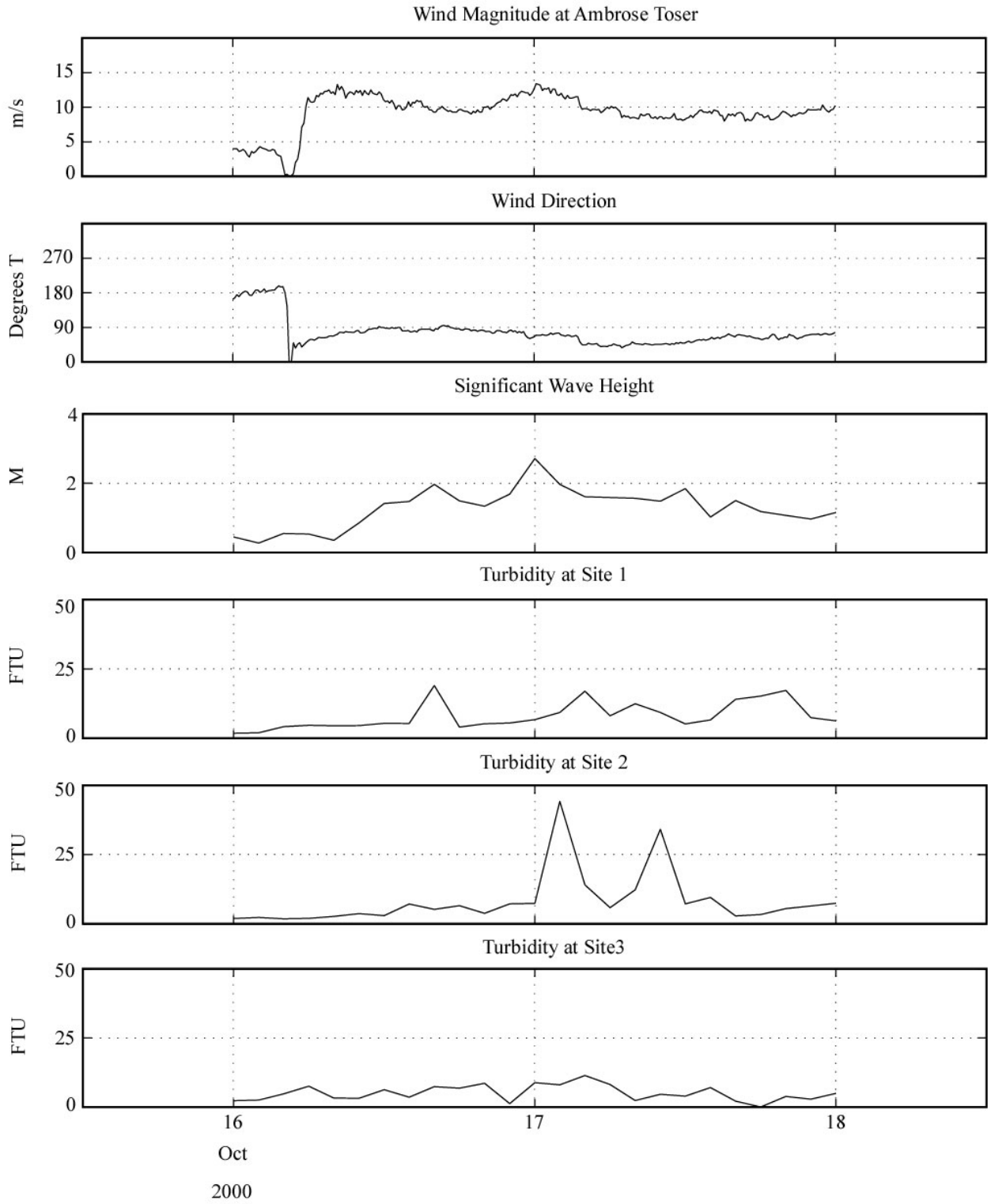

Figure 4-2. Environmental and turbidity data for a small wave event in the second deployment period, 16–18 October 2000. Wind data was recorded at NOAA station Ambrose Tower, and wave data was recorded by ARESS at Site 3.

4.2 Examination of Transport Pathways

Having examined some of the likely causes and sources of elevated turbidity, it is then useful to examine the likely sediment transport pathways around the HARS. Relying primarily on the extensive current data acquired during this study, this analysis attempts to define the dominant long-term current patterns at different levels in the water column, at different locations, and during different periods of the year. Because a major objective of this study was to measure the potential for suspended sediment transport, this analysis will be focused primarily around those periods of observed elevated turbidity.

Progressive Vector Diagrams

One of the simplest means for examining the correlation in horizontal currents between sites and the subsequent potential for transport of water between sites is to plot cumulative progressive vector diagrams (PVDs). Using current velocity data with observations that are regularly spaced in time, it is possible to plot a cumulative vector of the current observed at each deployment location; these plots provide an indication of the net excursion (distance and direction) of a parcel of water away from the measurement location over a defined period of time. It is important to keep in mind that this does not necessarily represent the true trajectory of a water parcel through space, as the currents cannot be extrapolated from one location to another. Nevertheless, it provides a useful representation for making first-order observations on the typical transport pathways of currents at the site.

In order to provide an initial overview of the data, progressive vector diagrams were generated in one-day increments for all of the current data for each of the main deployment periods (Figures 4-3 through 4-5). Only data from the lower sensors were plotted, both to simplify the plots and because the turbidity was typically higher at the lower sensor level. For the fall data (Figure 4-3), the northwest-southeast trends mentioned in previous sections are clearly visible at Sites 1 and 3. At Site 1, the predominant average flow to the northwest is also obvious. Trends to the east or west are rare, and do not typically represent large excursions from the deployment location (1 or 2 km). Closer to shore at Site 2, currents are more scattered and do not appear to be as bi-directional; the average current trend appears to be to the north or northeast, which is consistent with the rose diagrams presented in Section 3.

The highlighted vector shown in Figure 4-3 (from 16 October) illustrates the lack of coherence that was sometimes observed between the measurement sites. On this day, Site 3 near the HARS experienced a consistently southward flow that led to one of the largest southerly excursions that was detected in the data. At Site 2 near the shore, currents oscillated from westward to eastward, and at Site 1 to the north, currents oscillated from northward to southward; in both of these cases, little net excursion was noted. Thus, in the fall, while there were some similarities in long-term trends, currents were not necessarily well correlated from one site to another.

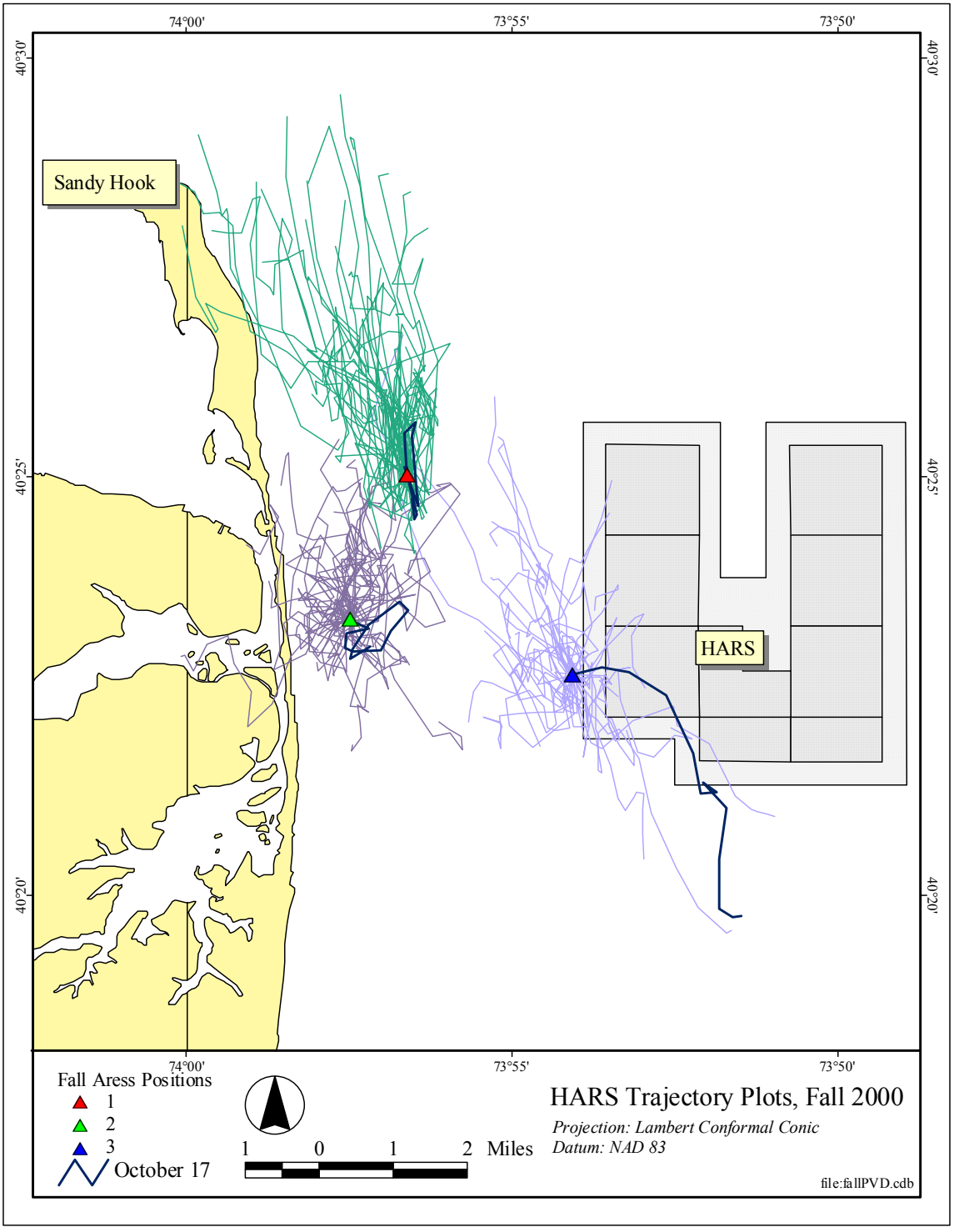

Figure 4-3. Progressive Vector Diagrams of raw currents plotted from 1 day periods in fall 2000. Average northward trends are clearly visible at all three sites, particularly at Sites 2 and 3. An event on 17 October demonstrates that currents are not necessarily coherent between sites in the fall.

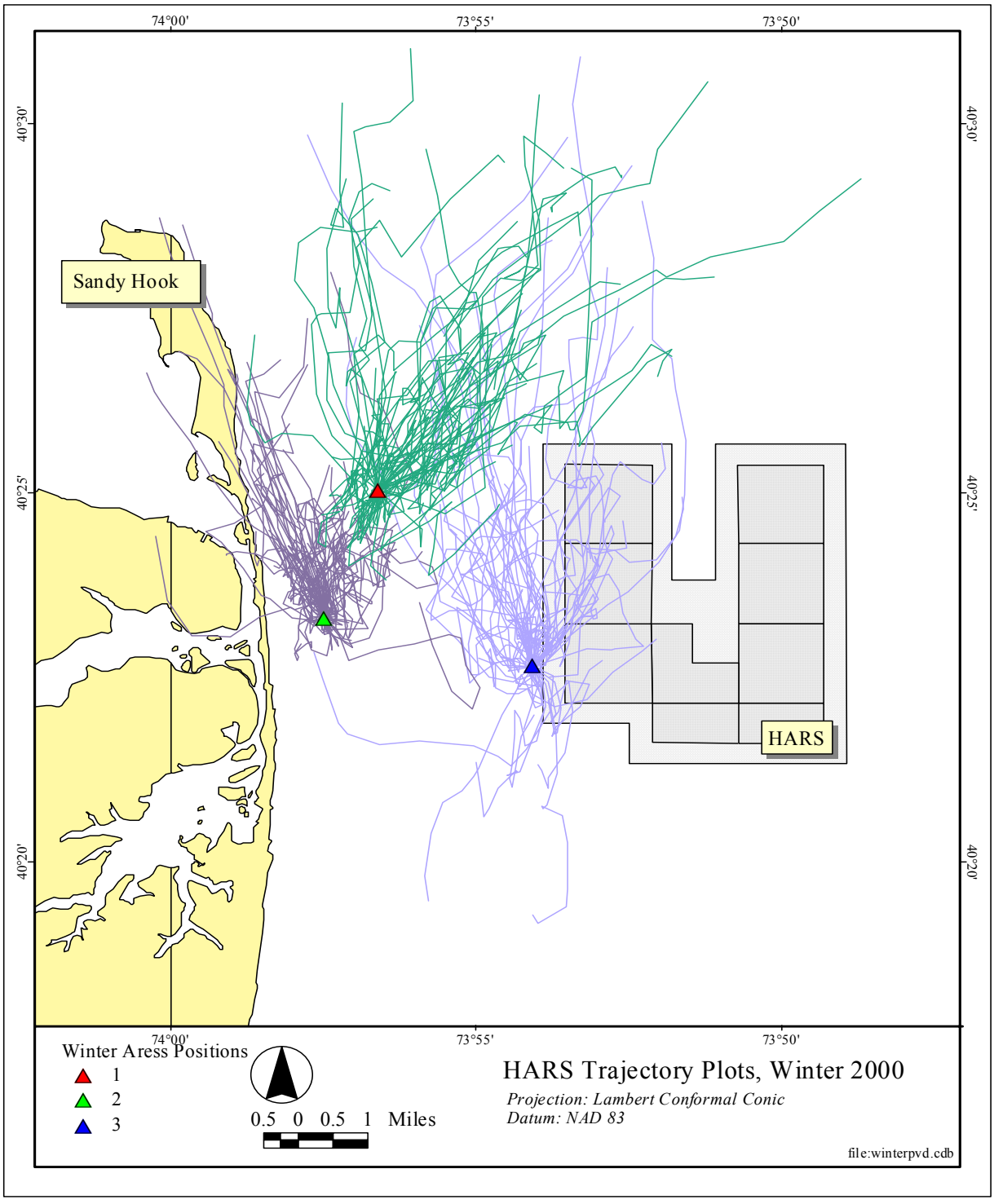

Figure 4-4. Progressive Vector Diagrams of raw currents plotted from 1 day periods in winter 2000–01. Average northward trends are clearly visible at all three sites, particularly at Sites 2 and 3, whereas Site 1 demonstrates more northeastward trends.

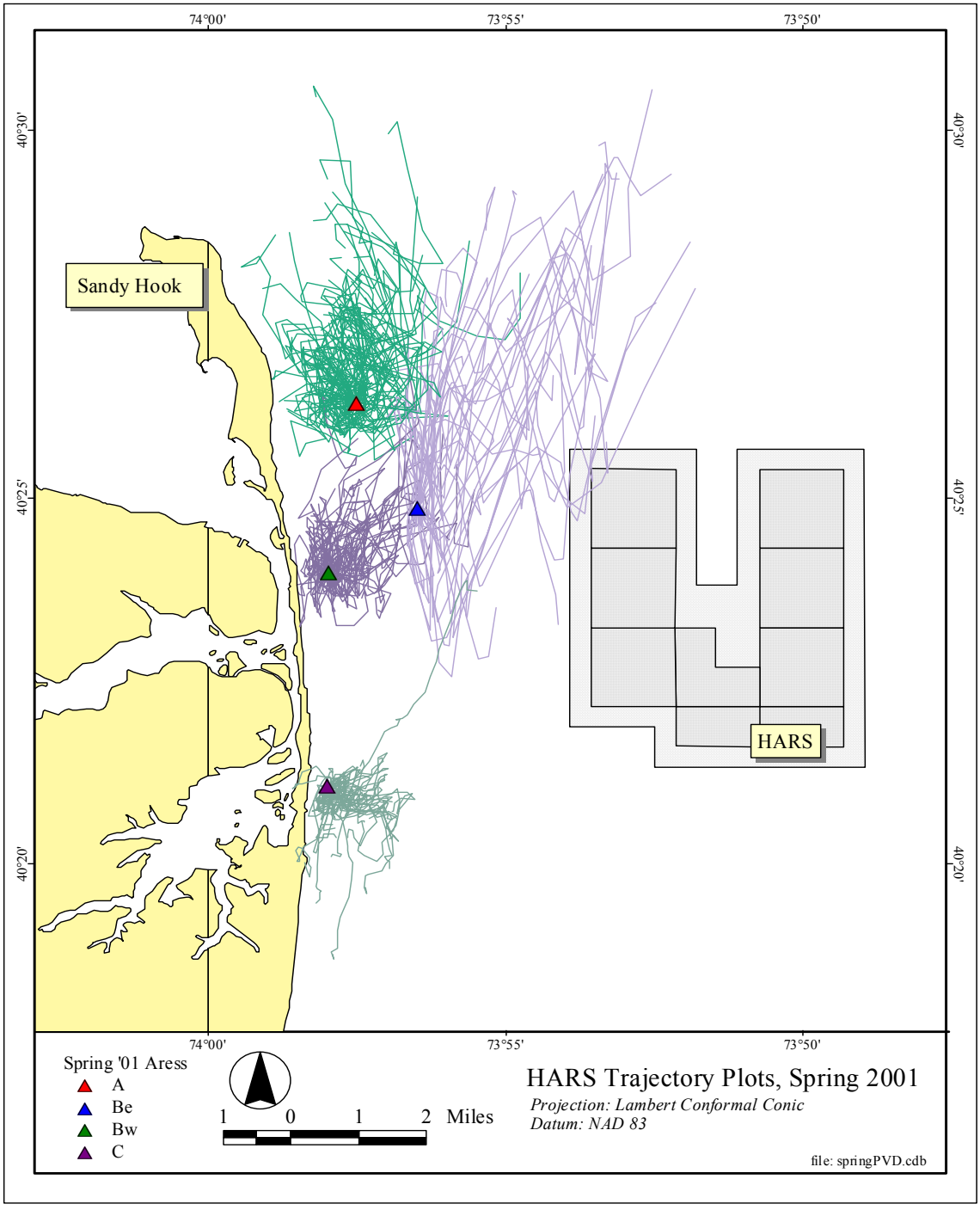

Figure 4-5. Progressive Vector Diagrams of raw currents plotted from 1 day periods in spring 2001. Site Be (concurrent in location with Site 1 in the fall/winter) demonstrates the most significant north-south excursions, while the near-shore sites are more scattered. Site C to the south shows markedly different trends to the east and south.

In the winter, all sites showed northward average trends, with generally greater daily excursions (Figure 4-4). East-west trends were still uncommon and total excursion in this direction was generally less than one to two km. In general, Sites 2 and 3 seemed to show the most coherence, with trends that were predominantly north to northwestward and oriented along the shore; Site 1 demonstrated more northeastward trends oriented away from shore. This suggests that, in general, a water parcel leaving the HARS (near Site 3) would have the tendency to flow alongshore to the north and then be advected offshore to the northeast. The PVDs for winter clearly demonstrate that westward currents are rare at all three measurement sites.

Although the average trends were somewhat different in spring than in winter or fall, it is still evident that significant westward excursions were rare (Figure 4-5). At Site Be, about 1.5 km offshore from the inshore sites, a relatively large north to northeastward excursion of the vectors dominated the observed current pattern. At the three near-shore sites (Sites A, Bw, and C) the excursions from the deployment location were not nearly as significant and appeared to decrease significantly farther down the coast. Average current trends were generally northward at both of the northern inshore sites (Sites A and Bw), though there was significant scatter in the vector plots and the average excursions were small. An entirely different current regime appeared to dominate at Site C to the south, where current trends were primarily to the east and south. It is likely that the presence of a prominent rocky shoal (Shrewsbury Rocks) oriented perpendicular to shore and located just to the south Site C had an impact on the observed current regime at this site.

30-Hour Low Pass Filtered Currents During High Turbidity Events

Because a specific intent of this study was to assess the likelihood of suspended sediment transport, it is also necessary to more closely examine the near-bottom and water-column current trends during specific periods of higher turbidity. One useful means of doing this is to closely analyze the longer-term, sub-tidal currents (30-hr low-pass filtered) at various depth levels in the water column over those narrow time periods of elevated turbidity. One particular period of interest was in late November 2000 and was discussed earlier in Section 4.1 (Figure 4-1). During this period, strong northeast winds generated waves up to 4 m and resulted in an increase in near-bottom turbidity to about 150 FTUs. During this period, the surface and mid-depth low-frequency currents were predominantly southward with relatively high velocities (around 20 cm/s). The average near-bottom currents were much weaker (<5 cm/s) and appeared to be transitioning from a southward to a northward direction during this period.

Another particular period of interest occurred at the end of September 2000, when a strong northeast wind event generated waves in excess of 3 m and a corresponding increase in near-bottom turbidity at all three sites. At Site 1, the increase in turbidity occurred during a period of strong southward sub-tidal currents in the surface and mid-depth levels (Figure 4-6); near-bottom currents were weak to the north-northwest (<5 cm/s). The background turbidity at this site before the event was less than 10 FTU. During the event, the turbidity reached just over 50 FTU on a few occasions, with an average for the duration of the event of approximately 30 FTU.

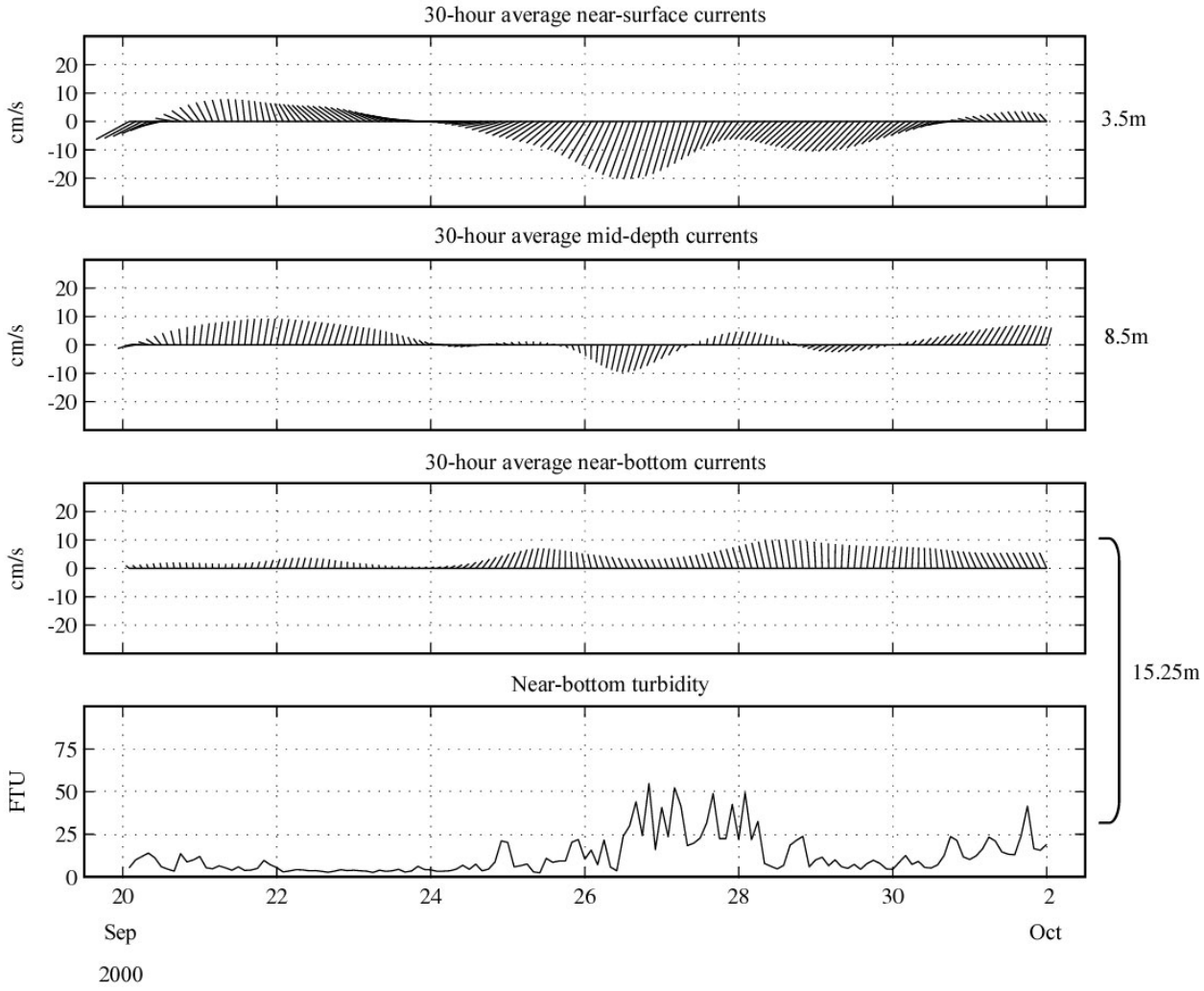

Figure 4-6. Vector plot of near-surface, mid-depth, and near-bottom 30 LPF currents and turbidity during a turbidity event in late September 2000 at Site 1. Upper water column currents show strong southward flow, while near-bottom currents are weak and to the north. Values to the right of plots indicate measurement depth.

Further inshore at Site 2, the near-bottom average currents were even weaker (<3 cm/s) and flowed mostly northward for this period (Figure 4-7). Turbidity at the lower sensor reached a maximum of approximately 90 FTU during the turbidity event and then appeared to become interfered with as the values continued to increase throughout the rest of the deployment; a trend that was not noted in the upper sensor at this site. Turbidity at the upper sensor reached a maximum of approximately 47 FTU, or a little more than half the value at the lower sensor level. At Site 3 (closest to the HARS), southwestward currents were noted in the surface and mid-depth levels, while southeastward currents were recorded at the near-bottom level (Figure 4-8). Turbidity levels reached a maximum of 60 FTU and averaged about 30 FTU; the duration of the elevated turbidity levels was similar to the other sites. During this turbidity event, near-bottom low-frequency currents were either northward or southward at all three sites, and water column currents were typically southward. Eastward or westward near-bottom currents were only noted during the brief transitions between northward and southward flow.

Another presentation of near-bottom currents during an elevated turbidity event is provided in Figure 4-9. During this mid-December 1999 time period, a strong northeast wind event generated waves above 4 m and resulted in turbidity levels as high as 200 FTU in the lower sensor, and 100 FTU in the upper sensor. During this event, low-frequency currents were predominantly southward, reaching almost 10 cm/s in the upper sensor level and approximately 5 cm/s at the lower level. A week later another northeast storm of lesser magnitude (10-12 m/s winds) produced 2 m waves and another smaller increase in turbidity levels. During this subsequent event, the near-bottom low-frequency currents were weak and to the north-northeast, though the current magnitude did increase soon after this event.

Summary

Analysis of the time series current, turbidity, and wave height data showed that the high turbidity events consistently occurred during periods of increased wave activity. In general, events having large waves were less frequent in spring than in winter, and subsequently significant turbidity events were also less frequent. It appeared that local resuspension was the likely source of suspended material at each of the monitoring sites, and that the extent of the resuspension was directly related to wave height and water depth (peak wave period during these events was typically short). The fact that turbidity returned to background levels relatively quickly following the passage of the large wave events, suggests that the increased turbidity noted during major storm events was due to local resuspension of coarser grained material. A closer inspection of current patterns during the individual turbidity events confirmed that low-frequency currents were almost exclusively weak and directed northward or southward during these turbidity events. While wave-induced orbital currents were likely responsible for causing sediment resuspension, the low-frequency near-bottom currents were generally weak and rarely directed westward. Based on these data, it appears that there is little potential for resuspended bottom material from the HARS to be transported in toward the New Jersey shoreline.

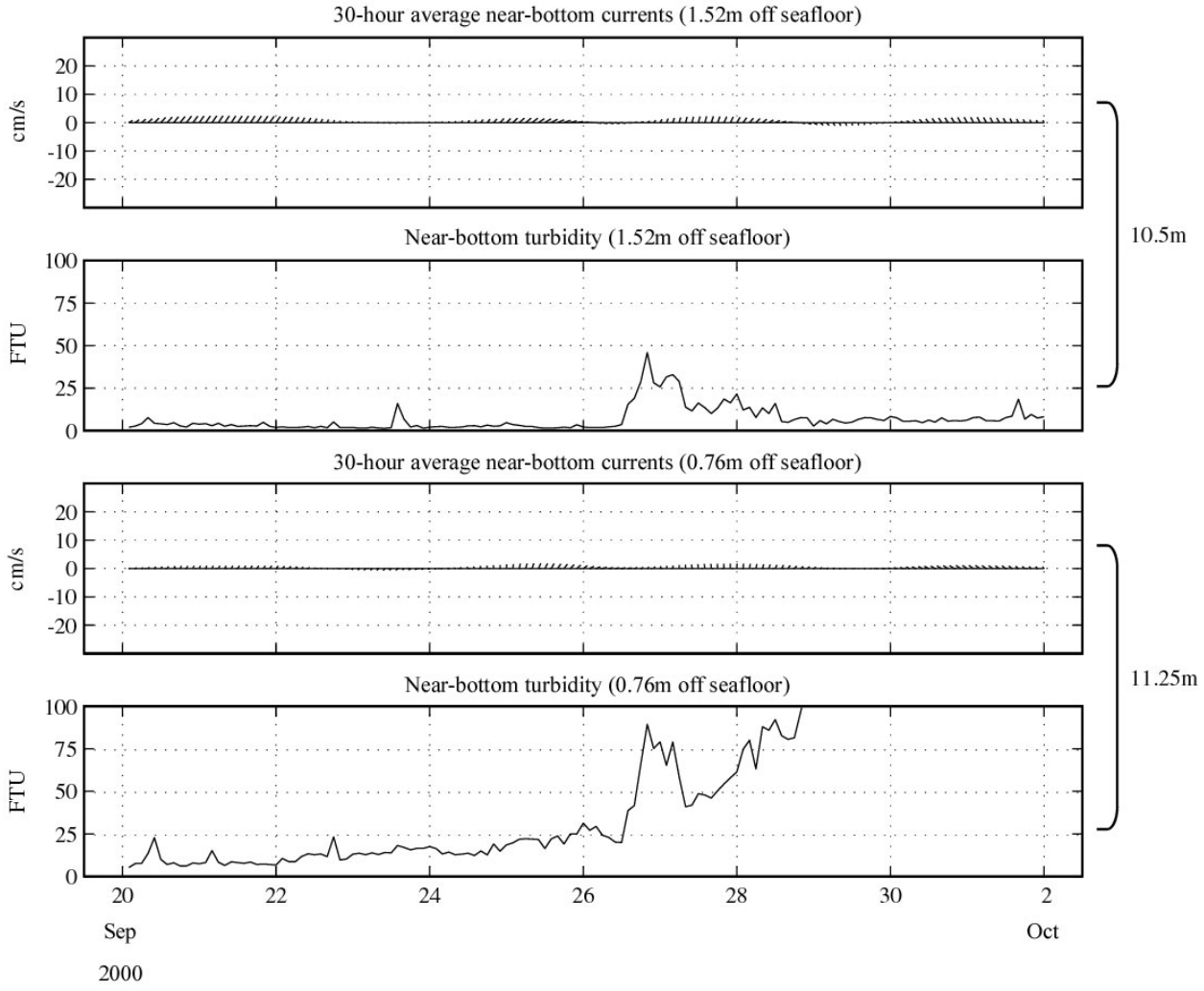

Figure 4-7. Vector plot of near-bottom 30 LPF currents and turbidity recorded by ARESS at two depth levels during a turbidity event in late September 2000 at Site 2. Average currents are extremely weak (<5 cm/s), and are directed either northward or southward. Brackets to the right of plots indicate sensor depth.

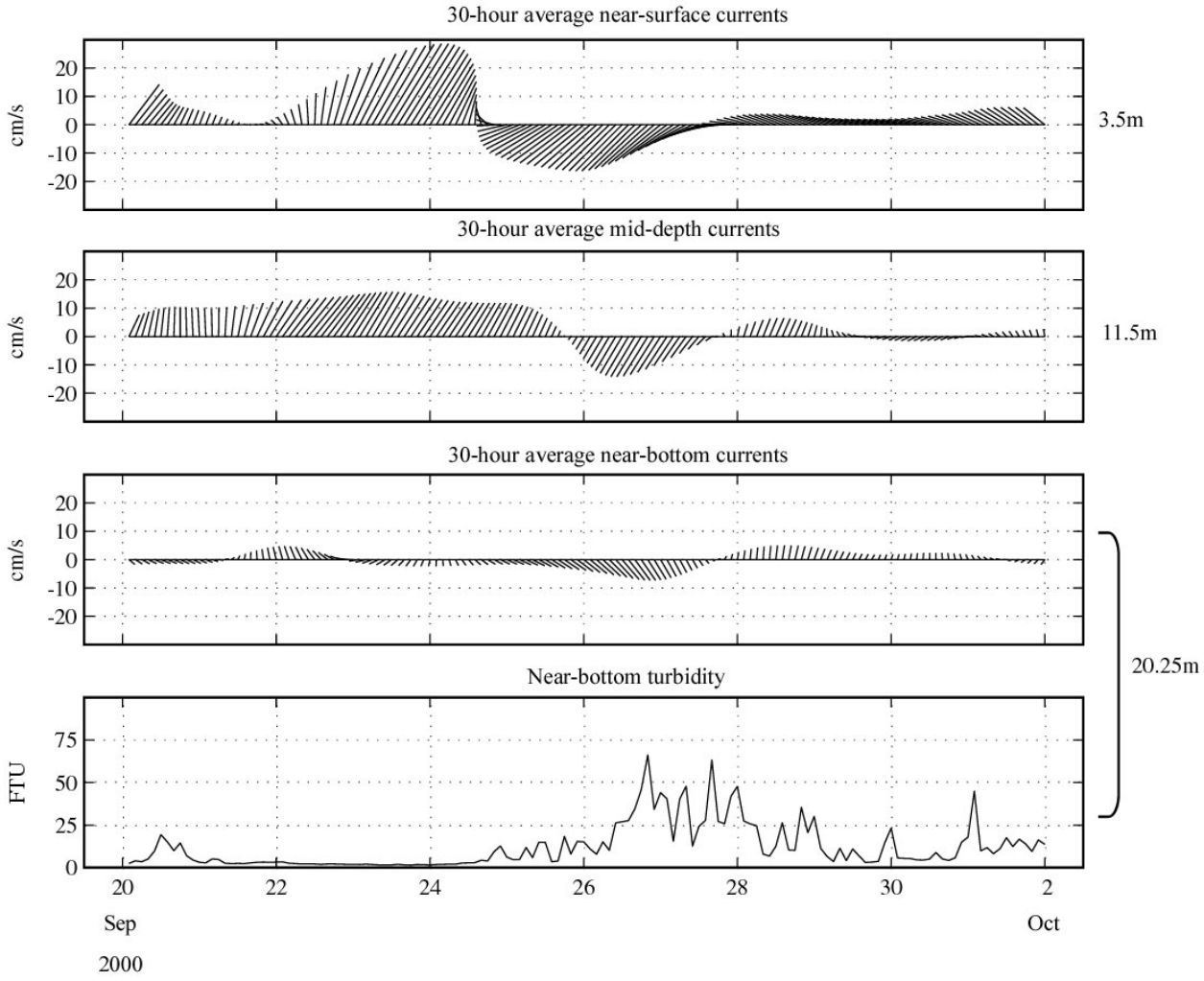

Figure 4-8. Vector plot of near-surface, mid-depth, and near-bottom 30 LPF currents and turbidity during a turbidity event in late September 2000 at Site 3. Upper water column currents show strong southward flow at first, switching to northward, while near-bottom currents are somewhat weaker (but reasonably strong for the near-bottom) and directed to the southeast, also switching northward. Values to the right of plots indicate measurement depth.

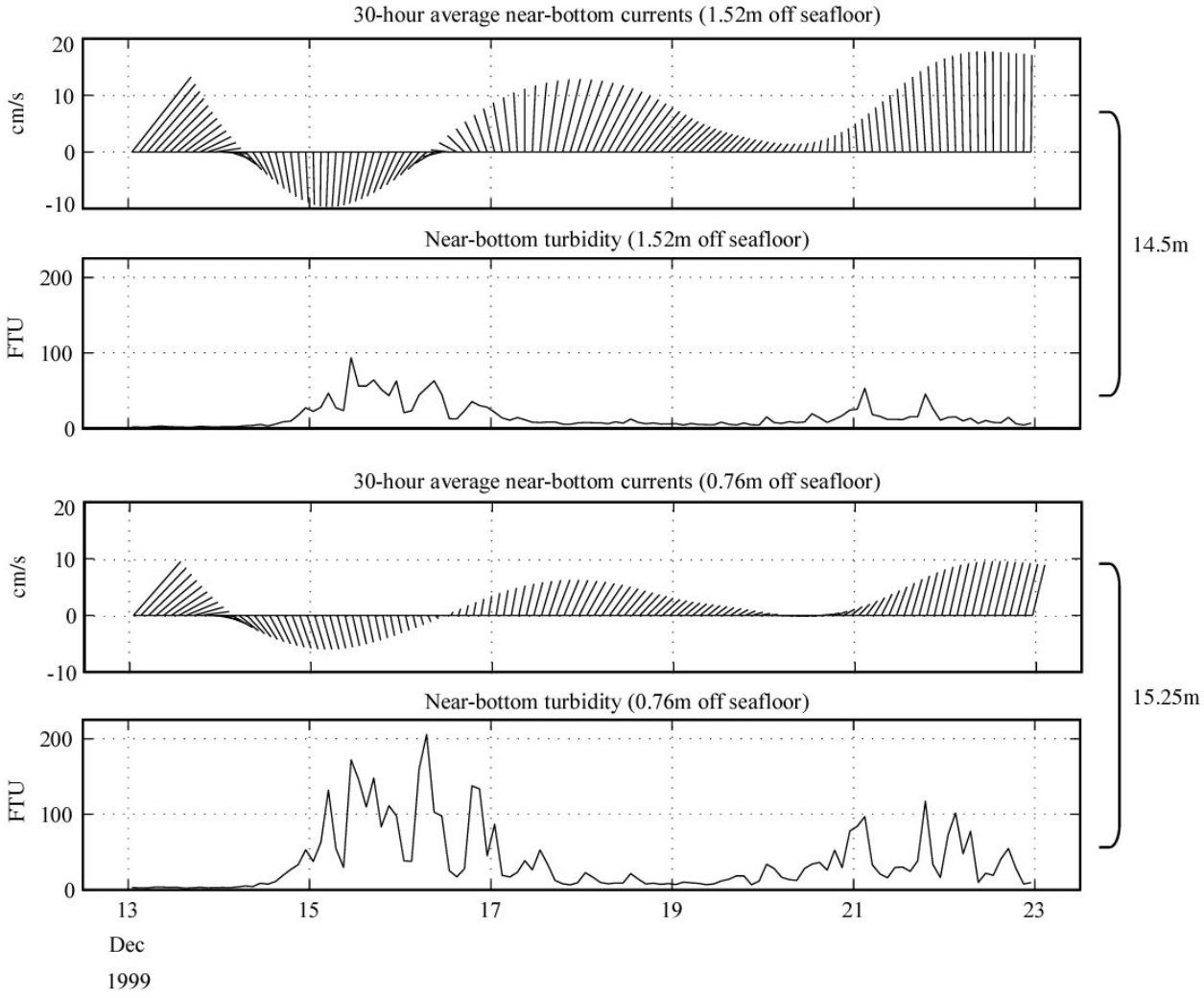

Figure 4-9. Vector plot of near-bottom 30 LPF currents and turbidity recorded by ARESS at two depth levels during a turbidity event in mid and late December 1999 at Site 1. Average currents are reasonably strong, directed southward, and then turn northward during the first event. Currents are very weak, and directed north-northeastward at the beginning of the second turbidity event, and then increase, particularly at the upper sensor level. Brackets to the right of plots indicate sensor depth.

5.0 CONCLUSIONS

The six-month measurement program conducted between the HARS and the New Jersey shoreline spanning the fall and early winter of 2000 and the spring of 2001 showed that there was little potential for the westward transport of suspended bottom sediment from the HARS in toward the New Jersey shoreline. Currents in the region were dominated by the semi-diurnal tide and showed predominantly northward and southward flow at all depth levels. Low frequency, sub-tidal near-bottom currents flowed principally northward, and on occasion southward, in response to storm events. Low frequency currents at the near surface demonstrated more variability, as wind and freshwater forcing had more direct impact in this region of the water column. Winds out of the east and northeast had the greatest capacity to generate large surface waves, though these conditions were observed infrequently during the study (only two wave events over 3 m in the 6 month period). Long-term average currents were typically weak and to the north (<10 cm/s) at the near-bottom, and more southward at the near surface.

Water properties exhibited primarily thermal stratification in the fall and saline stratification in the winter (after storms had overturned the water column and freshwater input to the system increased), but overall density stratification did not vary significantly. In the spring, peaks in river discharge corresponded to significant decreases in salinity at the surface and to stronger southward flows throughout the water column, but did not cause any corresponding increase in near-bottom turbidity. However, because there were no significant high river discharge events during the spring portion of this study, the subject data provided little conclusive insight into the potential impacts associated with the NY/NJHE system. Additional monitoring during periodic high river discharge events would be necessary to accurately quantify these impacts.

Background turbidity was typically low both near-shore and offshore, and events of elevated turbidity were very distinct, tending to occur at all measurement sites simultaneously. These turbidity events were well correlated with periods of higher wave activity, suggesting that the increased turbidity was due to the resuspension of bottom sediments by wave induced orbital velocities. This was further supported by evidence from some of the smaller storm events, where higher turbidity levels were noted at the shallower, inshore sites but not at the deeper sites closer to the HARS. An examination of the current data during the elevated turbidity events demonstrated that longer-term averaged currents flowed primarily in a northward or southward direction; the only instance when a consistent westward near-bottom current was noted at all measurement sites corresponded to a benign weather pattern and a period of low turbidity.

Based on ongoing and past water quality monitoring activities being conducted by federal, state, and local agencies throughout New Jersey coastal regions, there does not appear to be any compelling evidence supporting the claims of water quality degradation (by material from the HARS) specifically along the northern New Jersey shoreline. Furthermore, this recent oceanographic study has shown that there is little potential for sediment from the HARS to impact the New Jersey coast. Continued water quality monitoring, in conjunction with follow-on oceanographic studies, should provide additional insight into any potential HARS-related water quality impacts.

6.0 REFERENCES

Charnell, R. L. and D.V. Hansen, 1974. Summary and analysis of physical oceanography data collected in the New York Bight apex during 1969-70. Waterways Exp Station book GC 1080 M47 no.74-3, Waterways Experiment Station, Vicksburg, MS.

Ditsworth, G.R., Teeter A. M., and Callaway R. J., 1978. New York Bight suspended matter and oceanographic data, 1973-1974. Environmental Protection Agency Report no. EPA-600/3-78-022, EPA Office of Research and Development, Corvallis OR.

Harris, C.K, and Signell, R.P., 1999. Circulation and sediment transport in the vicinity of the Hudson Shelf Valley. *Estuarine and Coastal Modelling: Proceedings of the Conference of American Society of Civil Engineers.* New Orleans, LA.

Lyne, V., Butman, B., and Grant, W., 1990. Sediment Movement along the U.S. East Coast Continental Shelf II: Modelling suspended sediment concentration and transport rate during storms. *Continental Shelf Research*, vol. 10, no. 5, pp 429 – 461.

SAIC, 1995. Analysis of waves and near-bottom currents during major storms at the New York mud dump site. Report No. 20 of the New York Mud Dump Site Studies, SAIC technical report No. 346, Newport, RI.

Scheffner, N.W., 1994. New York Bight Study. Report 1, Hydrodynamic modeling. Technical report ; CERC-94-4 rept.1. Coastal Engineering Research Center, U.S. Army Engineer Waterways Experiment Station, Vicksburg, MS

APPENDIX A

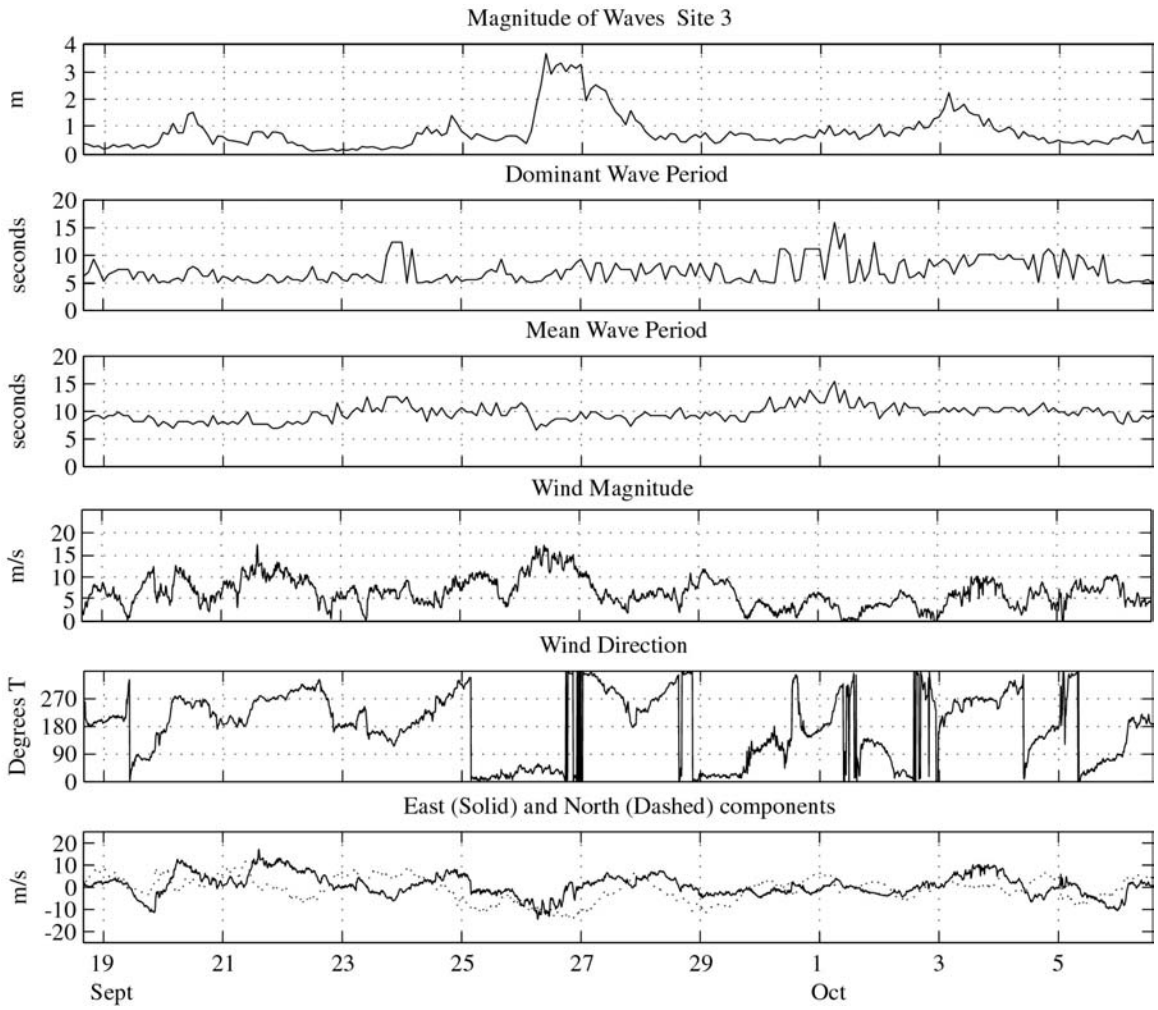

Figure A-1. Time series of Wave data recorded at Site 3 and Wind data from Ambrose Tower for the first deployment in fall 2000. Wave data is presented as significant wave height.

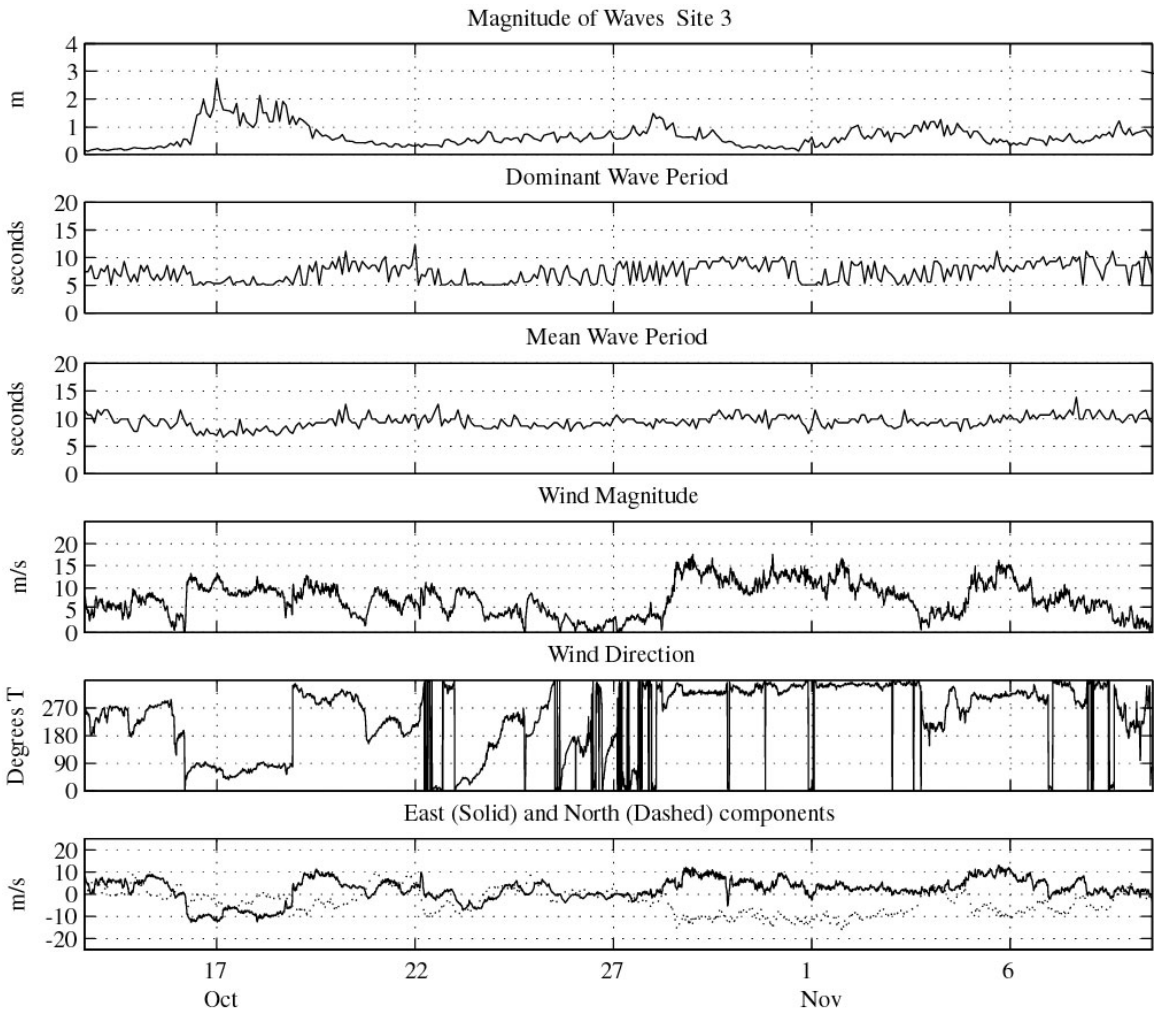

Figure A-2. Time series of Wave data recorded at Site 3 and Wind data from Ambrose Tower for the second deployment in fall 2000. Wave data is presented as significant wave height.

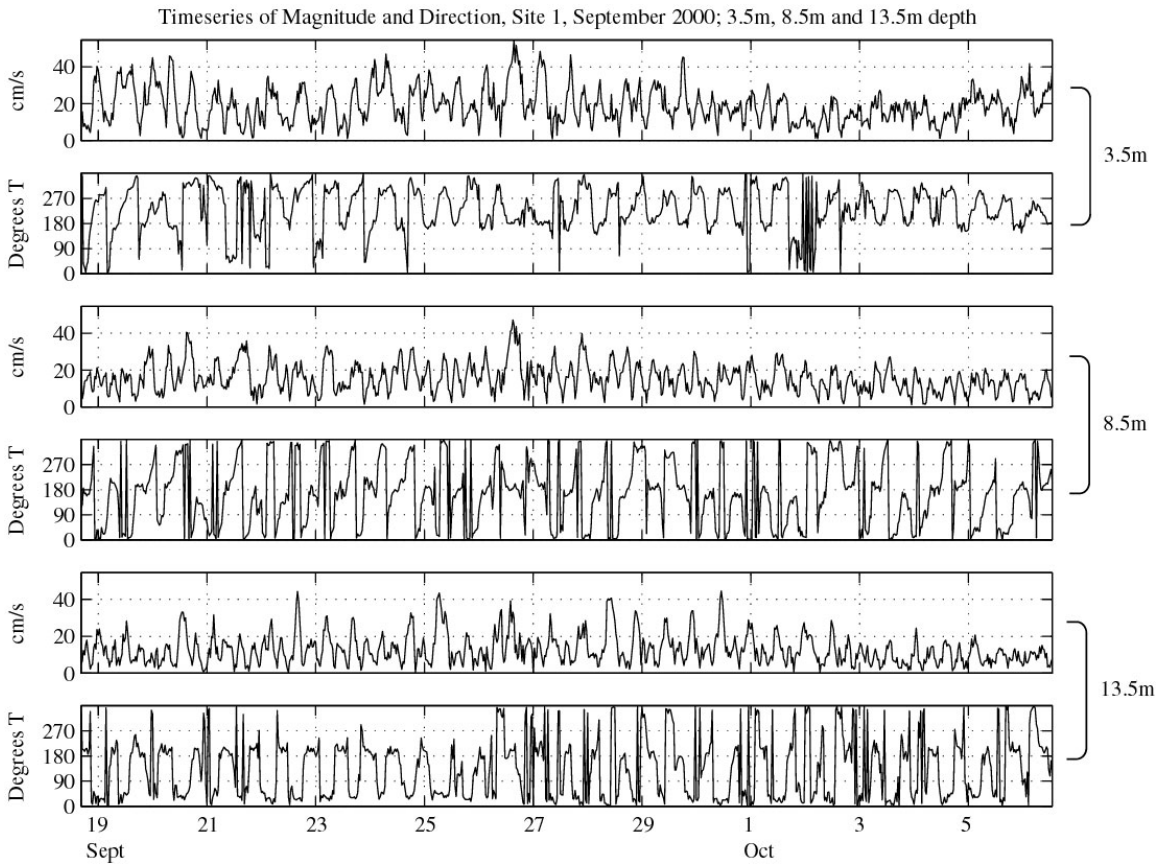

Figure A-3. Time series of current magnitude and direction from three depth levels as recorded by ADCP at Site 1 in the first deployment, fall 2000. Depth at the site was approximately 16 m. Values to the right of plots indicate measurement depth.

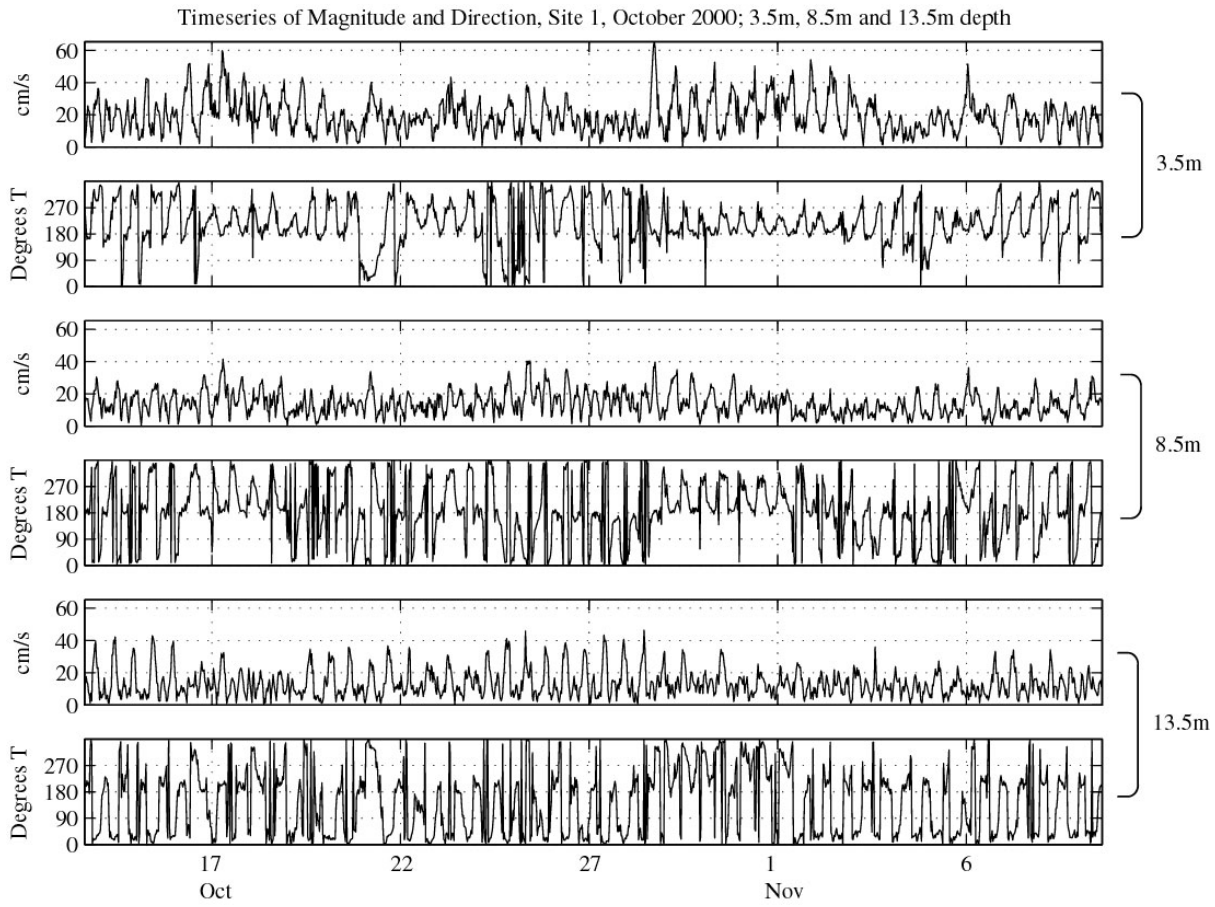

Figure A-4. Time series of current magnitude and direction from three depth levels as recorded by ADCP at Site 1 in the second deployment, fall 2000. Depth at the site was approximately 16 m. Values to the right of plots indicate measurement depth.

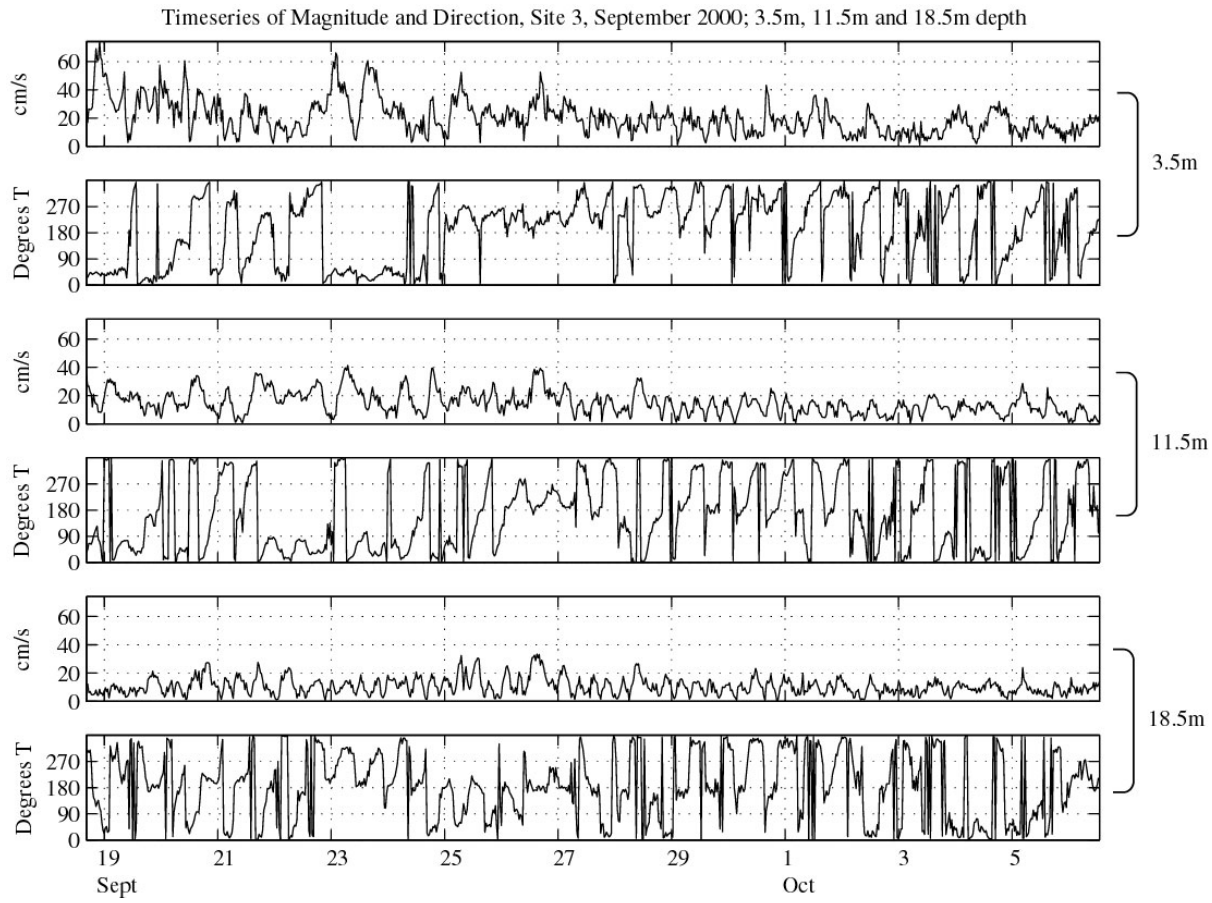

Figure A-5. Time series of current magnitude and direction from three depth levels as recorded by ADCP at Site 3 in the first deployment, fall 2000. Depth at the site was approximately 21 m. Values to the right of plots indicate measurement depth.

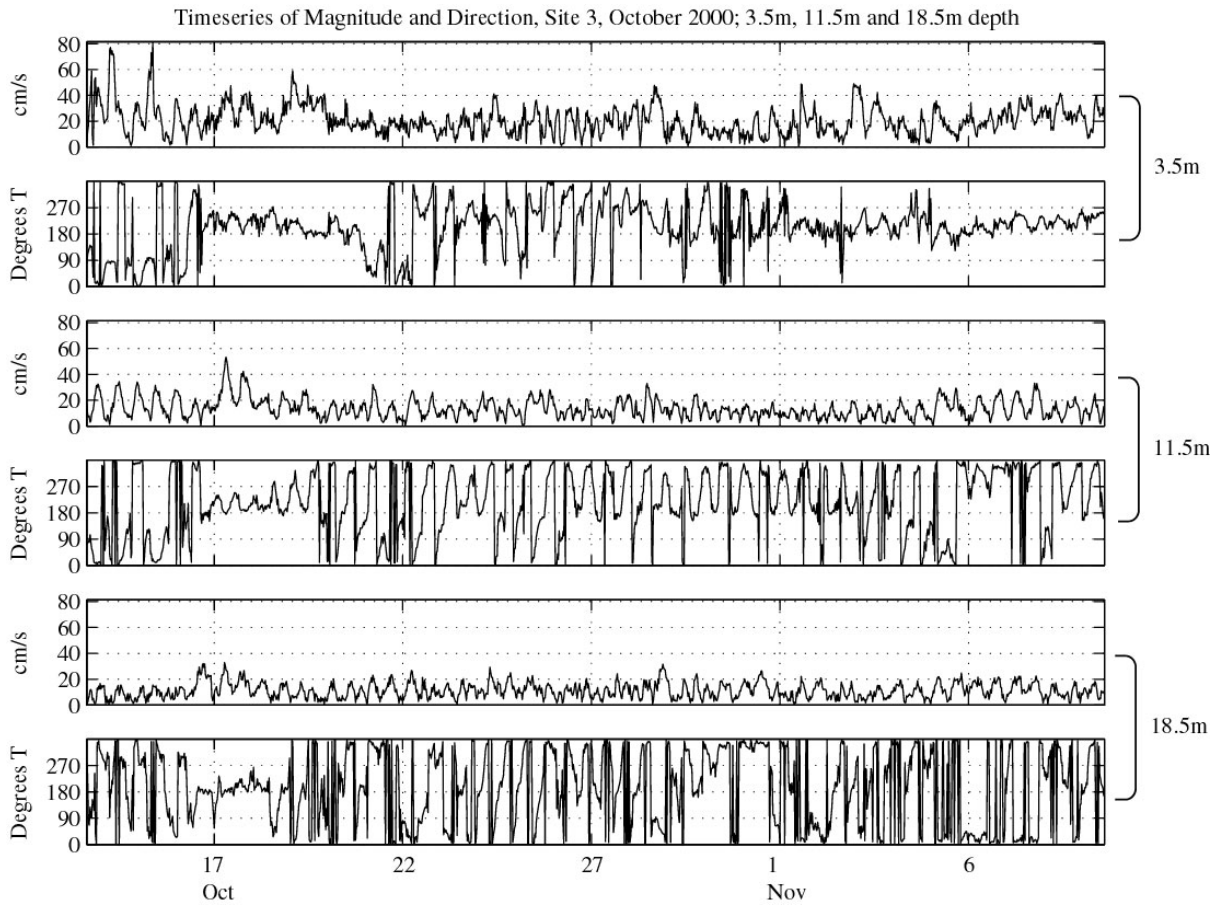

Figure A-6. Time series of current magnitude and direction from three depth levels as recorded by ADCP at Site 3 in the second deployment, fall 2000. Depth at the site was approximately 21 m. Values to the right of plots indicate measurement depth.

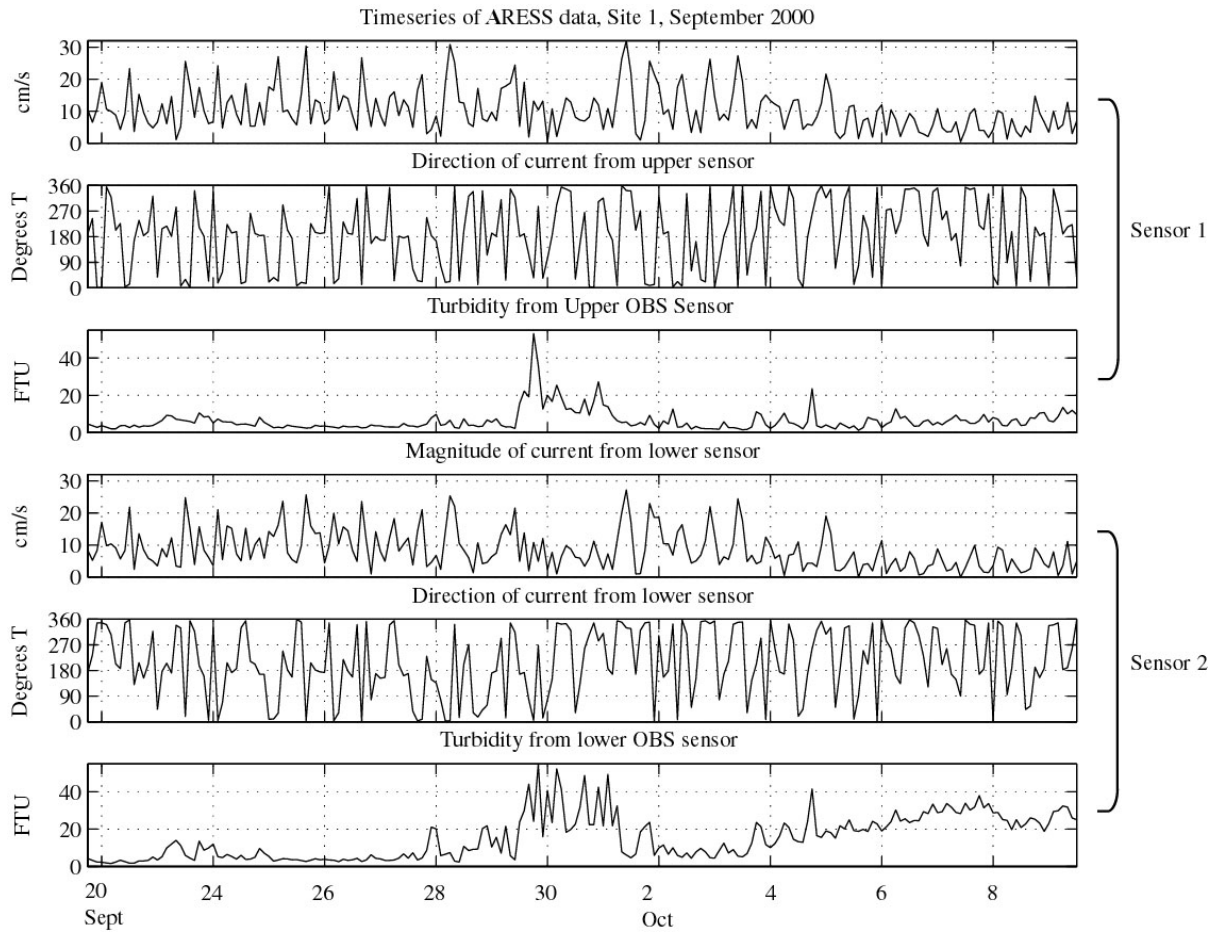

Figure A-7. Time series of near-bottom current magnitude and direction and near-bottom turbidity recorded by ARESS at Site 1 for the first deployment in fall 2000. Sensor one was situated at approximately 1.5 m off the seafloor, and sensor two was at 0.75 m off the seafloor. The depth at the site was approximately 16 m.

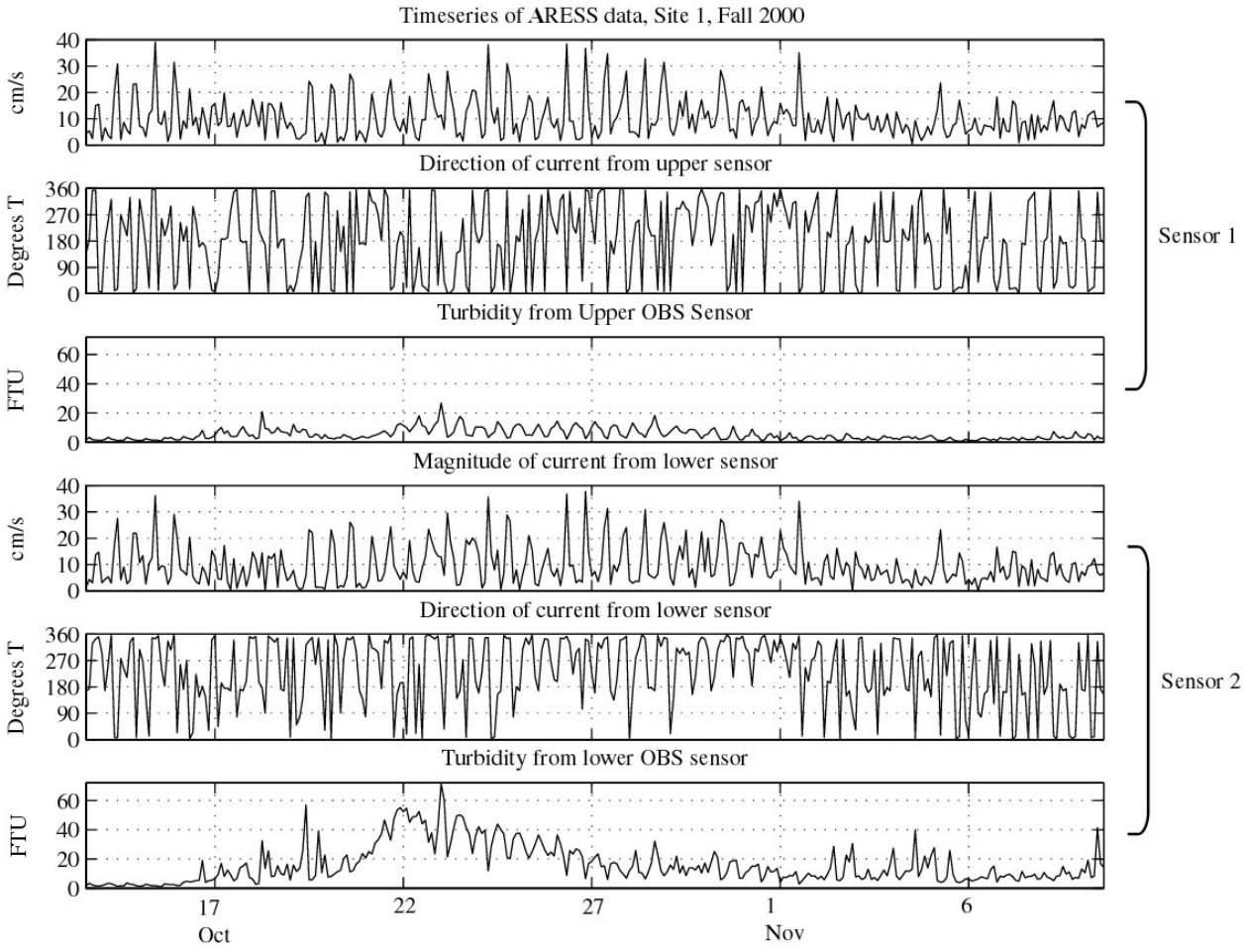

Figure A-8. Time series of near-bottom current magnitude and direction and near-bottom turbidity recorded by ARESS at Site 1 for the second deployment in fall 2000. Sensor one was situated at approximately 1.5 m off the seafloor, and sensor two was at 0.75 m off the seafloor. The depth at the site was approximately 16 m.

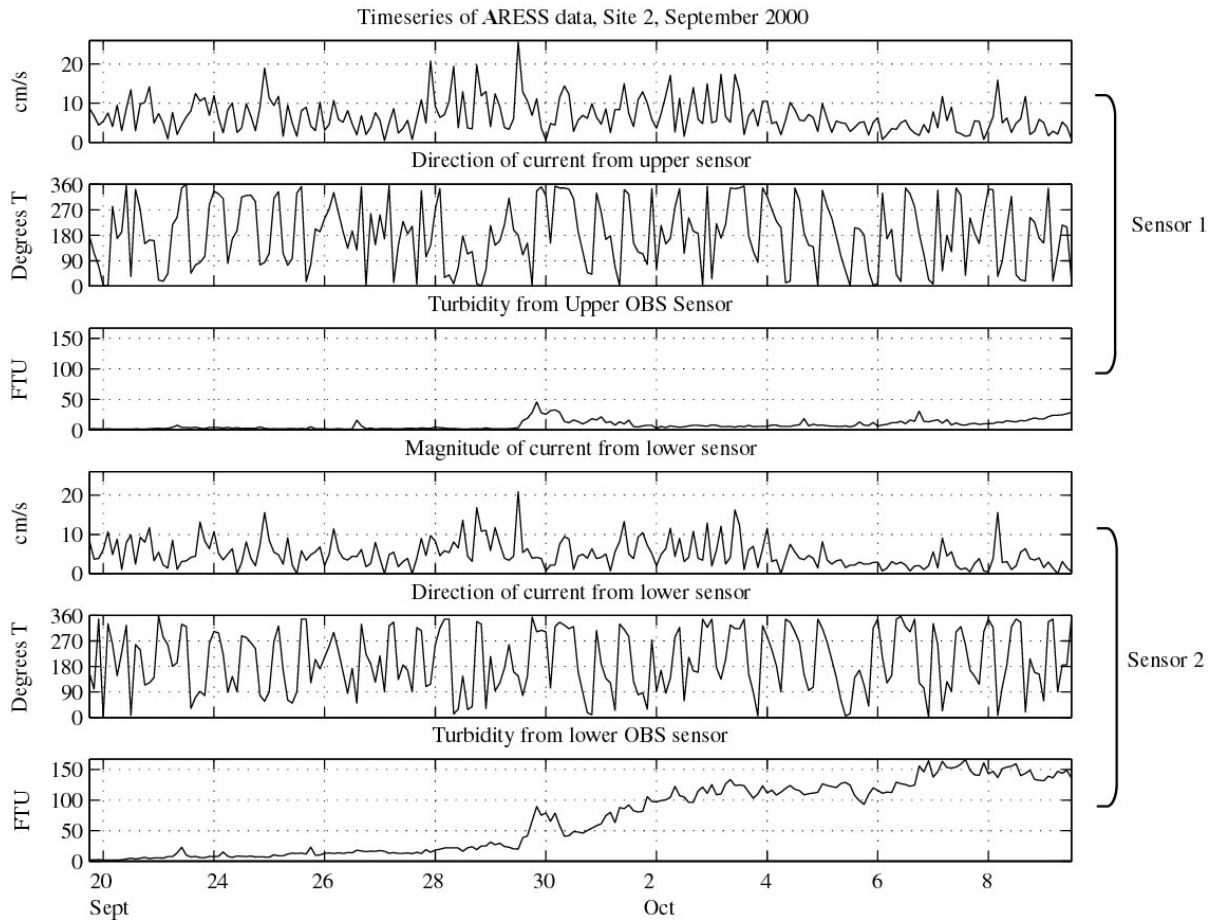

Figure A-9. Time series of near-bottom current magnitude and direction and near-bottom turbidity recorded by ARESS at Site 2 for the first deployment in fall 2000. Sensor one was situated at approximately 1.5 m off the seafloor, and sensor two was at 0.75 m off the seafloor. The depth at the site was approximately 12 m.

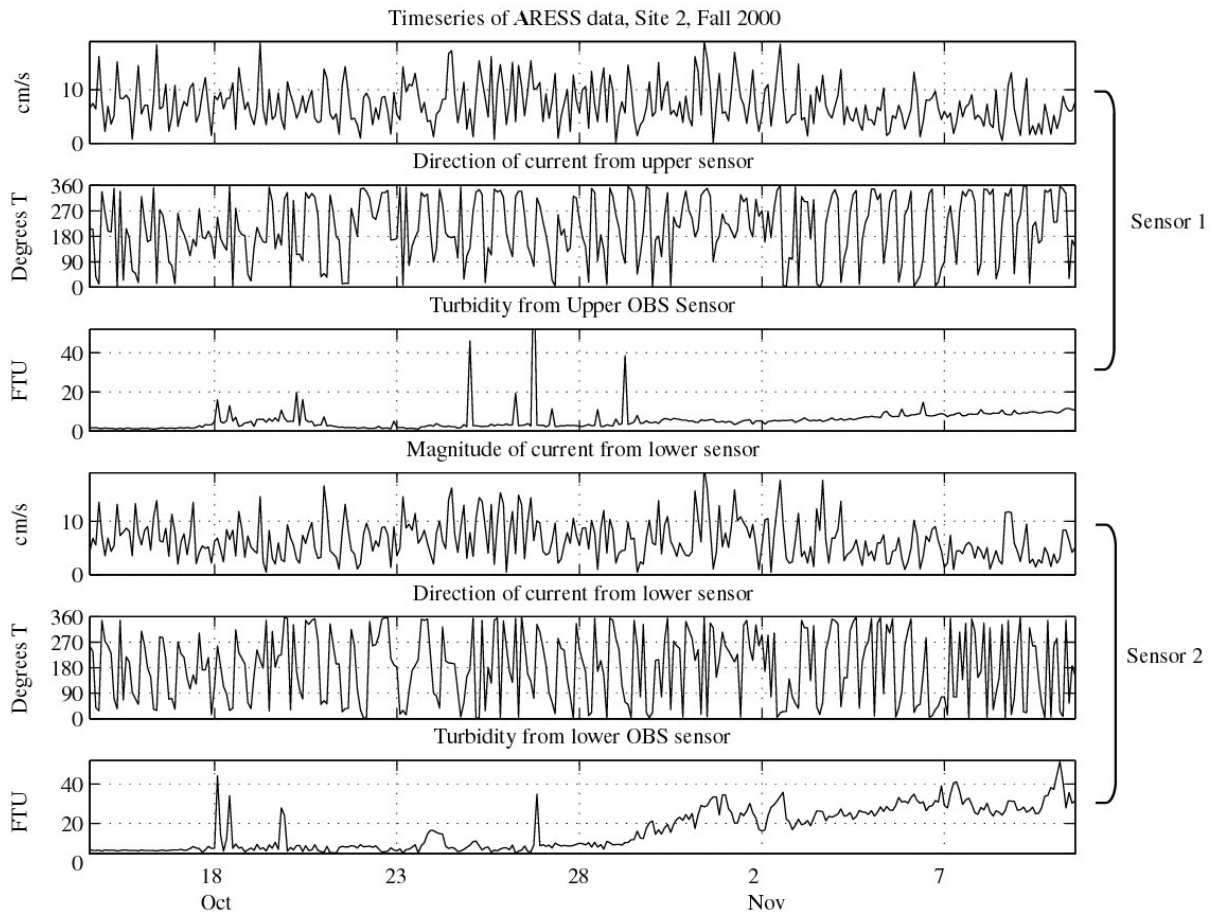

Figure A-10. Time series of near-bottom current magnitude and direction and near-bottom turbidity recorded by ARESS at Site 2 for the second deployment in fall 2000. Sensor one was situated at approximately 1.5 m off the seafloor, and sensor two was at 0.75 m off the seafloor. The depth at the site was approximately 12 m.

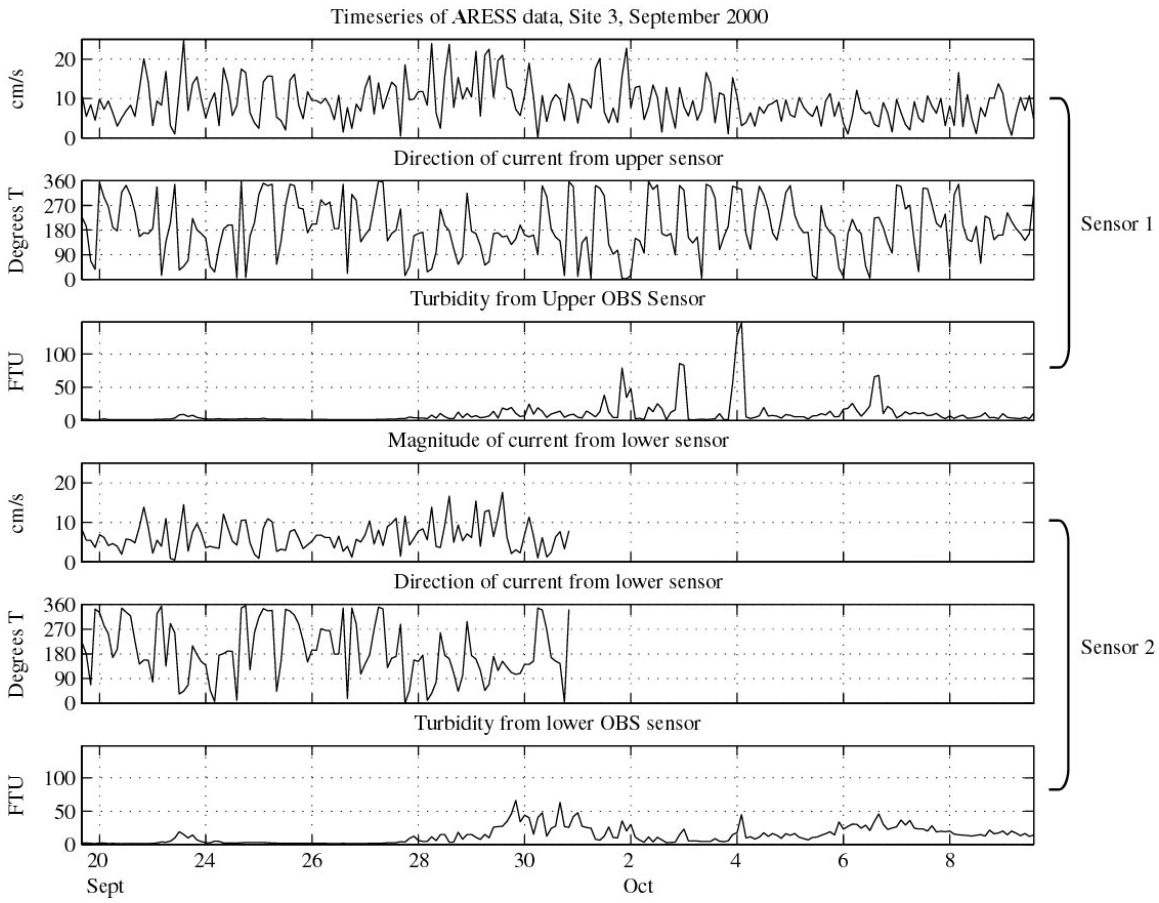

Figure A-11. Time series of near-bottom current magnitude and direction and near-bottom turbidity recorded by ARESS at Site 3 for the first deployment in fall 2000. Sensor one was situated at approximately 1.5 m off the seafloor, and sensor two was at 0.75 m off the seafloor. The depth at the site was approximately 21 m. Note that the current sensor at depth level 2 failed halfway through the deployment, whereas the turbidity sensor continued operating at this depth level.

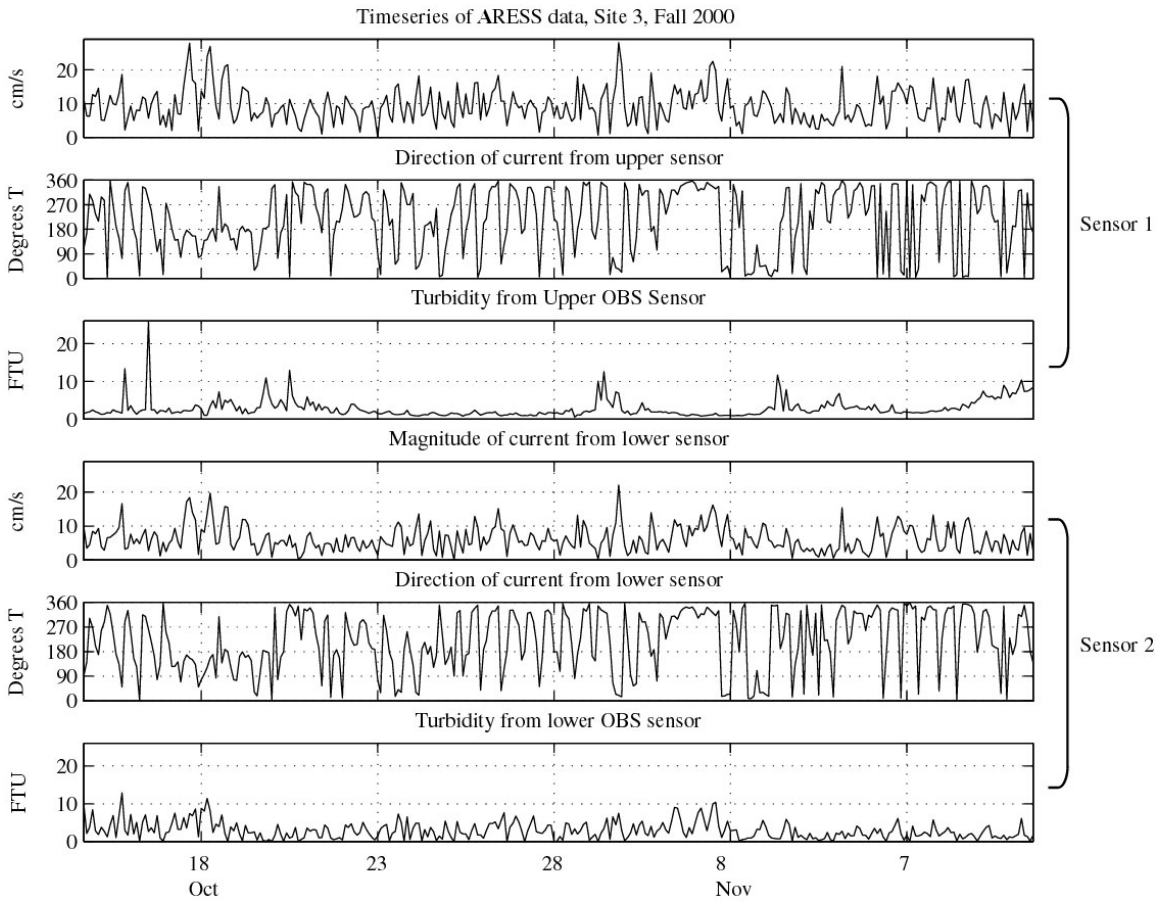

Figure A-12. Time series of near-bottom current magnitude and direction and near-bottom turbidity recorded by ARESS at Site 3 for the second deployment in fall 2000. Sensor one was situated at approximately 1.5 m off the seafloor, and sensor two was at 0.75 m off the seafloor. The depth at the site was approximately 21 m.

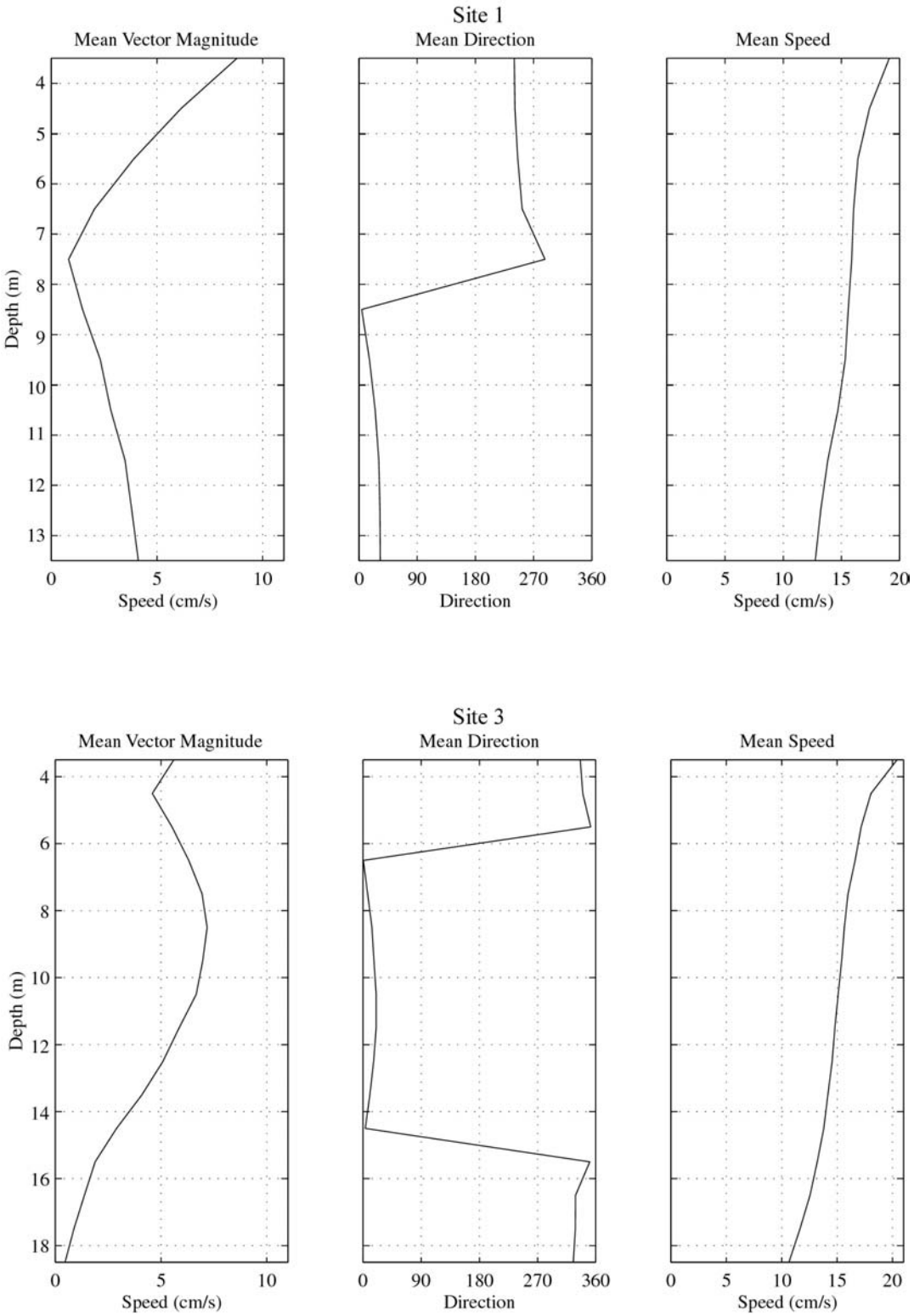

Figure A-13. Mean vector magnitude and direction, and mean speed throughout the water column from ADCP at Sites 1 and 3 in fall 2000 (Deployment 1)

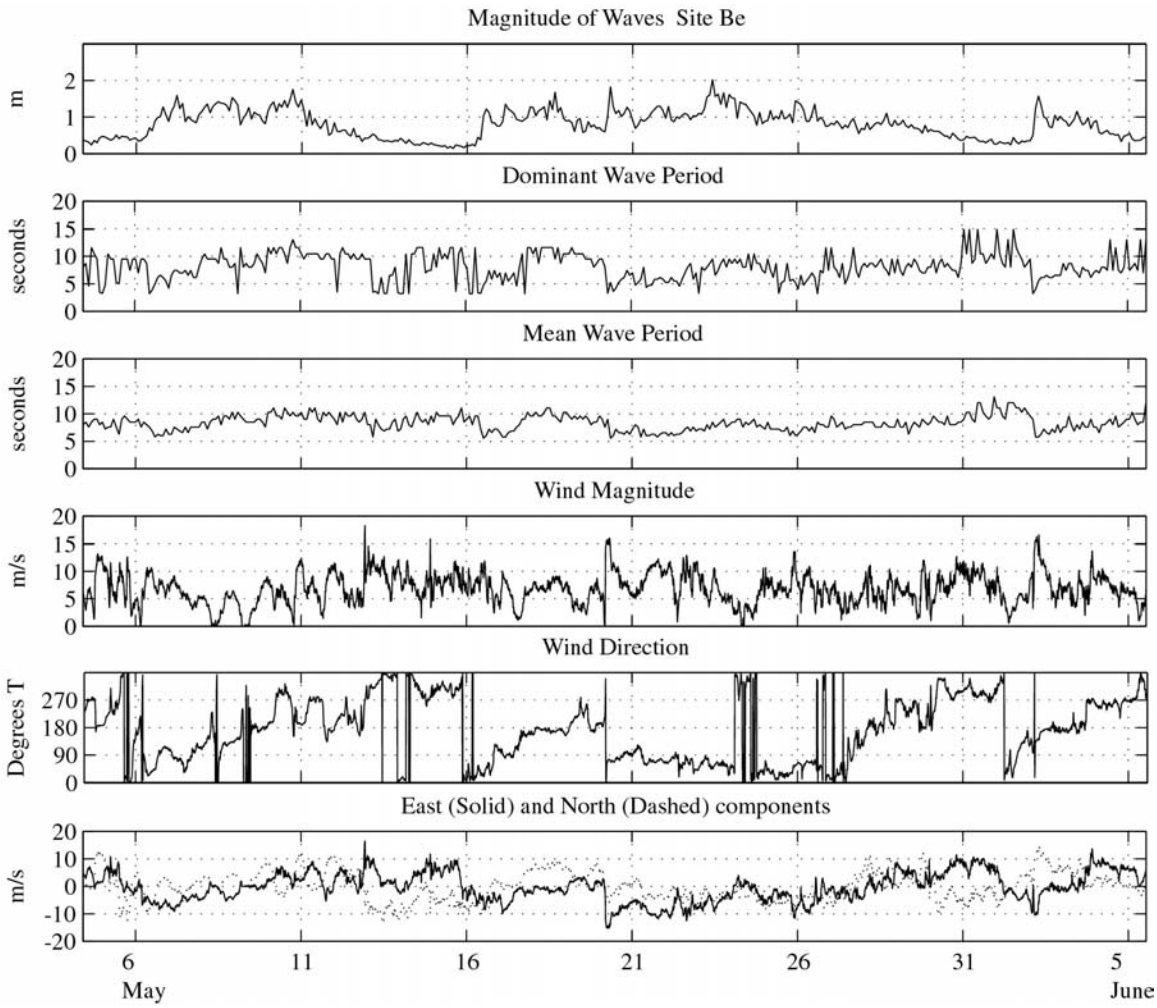

Figure A-14. Time series of waves recorded at Site Be and winds at Ambrose Tower for the fifth deployment in spring 2001. Wave data is presented as significant wave height.

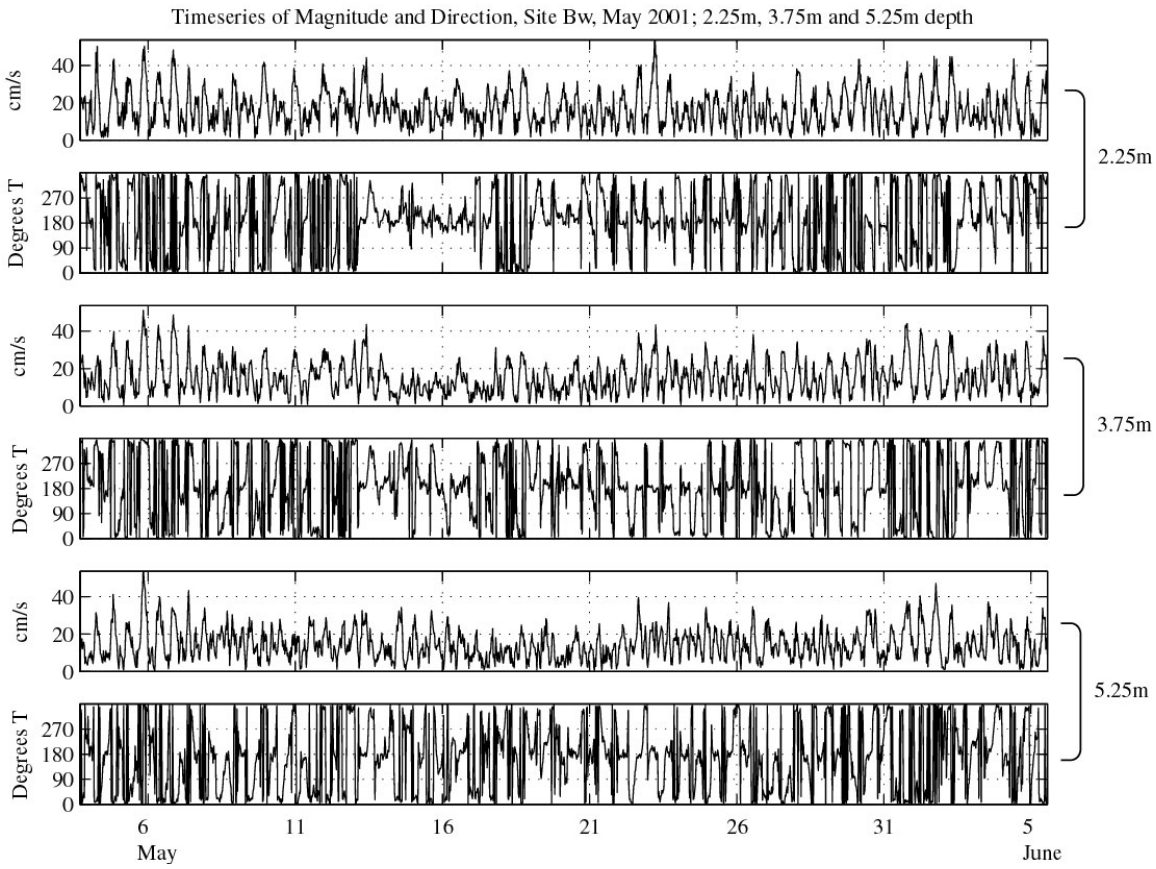

Figure A-15. Time series of current magnitude and direction from three depth levels as recorded by ADCP at Site Bw in the fifth deployment, spring 2001. Depth at the site was approximately 7.5 m. Values to the right of plots indicate measurement depth.

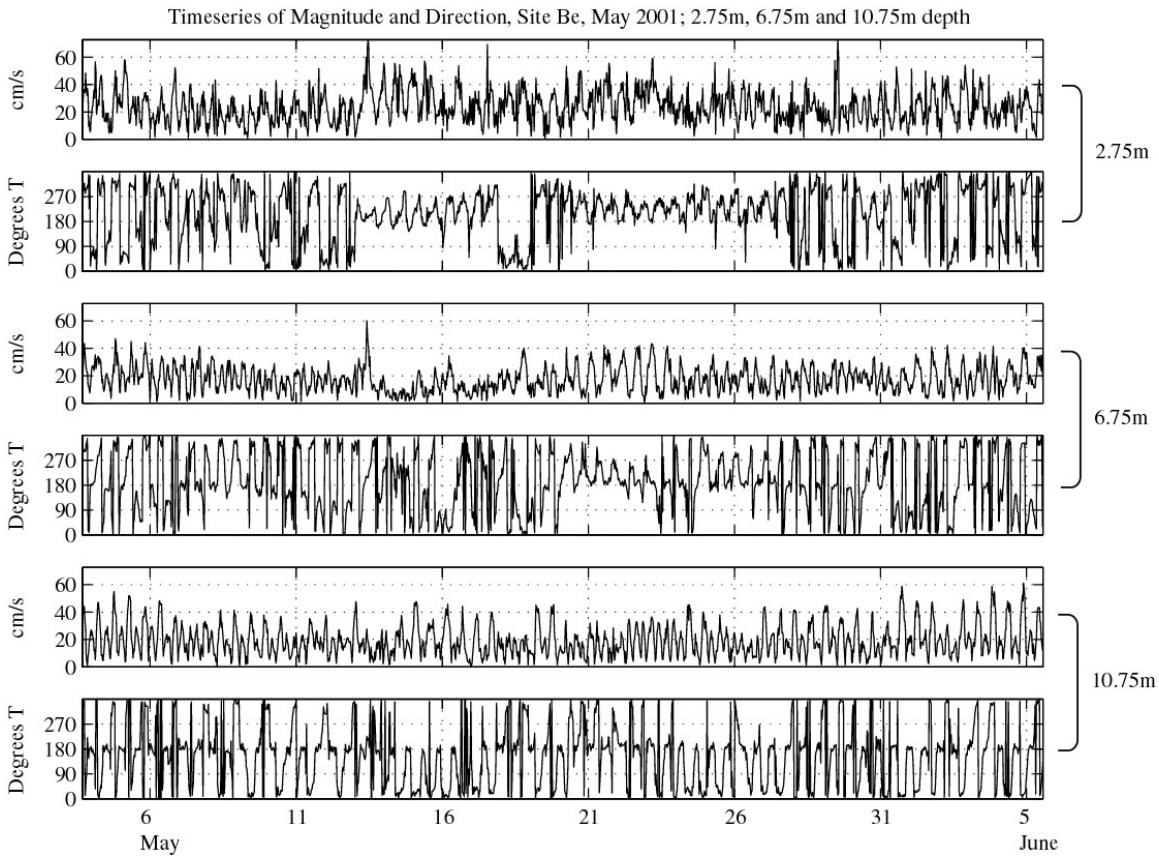

Figure A-16. Time series of current magnitude and direction from three depth levels as recorded by ADCP at Site Be in the fifth deployment, spring 2001. Depth at the site was approximately 13 m. Values to the right of plots indicate measurement depth.

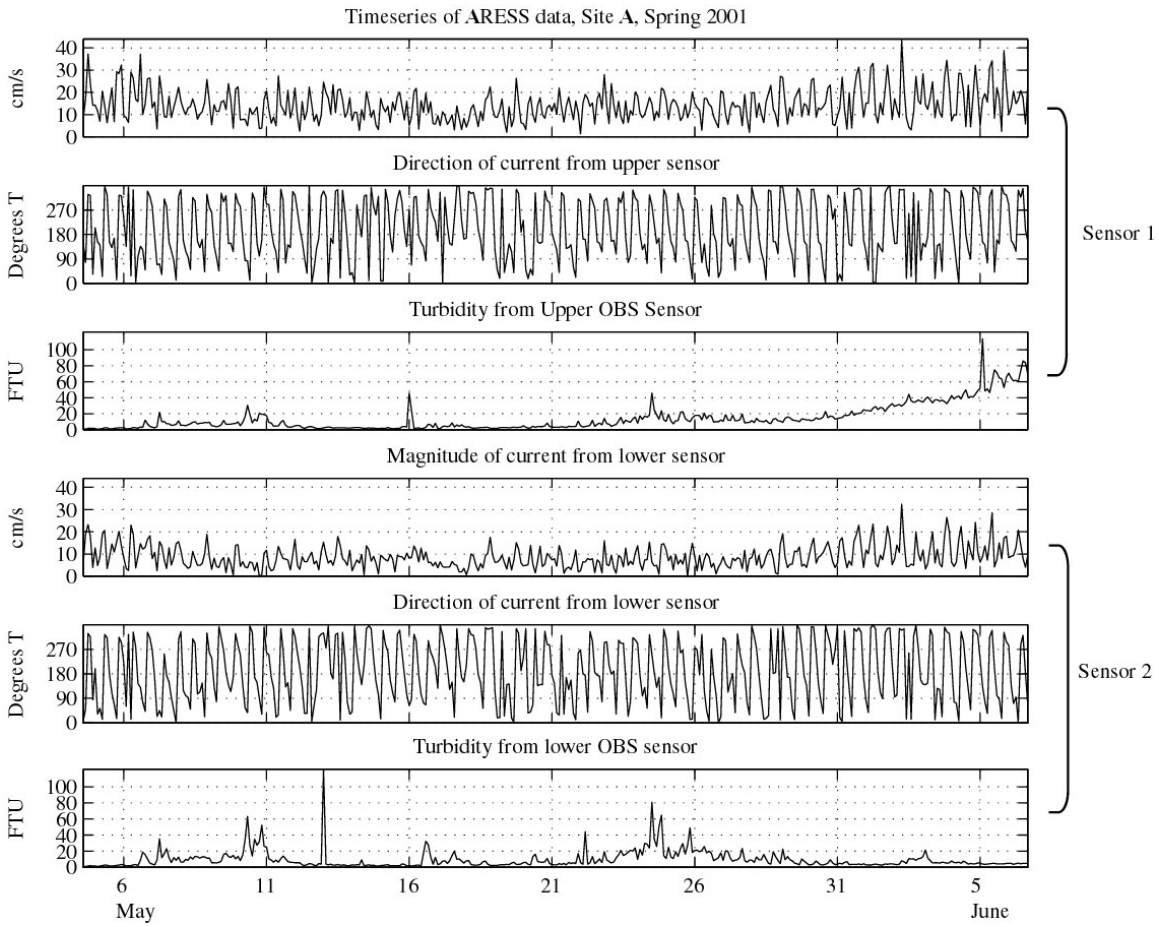

Figure A-17. Time series of near-bottom current magnitude and direction and near-bottom turbidity recorded by ARESS at Site A for the fifth deployment in spring 2000. Sensor one was situated at approximately 1.5 m off the seafloor, and sensor two was at 0.75 m off the seafloor. The depth at the site was approximately 7.5 m.

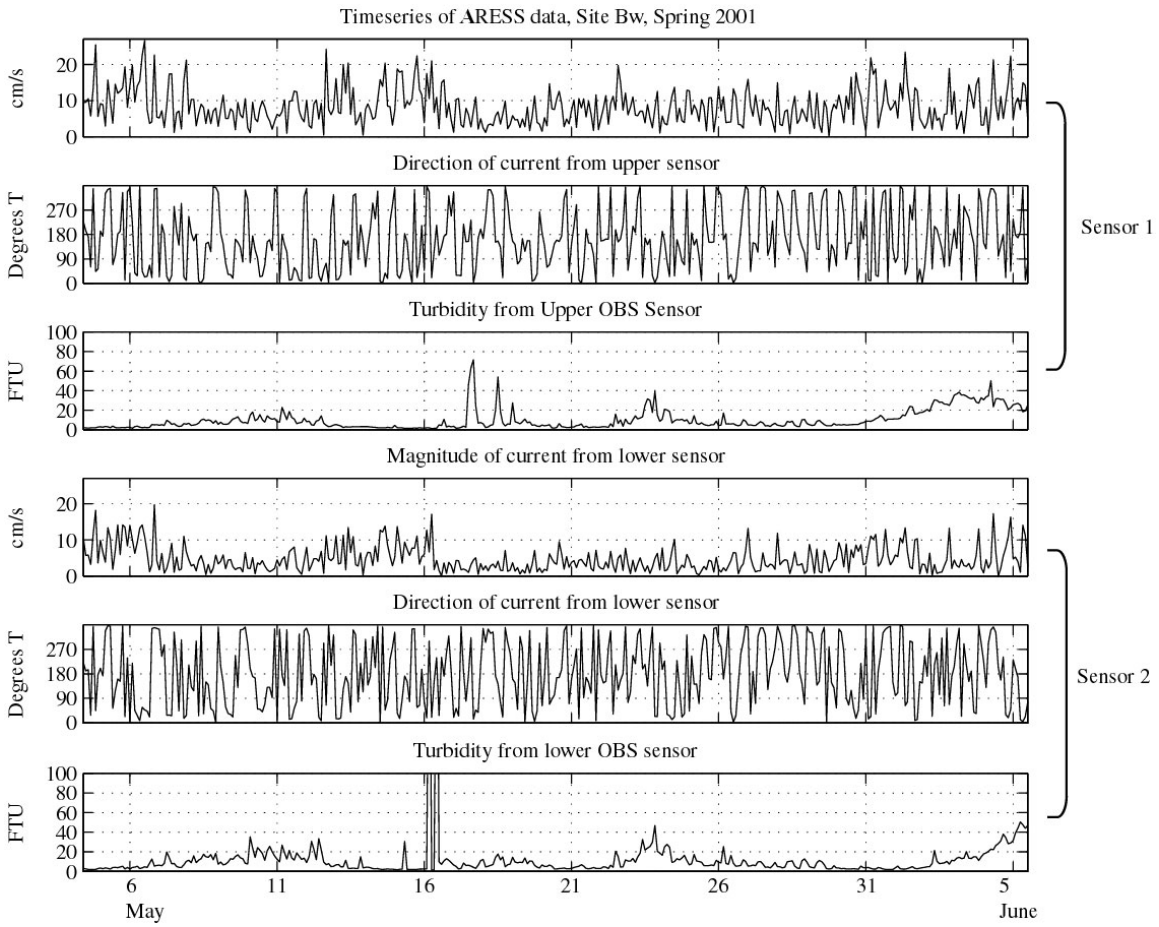

Figure A-18. Time series of near-bottom current magnitude and direction and near-bottom turbidity recorded by ARESS at Site Bw for the fifth deployment in spring 2000. Sensor one was situated at approximately 1.5 m off the seafloor, and sensor two was at 0.75 m off the seafloor. The depth at the site was approximately 7.5 m.

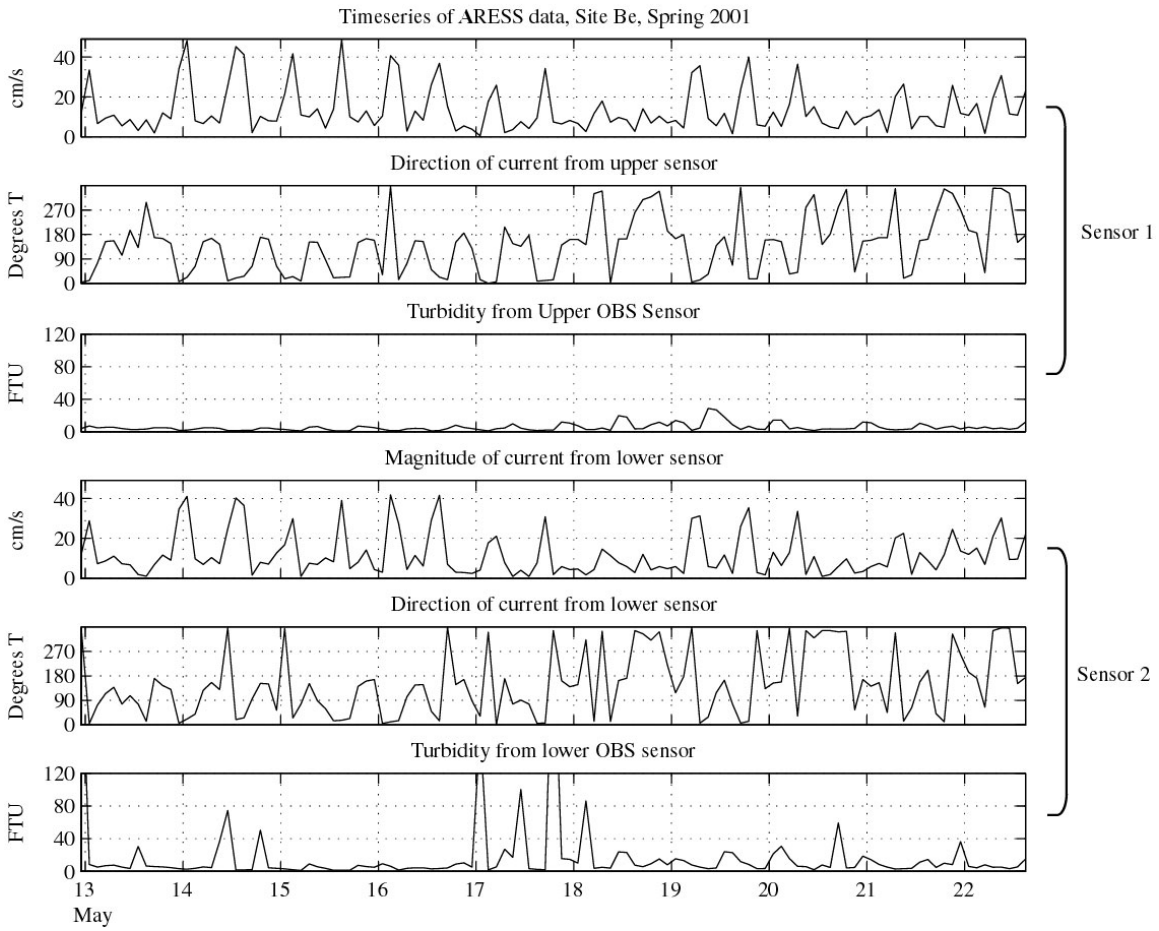

Figure A-19. Time series of near-bottom current magnitude and direction and near-bottom turbidity recorded by ARESS at Site Be for the fifth deployment in spring 2000. Sensor one was situated at approximately 1.5 m off the seafloor, and sensor two was at 0.75 m off the seafloor. The depth at the site was approximately 13 m. Note: the record length was truncated due to data recorder difficulties.

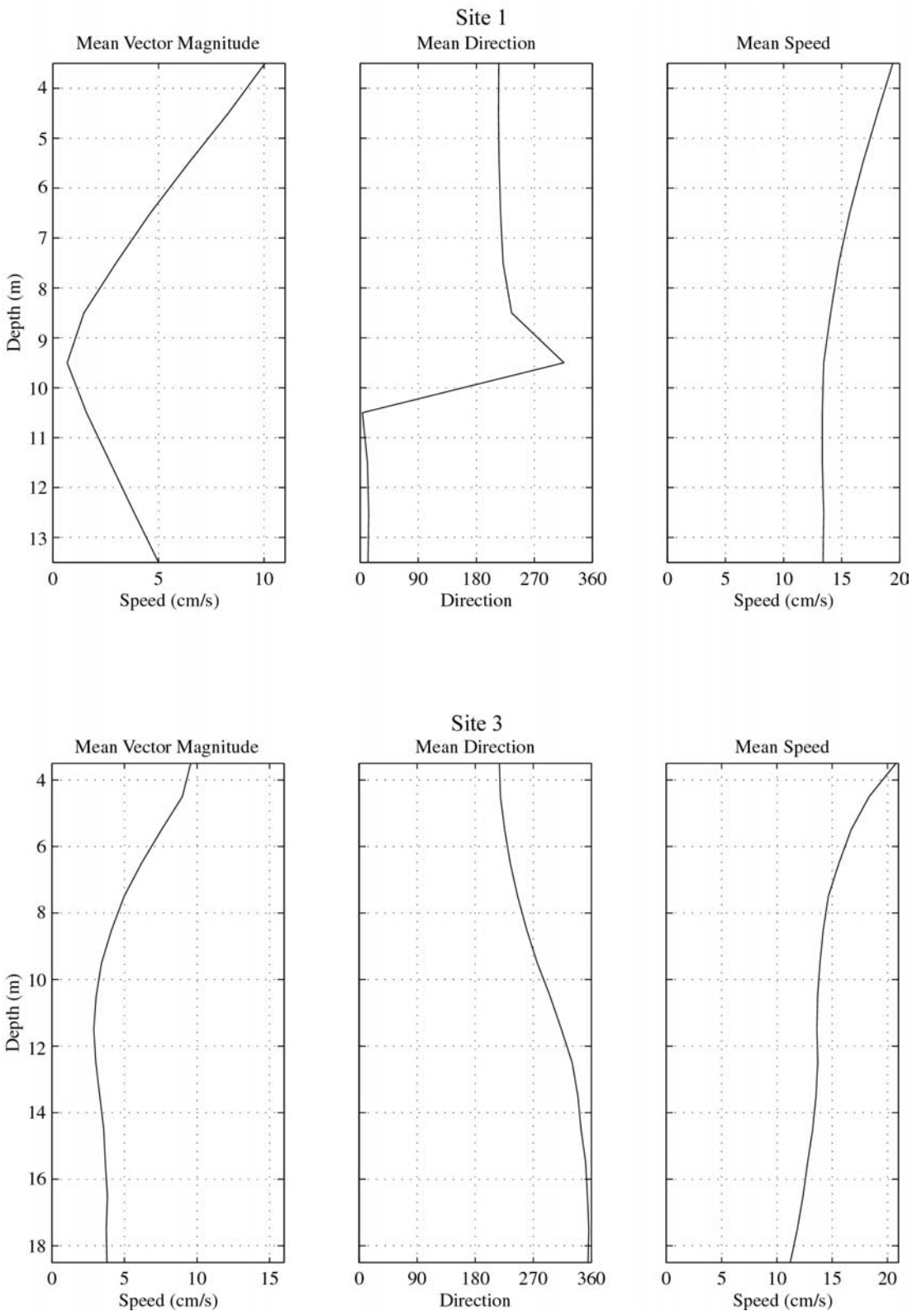

Figure A-20. Mean vector magnitude and direction, and mean speed throughout the water column from ADCP at Sites 1 and 3 in fall 2000 (Deployment 2)